

01 Aug 1965

## Structural performance of light gage steel diaphragms

Larry D. Luttrell

George Winter

Follow this and additional works at: <https://scholarsmine.mst.edu/ccfss-library>



Part of the [Structural Engineering Commons](#)

---

### Recommended Citation

Luttrell, Larry D. and Winter, George, "Structural performance of light gage steel diaphragms" (1965).  
*Center for Cold-Formed Steel Structures Library*. 140.  
<https://scholarsmine.mst.edu/ccfss-library/140>

This Technical Report is brought to you for free and open access by Scholars' Mine. It has been accepted for inclusion in Center for Cold-Formed Steel Structures Library by an authorized administrator of Scholars' Mine. This work is protected by U. S. Copyright Law. Unauthorized use including reproduction for redistribution requires the permission of the copyright holder. For more information, please contact [scholarsmine@mst.edu](mailto:scholarsmine@mst.edu).

Department of Structural Engineering  
School of Civil Engineering  
Cornell University

Report No. 319

STRUCTURAL PERFORMANCE OF LIGHT GAGE STEEL DIAPHRAGMS

by

Larry D. Luttrell

George Winter

Project Director

A Research Project Sponsored by the  
American Iron and Steel Institute

Ithaca, New York

August, 1965

## TABLE OF CONTENTS

	Page
ABSTRACT	1v
1. INTRODUCTION	1
1.1 Definition of Shear Diaphragms	1
1.2 Uses for Shear Diaphragms in Framed Structures	1
1.3 Purpose of the Investigation	3
1.4 Scope of the Investigation	3
2. THEORETICAL DIAPHRAGM SOLUTIONS	5
2.1 Review of Literature	5
2.2 General Shear-Deflection Theory	7
3. TEST VARIABLES AND PROCEDURE	16
3.1 Major Test Parameters	16
3.2 Test Procedures	21
4. TEST RESULTS	24
4.1 Introduction	24
4.2 Heavy Frame Tests	24
4.3 Light Frame Tests	26
4.4 Small Diaphragm Tests	41
4.5 Discussion and Conclusions	43
5. DIAPHRAGM DEFLECTIONS	59
5.1 The Deflection Problem	59
5.2 Deflection Analysis of Cantilever Tests	59
5.3 Diaphragm Deflections in Buildings	62
5.4 Conclusions	68

6.	MILL BUILDING INVESTIGATION	70
6.1	Introduction	70
6.2	Prototype Building	70
6.3	Structural Analysis	72
6.4	Model Analysis	77
6.5	Model Materials	79
6.6	The Model Buildings	81
6.7	The Model Tests	82
7.	LOAD FACTORS AND STANDARD TEST PROCEDURES	85
7.1	Introduction	85
7.2	Load Factors for Light Gage Steel Diaphragms	85
7.3	Standard Test Procedure for Light Gage Steel Diaphragms	93
8.	SUMMARY	100
8.1	General Diaphragm Behavior	100
8.2	Diaphragm Deflections	103
8.3	Load Factors	103
8.4	Diaphragm Influence in Mill Buildings	104
8.5	Possibilities for Future Investigations	104
	APPENDIX A - NOTATION	106
	APPENDIX B - COMPUTER ANALYSIS OF MILL BUILDINGS	108
	REFERENCES	115
	TABLES	116
	FIGURES AND ILLUSTRATIONS	125

## ABSTRACT

Light gage steel roof, wall, and floor systems may be used to transfer in-plane shear forces from one part of a framed structure to another, leading to reduced loads in parts of the structure. This is particularly noticeable in buildings having rigid end walls and under lateral loading. The diaphragms transfer forces from the interior frames into the foundation through the rigid end walls, resulting in lower loads for the interior frames. The amount of force transfer is dependent upon the in-plane shear strength and is particularly sensitive to the shear stiffness of the diaphragm.

The results from some 60 full scale diaphragm shear tests and several smaller tests are presented. The test diaphragms were fabricated from several different panel shapes and thicknesses and had three basic types of connections. These were welds, screw type fasteners, and backed up fasteners. The assembly method generally followed that recommended by the panel manufacturer except in a few cases where it was desirable to study the influence of fastener spacing. The tests included 22, 26, and 28 gage diaphragms under static, pulsating, and reversed loading.

It is shown that the shear strength per foot of diaphragm is relatively independent of length along the corrugations provided a regular fastener arrangement is used throughout. The addition of sidelap fasteners increases the shear strength

in proportion to the number of fasteners added. The strength is also dependent on the intensity and number of cyclic loads, being lower than the static strength if the number of cycles is large and the cyclic load is intensive. However, cyclic loads up to  $\pm 0.3$  of the static strength and applied for up to 30 cycles, result in only a small strength reduction.

A critical measure of diaphragm performance is the shear stiffness. For a given panel configuration and a fixed fastener arrangement, the stiffness is very strongly dependent on the panel length. This is due to the introduction of accordion-like warping across the panel ends which penetrates into the diaphragm and reduces the shear stiffness. The penetration is relatively independent of length and as the diaphragm becomes longer, the warping influence at the ends becomes less significant. This accounts for a variation in shear stiffness with length. A method is presented to predict the shear stiffness for diaphragms of any length on the basis of a single test.

A method of analysis for framed structures having diaphragms is given and it is illustrated by simple examples. Gable frame mill buildings are investigated in considerable detail by theoretical means as well as by model analysis. The investigation shows that roof diaphragms are very influential in reducing interior frame loads when the buildings have stiff end walls.

Load factors for light gage steel diaphragms under in-plane shear were determined on the basis of extensive reversed

load tests. The factors were derived within the framework of the American Iron and Steel Institute Light Gage Cold-Formed Steel Design Manual (1962) Specifications. The recommended values cover wind loads, earthquake loads, dead loads, and gravity live loads.

## INTRODUCTION

### 1.1 Definition of Shear Diaphragms.

Shear diaphragms are membrane-like devices which are capable of resisting deformation when loaded by in-plane shear forces. The ideal diaphragm is a thin sheet of material attached to a supporting framework in such a way that shear loads are resisted by diagonal tension fields.

A broader and more practical definition which will be used throughout this work includes all thin web structures regardless of whether or not they are plane. This definition includes such diaphragms as thin web plate girders, stressed skin surfaces of aircraft, and light gage steel roof or wall sections under in-plane shear. The present investigation deals with the last category and includes light gage steel roof, wall, and floor diaphragms as they are currently used in buildings.

### 1.2 Uses for Shear Diaphragms in Framed Structures.

Roof and wall sections in buildings are used primarily to transfer the normal components of surface loads into the structural framework. In order to do this efficiently, they will ordinarily be corrugated or otherwise stiffened. The stiffeners increase the normal load strength but introduce complexities into shear strength analysis which are so difficult to deal with that in-plane shear forces have been almost totally ignored in past analysis and design.

In practically all steel buildings, the end frames are covered with a diaphragm or otherwise braced by a stiff end wall. Thus, the end frame will seldom be loaded to design capacity, loads being transferred into the foundation by shear action of the end walls. The stiff end frame and wall assembly could be used to carry an appreciable part of the interior frame loads if a method of force transfer were present. Roof, wall, and floor diaphragms can perform this function. Depending on the type of diaphragm, it is possible that all wind bracing might be eliminated and even more attractive is the possibility that diaphragm strength might be used to reduce the size of interior framing members. It is, however, necessary to know the diaphragm strength, stiffness, and what safety factors to use before any of this can be realized. Strong emphasis should be placed on stiffness which is a measure of the shear force to shear deflection ratio. Many diaphragms are strong but are so flexible that their use as shear load carrying devices in framed structures is virtually impossible.

The most apparent use for floor and roof shear diaphragms is to resist lateral earthquake and wind loads. In buildings which have sloped roofs, they may also be used to transfer vertical live load shear forces into the end walls. However, they may be used to resist dead load forces only when special erection techniques are employed since most dead load deflections will have occurred prior to completion of the diaphragm system.

### 1.3 Purpose of the Investigation.

Light gage steel diaphragms are almost infinite in variety when all possible parameters are considered. In this light, several different diaphragms were studied theoretically and experimentally in order to clarify the following points:

1. Typical ultimate shear strength values for several types of diaphragms.
2. The variation of in-plane shear deflection with load.
3. Shear strength variation with several parameters, particularly with length along the diaphragm corrugations.
4. Maximum reliable strength under dynamic load conditions.
5. Required load factors for diaphragms under in-plane shear.
6. Methods to deal with diaphragm influence in structural analysis.
7. Factors to consider in establishing standard test procedures for shear diaphragms.

### 1.4 Scope of the Investigation.

The study was limited to light gage steel diaphragms having "open" corrugated shapes typified by those in Fig. 3-1. Cellular panel diaphragms having continuous flat plate elements and composite systems such as concrete and steel roofs were not studied. In the course of the investigation, some 60 large diaphragms and 40 small diaphragms were tested. The primary test variables were: 1) panel configuration, 2) panel

length and thickness, 3) type of fasteners and their arrangement, 4) edge member flexibility, 5) restraints of interior frame members such as girts or purlins, 6) type of loading, and 7) diaphragm material properties.

A general procedure to consider the diaphragm influence in structural analysis was developed. It was used for several mill building solutions and was checked by model analysis of mill buildings.

## 2. THEORETICAL DIAPHRAGM SOLUTIONS

### 2.1 Review of Literature.

The most straightforward solutions for determining in-plane shear stresses and deflections of diaphragms are those for thin plane diaphragms. The diaphragms may be attached to either infinitely stiff edge beams or to flexible beams; solutions for both cases are well known.<sup>1</sup>

The problem becomes much more complicated when corrugated diaphragms are considered. These will usually be attached to the supporting framework along the bottom of the corrugations. All force transfer between the diaphragm and the frame will occur in the plane of attachment and consequently the shear forces will be eccentric with respect to the mid-plane of the diaphragm. The eccentricity of loading will give rise to accordion-like end warping in the case where end connections are not continuous. This type of end warping is shown in Fig. 4-20.

Theoretical solutions have been obtained for the case of rectangularly corrugated diaphragms<sup>2</sup> and for diaphragms having cross sections which can be represented by a series of circular arcs.<sup>3</sup> Finite length diaphragms of a somewhat more general shape have been investigated for cases when the corrugation ends are continuously connected to a heavy edge member.<sup>4</sup>

---

1. Superscripts refer to the references on page 115.

These solutions were obtained on the assumption that the diaphragm was either infinitely long or that all section lines along the corrugations remained straight under loading. (Length will always denote the dimension parallel to the corrugations.) Both assumptions place serious restrictions on the solutions since they exclude localized warping across the corrugation ends. It is precisely the neglect of end warping which causes the theories to overestimate the shear stiffness when end fasteners are located at discrete points across the corrugation ends.

Other investigators<sup>5,6,7,8</sup> have studied more practical roof and wall diaphragms, determining shear strength and stiffness characteristics by experiment. They have developed procedures for using diaphragms once the stiffness and strength have been determined but have not presented theoretical procedures for establishing the shear characteristics as a function of diaphragm configuration.

Consider an infinitely long diaphragm in which uniformly distributed shear forces are applied along the corrugation edges. All sections at right angles to the corrugations will be identical regardless of where they are taken along the length. This means that a line scribed along the crest of a corrugation might move but it will always remain parallel to its original position. If the diaphragm is now made finite but long, sections near the middle will remain very much as they were in the infinitely long diaphragm under shear loads. As sections nearer and nearer to the ends are considered,

warping due to the eccentricity of end shear forces will become more pronounced until it reaches a maximum at the diaphragm ends. The end warping extends into the diaphragm but it is more pronounced near the ends.

It is now necessary to develop a method for predicting shear stiffness as a function of the corrugation shape as well as the diaphragm length which will account for end warping influences. The theory should have two applications:

1. To predict the shear stiffness.
2. To extend test data to diaphragms having lengths different from those tested.

A completely theoretical prediction of shear stiffness involves an assumption as to how the end warping penetrates into the diaphragm. Since diaphragms will be tested regardless of the theoretical predictions, the second concept is much more practical. From any one test, it is possible to find certain parameters in the theory which are independent of diaphragm length. From these, the stiffness for any other length of diaphragm can be determined, avoiding any assumptions connected with the influence of end warping.

## 2.2 General Shear-Deflection Theory.

The elastic shear deflection, and consequently the stiffness, may be determined from the superposition of two separate elastic solutions. The first is obtained by assuming that the entire perimeter of the diaphragm is continuously connected to the marginal frame members. The second solution accounts for the removal of fastener continuity across the corrugation

ends and allows end shear forces to be concentrated at discrete points.

a) Part 1. Suppose an infinitely long plane diaphragm having a finite width  $w$  is loaded by uniformly distributed shear forces as shown in Fig. 2-1. The in-plane deflection  $\Delta'$  of one edge with respect to the other is:

$$\Delta' = w \frac{2(1+\nu)}{E} \tau_{xy} \quad (2-1)$$

where  $E$  is the elastic modulus,  $\nu$  is Poisson's ratio, and  $\tau_{xy}$  is the shear stress. If the diaphragm is cut to a finite length  $l$  as in Fig. 2-2 but is attached to perfectly rigid edge members with continuous connections, equation 2-1 is unchanged. Fastener continuity across the ends at the perfectly rigid marginal beams force the end section to have the same shape as in the infinitely long diaphragm and consequently, shear stresses are identical everywhere.

The diaphragm in Fig. 2-3 is loaded by a concentrated load which is applied through the edge beam. It may be assumed that the shear transfer into the diaphragm is continuous and uniform if the edge fasteners are continuous and the longitudinal strains in the beam are small. Edge fasteners generally will not be continuous but the intervals between them usually will be small in relation to the overall diaphragm dimensions and shear transfer will be assumed to be continuous. The shear stress may be expressed as:

$$\tau_{xy} = P/lt \quad (2-2)$$

where  $P$  is an external concentrated shear force,  $t$  is the

diaphragm thickness, and  $l$  is the dimension along the corrugation.

Common roof and wall panels can be represented as surfaces generated by moving a line at right angles to a particular plane path. The plane path is of course the shape of the cross section. When such an infinite panel is shear loaded, all lines will remain parallel because all cross sections will be identical. The same observation holds for finite length diaphragms when corrugation ends are continuously connected to infinitely rigid edge beams. Since no warping occurs, the only influence of introducing the corrugations is to increase the effective shear width  $w$  in equation 2-1. One corrugation from a typical perfectly connected diaphragm is shown in Fig. 2-4. It can be seen that the effective shear width is increased in the ratio of  $L/h$  where  $L$  is the developed corrugation width and  $h$  is the corrugation pitch. Modifying equation 2-1 and using equation 2-2:

$$\Delta' = w \frac{2(1+\nu)}{E} \cdot \frac{P L}{l t h} \quad (2-3)$$

b) Part 2. Corrugated diaphragms are almost never continuously connected across the corrugation ends, the fasteners being concentrated in the corrugation valleys. Thus, shear stresses across sections  $mno$  in Fig. 2-4 cannot exist and their influence must be removed from the solution in equation 2-3 in order to account for end warping. The stresses across the sections  $mno$  may be replaced by a resultant force  $P'$  through the shear center of the section and parallel to the

plane of attachment between the diaphragm and the frame as shown in Fig. 2-4. The influence of end warping may now be considered by placing an equal but opposite force through the shear center as shown in Fig. 2-5 and then determining its influence on the shear deflection. The force  $P'$  is given by:

$$P' = \tau_{xy} h t = P \frac{h}{\ell} \quad (2-4)$$

This set of  $P'$  forces are held in equilibrium by an undetermined set of forces along the lines  $mm'$  and  $oo'$  in Fig. 2-5. The distribution will be uniformly varying only for the case when all lines along the corrugation are straight. Shear forces parallel to and along  $mm'$  and  $oo'$  have already been considered in equation 2-3 and are nonexistent in this part of the solution. Lines  $mm'$  and  $oo'$  are perfectly free to move longitudinally with respect to each other in the second part of the solution. They must remain parallel since end fasteners are assumed to be in every valley. A line  $nn'$  along the corrugation crest may rotate with respect to the edge lines but due to the antisymmetry of loading, it must always rotate about the midlength of the corrugation. It is also obvious that either half of the corrugation length is in equilibrium and that no shear stresses can exist across the section at the midlength. The investigation may now be directed to the free body in Fig. 2-7.

An important boundary condition may be deduced from an inspection of Fig. 2-6 which represents any cross section of the corrugation in Fig. 2-7. The ends of all corrugations

are loaded in the same sense by loads  $P'$  through the shear centers. The deflected shapes are all identical and any moments  $M$  at the corrugation valleys must be identically zero. Therefore, no bending moments can exist along lines  $mm''$  and  $oo''$  and the forces  $P'$  must be resisted only by forces  $u(x)$  and  $v_1(x)$  which must vary from zero when  $x = 0$  to a maximum when  $x = \ell/2$ . Similarly, the forces  $P'$  must vary from zero to a maximum with  $x$ .

The displacement  $\delta'(x)$  of a point on the corrugation crest as shown in Fig. 2-7, must vary from zero at  $x = 0$  to a maximum at  $x = \ell/2$  due to the antisymmetry of loads  $P'$  at either end of the corrugation (See Fig. 2-5).

The  $\delta'(x)$  deflections can be represented as those for a series of arches  $dx$  long as indicated by the shaded area in Fig. 2-7. The load  $p(x)$  through the shear center of each "arch" must be equivalent to the resultant of the shears on the faces  $x$  and  $x + dx$ . Torsional effects are an order smaller and will be ignored. The edge forces  $u(x)$  are assumed to vary as an  $n$ th degree parabola between  $x = 0$  and  $x = \ell/2$ . By integrating the forces  $u(x)$  between the limits  $x = 0$  and  $x = \ell/2$  and summing the forces in the direction of  $p(x)$  yields:

$$p(x) = 2(n+1) \frac{ph}{\ell^2} \left(\frac{2x}{\ell}\right)^n dx \quad (2-5)$$

where  $n$  fixes the degree of parabolic variation. An  $n = 1$  is equivalent to assuming that the warping varies linearly from a maximum at the ends to zero at the midlength.

The rate of change in the rotation of line  $nn''$  is denoted by  $d\phi$ :

$$d\phi = \frac{d}{dx} [\delta'(x)] \quad (2-6)$$

The line  $nn''$  must meet a line connecting points  $m$  and  $o$  at right angles. Consequently, the additional shear deflection due to the removal of the  $P'$  forces which must be added to equation 2-1 is, for one corrugation:

$$\delta_w = h\phi \quad (2-7)$$

where  $\delta_w$  is the additional shear deflection due to warping and  $\phi$  is the angle denoted in Fig. 2-7. There are  $w/h$  corrugations in the diaphragm. The final value of  $\Delta'$  is:

$$\Delta' = \frac{2(1+\nu)}{E} \frac{Pw}{\ell t} \frac{L}{h} + w\phi \quad (2-8)$$

The deflection of the arch element at its top point may be found from the bending energy approach. Let  $p(x)$  be the real load through the arch shear center and  $q(x)$  be a dummy load applied to the crest in the direction of the desired deflection. The bending energy  $U$  is given by:

$$U = \int_0^L \frac{M^2 d\xi}{2EI} \quad (2-9)$$

where  $\xi$  measures distance along the developed arch length  $L$ .  $I$  is the cross sectional moment of inertia  $t^3 dx/12$ ,  $t$  being the arch thickness.

The bending moment on any section is a function of  $p(x)$ ,  $q(x)$ , and  $\xi$ . Thus, equation 2-9 can be written in completely general terms as:

$$U = \frac{6}{Et^3 dx} \int_0^L [p(x), q(x), f(\xi)]^2 d\xi \quad (2-10)$$

where the substitution has been made for I.

Differentiating equation 2-10 with respect to  $q(x)$  and then allowing  $q(x)$  to go to zero yields the deflection  $\delta'(x)$ :

$$\delta'(x) = \frac{\delta v}{\delta q(x)} \Big|_{q \rightarrow 0} = \frac{6 p(x)}{Et^3 dx} \int_0^L [f(\eta)]^2 d\xi \quad (2-11)$$

where  $f(\eta)$  involves cross products of the terms in the integrand of equation 2-10. All  $f(\eta)$  terms are composed of corrugation cross sectional dimensions only and are entirely independent of corrugation length. The integral in equation 2-11 may therefore be replaced by a constant  $K$  for all diaphragms of a particular type. Making use of equation 2-5,  $\delta'(x)$  may be rewritten:

$$\delta'(x) = \frac{12(n+1) Ph}{Et^3 \ell^2} \cdot \left(\frac{2x}{\ell}\right)^n K \quad (2-12)$$

After applying equations 2-6 and 2-7 to the above, the final shear deflection for a particular series of diaphragms is:

$$\Delta' = \frac{2(1+\nu)}{E} \frac{Pw}{\ell t} \frac{L}{h} + w \left[ \frac{24n(n+1) Ph}{Et^3 \ell^3} \left(\frac{2x}{\ell}\right)^{n-1} k \right] \quad (2-13)$$

The  $(2x/\ell)^{n-1}$  term is a measure of  $\delta_w$  in Fig. 2-7. It is always evaluated at  $x = \ell/2$  and is always unity. Equation 2-13 is modified slightly to read:

$$\Delta' = \frac{Pw}{E \ell t} \left[ \frac{2(1+\nu)L}{h} + \frac{24n(n+1) h K}{(\ell t)^2} \right] \quad (2-14)$$

where  $n$  and  $K$  are the only undetermined parameters. It can be seen that the second term on the right in the above equation

approaches zero as  $\lambda$  becomes infinite and that the solution reduces to that in equation 2-3.

At this point, it becomes necessary to assign numerical values to  $n$  and  $K$  or to determine them experimentally. In previous solutions<sup>3</sup>,  $n$  has been assumed equal to 1. It is obvious that warping is more pronounced near the corrugation ends and any  $n$  greater than 1 is more realistic. This in no way limits the theory to less generality than those proposed before; it introduces more flexibility.

The constant  $K$  may be determined from the bending energy approach and corresponds to the integral in equation 2-11. It is dependent upon  $n$  and becomes increasingly more difficult to evaluate as the number of corrugations between the end fasteners increases. With no loss in generality, the entire numerator of the right expression in equation 2-14 may be replaced by a constant  $K_2$ :

$$\Delta' = \frac{Pw}{E\lambda t} \left[ \frac{2(1+\nu)}{h} L + \frac{K_2}{(\lambda t)^2} \right] \quad (2-15)$$

$K_2$  is a function of the diaphragm cross-section shape and the end fastener spacing. It is independent of diaphragm length and can be determined by testing any length diaphragm and placing the test results in equation 2-15. The shear deflection for any other diaphragm having similar cross sections and end fastener spacing can now be found from the equation.

It is convenient to rearrange equation 2-15 and define the shear stiffness  $G'$ :

$$G' = \frac{P}{\Delta'} \frac{w}{\ell} = \frac{Et}{\left[ \frac{2(1+\nu)}{h} L + \frac{K_2}{(\ell t)^2} \right]} \quad (2-16)$$

The last equation is used to extend shear stiffnesses from test results as shown in Fig. 4-24.

### 3. TEST VARIABLES AND PROCEDURE

#### 3.1 Major Test Parameters.

The primary variables in the diaphragm tests included panel configuration, frame types, panel cover width, material properties, and methods of attachment. Several different diaphragm sizes were used, the largest being 144" x 120" and the smallest being 17 3/4" x 24". The term full sized diaphragm often will be used in the discussion of tests and it refers to the 144" x 120" diaphragms. Other diaphragms are referred to as small diaphragms.

a. Panel Configuration. Cross sections of the panels with nominal dimensions are shown on Fig. 3-1. The cover widths ranged from 18" to 36" but the majority of tests were made on diaphragms having 24" panels. The various types of corrugations are indicated for the panels; the thickness was between 22 and 28 gage. The majority of the panels were 26 gage standard corrugated shapes. The panel lengths varied between 17 3/4" and 144". Material yield strengths varied between 30,000 psi and 150,000 psi.

b. Diaphragm Test Frames. Two types of frames were used for diaphragms having panel lengths of 6' or greater. The first, which is referred to as the heavy frame, was fabricated from 10 WF 21# beams and 4" - 7.25# American Standard Channels. The beams were used as marginal members and the channels as purlins. Typical frame details and centerline dimensions are shown in Fig. 3-2. The purlin spacing was variable and they

could be used to span either the long or short direction of the frame depending on the type of test. Purlin-to-frame connections were made with light clip angles as shown in Fig. 3-2. The heavy frame had marginal member centerline dimensions of 120" x 144" which allowed tests on either 10' or 12' panels with the end fasteners falling slightly inside the beam webs. The second series of tests was made on a lighter frame which was made from 6" x 1 1/2" cold formed channels. Fourteen gage material was used for the edge beams and 16 gage for the purlins. Frame details are shown in Fig. 3-3. The marginal member frame dimensions were 120" x 141" to allow for testing 12' panels with the end fasteners about 1 1/2" from the panel ends. The slight change in dimensions between the heavy frame and light frame introduces no inconsistencies since panel-to-frame connections on the heavy frame were made inside the web.

The frames were horizontal cantilevers with two point reactions. A typical light frame test is shown on Fig. 3-5 where north is to the left foreground as indicated. The southeast corner reaction was taken out of the diaphragm by a pinned connection at the centerline of the south edge beam (See Figs. 3-2 and 3-3, section a-a). The other corner reaction was taken out through a greased bearing plate on the end of the north edge beam in the heavy frame tests. For the light frame tests, the greased bearing was replaced by a doubly pinned link in order to permit loads from either the north or the south. Details of the link are shown on Fig. 3-3.

Since the marginal members were all pinned at their ends and since the purlin-to-edge beam connections were made with light clip angles, there was no appreciable resistance to horizontal movement prior to attaching the diaphragm. All interior frame connections could be considered as pinned.

Additional light frame tests were made on 6' x 6', 6' x 10', and 6' x 12' frames. These small frames were identical to the larger light gage steel frame described above except for the changes in marginal member lengths.

The fourth type of frame was made from 1 1/2" x 1/4" equal leg angles and was used for the smallest diaphragm tests. The frame was fitted into an apparatus which adapted a 400,000 lb. testing machine to shear panel testing. Two sizes of these frames were used. The first had centerline dimensions of 16 1/4" x 24" and is shown in Fig. 3-4. The second was identical in all respects except the 16 1/4" dimension was changed to 26 1/2". These sizes permitted testing of diaphragms with lengths of 17 3/4" and 28" respectively with end fasteners about 3/4" from the panel ends. All diaphragms for these frames were cut from a length of standard corrugated panel which had a cover width of 24". Typical test setups are shown in Figs. 3-6 and 3-7.

The small frames were loaded through a roller system as shown on Fig. 3-4. A pinned support was provided for upper left corner reaction and a roller was used at the lower left corner. The vertical supporting beam was cantilevered up from the base of the testing machine and a smooth guide was

used at the lower right to prevent out of plane warping.

c. Fasteners. The diaphragm connections fall into 4 general categories: screws, welds, backed up fasteners, and structural lock rivets. Fastener locations generally follow the manufacturer's recommendations except in some cases where side lap fasteners were either omitted or spaced above the recommended values.

The term intermediate fastener is used to define all fasteners along the panel edges except those at the purlins or those in the marginal members at the purlin ends. The term includes intermediate sidelap fasteners which connect adjacent panels at points between the purlins. It also includes the intermediate edge fasteners which connect the edge panels to the longitudinal frame members at points between the purlins. Fasteners which connect two adjacent panels at the purlins are referred to as purlin sidelap fasteners as distinguished from the intermediate sidelap fasteners which were defined above. These fasteners pass through both panels and into the purlins in all cases except in the box rib panels where they connected the two sheets without passing into the purlins. Other fasteners, passing through the panels and into the frame, are referred to as panel-to-frame fasteners. All fasteners along a panel-to-panel side lap may be referred to as sidelap fasteners. This definition includes both purlin and intermediate sidelap fasteners.

Caulking, pressure sensitive tapes, or other water proofing devices were not used. The fastener arrangement and purlin spacing for each test is indicated in the legend on the graphical test results in Figs. 4-1 through 4-19.

Screw connections were made with number 14 Type B self threading screws and with number 10 x 5/8" sheet metal screws. The Type B screw, which had an aluminum backed neoprene washer assembly, was used for panel to frame connections in the corrugated diaphragms as well as in the box rib tests. These screws were used in predrilled holes which were slightly less than the minimum throat diameter of the threads. The number 10 screws were used as intermediate side lap fasteners in most standard corrugated tests. These were placed in holes punched by a thin awl, the holes being just large enough to allow the screw to start into the hole.

Welded connections were used for some roof deck tests. The panel-to-frame welds were puddle welds with diameters of about 1/2". In the light frames, just enough heat was used to allow a small protuberance of molten metal to form on the under side of the flange in the frame member. Purlin side-lap welds were made by welding through both sheets and into the purlin. In the cases where intermediate side lap fasteners were used, these were also puddle welded but considerable care had to be used to prevent burn through in the panels.

The backed up fasteners were of two types but both working on the same principle. They were inserted into predrilled holes and by either pulling or twisting on the top, a spreading

device in the back was activated. The general principle is similar to that of the molly-bolt. Cross sections of the fasteners are shown in Fig. 3-11.

Special purlin connections were used in a few tests where it was desirable to eliminate purlin restraints and yet prevent overall panel out-of-plane buckling. These connections are shown in Fig. 3-8. They were made through an oversized hole in the diaphragm and used greased cover plates. The bolt was not allowed to contact the diaphragm and thus, no shear forces were transferred into the purlins.

### 3.2 Test Procedures.

a. Loading. For all diaphragms which were tested in the horizontal position such as the one shown in Fig. 3-5, the loading apparatus consisted of two 50 ton hydraulic jacks in conjunction with load cells. Loads were applied in increments of 200 lbs. or 400 lbs. in the plane of attachment between the diaphragm and the frame.

The loading may be divided into three types: static, pulsating, and reversed. The static or direct loads were applied in even increments from zero to failure at the southwest corner of the diaphragm. (North is to the left in Fig. 3-5). Pulsating loads were also applied at this corner in even increments from zero to some percentage of the expected ultimate load, then unloaded and so on until the desired number of cycles was reached. The expected ultimate load was determined by static load tests on an identical diaphragm to that being tested under dynamic load conditions.

The reversed load tests were similar to pulsating loads except that a jack was added at the northwest corner of the diaphragm. The direct load jack was loaded and then unloaded, the opposite jack loaded and then unloaded, and so on until the desired number of load cycles was reached. The reversed load intensity was also predetermined from static load tests. The time between successive applications of the incremental loads was about 45 seconds.

Small diaphragms of the type shown in Fig. 3-4 were all loaded from zero to failure in a testing machine. The loads were applied through a roller in accordance with the above definition for static loads. Reversed and pulsating loads were not used in these tests.

b. Deflections. In-plane corner movements at right angles to the edge beams were recorded from dial gage readings after each application of load. Dial gage locations are shown in Fig. 3-9. From these measurements, it was possible to correct for support movement and arrive at the true diaphragm deflection. The deflection  $\Delta$  (in inches) as shown on Figs. 3-2 and 3-9 included both bending and shear deflections.

$$\Delta = E - \left( A + \frac{a}{b} (B + G) \right) \quad (3-1)$$

where A, B, E, and G are the measured corner deflections and  $a/b$  is the ratio of the diaphragm dimension perpendicular to the loading direction to that parallel to the loading direction.

Deflections were recorded in the same manner for the small diaphragms. However, the support was provided through

a vertical cantilever as shown in Fig. 3-10 and both the roller and pinned supports could move in the same direction.

The net deflection was given by:

$$\Delta = E - \left( A + \frac{a}{b} (B - G) \right) \quad (3-2)$$

c. Material Properties. Standard tensile coupons were taken from several panels in each shipment of material. These were tested with a 2" extensometer and drum recorder to plot the load-deflection curves. The tensile properties are given in Tables 4-2 and 4-3.

## 4. TEST RESULTS

### 4.1 Introduction.

The data from all tests are presented in groups according to the type of test frame used. The figures giving the graphical data show the total shear force versus the diaphragm deflection. The data are reduced in accordance with section 3.2b of Chapter 3. The type of loading, purlin spacing, and fastener arrangement are indicated in the legend of each figure. Panel shapes are shown on Fig. 3-1.

### 4.2 Heavy Frame Tests.

All heavy frame diaphragms were loaded from zero to failure by static loads from the south jack. The results are shown in Figs. 4-1 through 4-6 and in Table 4-1. The results of tensile coupon tests are given in Table 4-2. Since the type of loading was not a variable, it is easy to describe the test behavior in terms of the weakest part of the system, the fasteners. The descriptions are divided into two sections, one for screw connected or lock riveted diaphragms and the other for welded diaphragms.

Screw connected and lock riveted diaphragms behaved similarly, characterized by the following stages.

a. Slip along the lap between adjacent panels which resulted in bearing contact at all sidelap fasteners. The slip was shortly followed by tilting of the sidelap fasteners and a slight distortion in the panel around the fasteners.

b. Local deformations in the panel at the intermediate

sidelap fasteners accompanied by a pile up of material ahead of the fasteners and tearing in the panels.

c. Accordion-like behavior across the panel ends and slight buckling at diagonally opposite corners of the individual panels.

d. Failure at panel-to-panel fasteners, tearing around fasteners at the panel ends, and buckling of diagonally opposite corners of the individual panels.

Steps a, b, and c were closely associated, occurring at about 50% of the ultimate load.

The welded diaphragms had a somewhat similar behavior to that described above. The characteristic steps follow.

a. Slight distortion around the intermediate and purlin sidelap welds resulting in local yielding of the diaphragm at the connection.

b. Slight accordion behavior at the panel ends and further yielding in the panel around the sidelap fasteners.

c. Failure at the sidelap fasteners by tearing in the panel around the welds and buckling of individual panels on diagonally opposite corners. Buckling of the corners usually occurred at 6" to 8" from the end of the panel.

Steps a and b in the welded diaphragms occurred at about 50% of the ultimate load and at deflections of about 20% of the maximum ultimate load deflection.

A special note should be made regarding the behavior of Test 7. As indicated in Fig. 4-4, this diaphragm showed comparatively large deflections at low loads. Upon close

inspection, hairline cracks were observed along the ridges and valleys of the corrugations. These apparently were due to the cold forming of this rather brittle material since some of the same type cracks were found in untested panels. The material in these panels had a yield strength of 153 ksi and an elongation of 3.5% in 2 inches. New material was ordered and Test 7 was disregarded in future comparisons. The test was replaced by 7A but a slightly different fastener arrangement was used (See Fig. 4-4).

#### 4.3 Light Frame Tests.

These tests had all the variable present in the heavy frame series plus the introduction of cyclic loading. The test results are strongly influenced by the method of loading, which makes generalizations of the type in Section 4.2 difficult. The tests are discussed individually according to the diaphragm type. The light frame test results are given in Table 4-5.

##### 26 Gage Standard Corrugated Diaphragms

These tests were made on diaphragms which were 144" long and 120" wide and had 4 spans with a nominal 3' length as shown in Fig. 4-10. Sidelap fasteners were used at 18" cc. as indicated in the legends of the results in Figs. 4-10 through 4-13. The intermediate sidelap fasteners were #10 sheet metal screws and all the panel-to-frame fasteners were #14 screws with aluminum backed neoprene washers. The average material properties for these diaphragms are given in Table 4-5. All reversed load tests are based on an expected ultimate

load  $P_u$  of 7200 lbs. from Test 5P unless otherwise specified.

Test 5P. Fig. 4-7.  $P_u = 7200$  lbs. In this statically loaded test, the first deformation around the intermediate sidelap fasteners occurred at about  $0.58 P_u$ . At  $0.94 P_u$ , slip was noted at the sidelaps in conjunction with splitting in the panels around the sidelap fasteners. The failure mode was typical of this series in that it was due to tilting of the intermediate sidelap fasteners and splitting in the sheets around the sidelap fasteners.

Test 5R. Fig. 4-8.  $P_u = 5000$  lbs. This test was identical to 5P except that it was loaded for five cycles of reversed load from zero to  $\pm 0.4 P_u = \pm 0.4 \times 7200$  lbs. =  $\pm 2900$  lbs. The 6th load application was from zero to failure. Panel slip and tearing around the intermediate sidelap fasteners was first noted at  $0.88 P_u$ . It was found that the reversing load caused an elliptic elongation of the fastener holes at the sidelaps and a consequent loosening of the #10 screw type intermediate sidelap fasteners. A 30.6% reduction in strength from that in 5P was apparently associated with load reversal at this intensity.

Test 5R-2. Fig. 4-8.  $P_u = 6300$  lbs. This diaphragm was identical to 5R and was loaded in the same way as Test 5. On the 6th application of direct load, it was loaded to failure. Considerable end warping such as that shown in Fig. 4-20 and tilting of the intermediate sidelap fasteners occurred at about  $0.82 P_u$ . Failure was by splitting of the panels around the sidelap fasteners. There was a 12.5% reduction in the

ultimate strength from that in 5P.

Test 5R-3. Fig. 4-7.  $P_u = 5000$  lbs. This reversed load test was loaded for 29 cycles from zero to  $\pm 0.3 P_u = \pm 2160$  lbs. and then to failure. Failure was due to tearing around the sidelap fasteners on the second lap from the east marginal member. There was a 30.6% reduction in strength from that in 5P due to reversal at this intensity. This reduction was the same as that in 5R due to 5 cycles at  $0.4 P_u$ .

Test 5R-4. Fig. 4-8.  $P_u = 6300$  lbs. This test was identical to 5R and 5R-2. Failure was due to splitting in the panels around the sidelap fasteners. There was a 12.5% strength reduction from that in 5P due to reversal at  $0.4 P_u$ . This test was made to check the discrepancy between the ultimate loads in 5R and 5R-2.

Test 5R-5. Fig. 4-7.  $P_u = 6800$  lbs. This test was identical to 5R-3 being loaded for 29 cycles from zero to  $\pm 0.3 P_u = \pm 2160$  lbs. and a 30th load to failure. Failure was by splitting around the sidelap fasteners. There was a 5.5% reduction in strength from the static load ultimate strength in Test 5P.

Test 5R-6. Fig. 4-7.  $P_u = 7250$  lbs. This test was identical to Tests 5R-3 and 5R-5. End distortions and first intermediate sidelap fastener tilting was noted at  $0.66 P_u$  and failure was due to splitting around the sidelap fasteners. There was no ultimate strength reduction from that in Test 5P.

The following two tests were identical in fastener arrangements to the other tests with a 5P prefix except that a

5/16" diameter screw type fastener with a spreading back was substituted for the #10 sheet metal screws at the intermediate sidelaps. This type of fastener is shown in Fig. 3-11.

Test 5P-A. Fig. 4-9.  $P_u = 7350$  lbs. In this statically loaded test, no failures were noted around the intermediate sidelap fasteners. Failure was due to local buckling at the compression corners of the individual panels. There was a 2% strength increase over that in 5P which was apparently associated with the use of the backed up type intermediate sidelap fastener instead of the #10 sheet metal screws.

Test 5PA-R. Fig. 4-9.  $P_u = 7170$  lbs. The fastener details were the same as in Test 5P-A but the diaphragm was loaded for 29 reversals of  $\pm 0.4 P_u = \pm 0.4 \times 7350 = \pm 2950$  lbs. where the expected ultimate load  $P_u$  was taken from 5P-A. The 30th load application was from zero to failure. Failure occurred by local buckling of the individual panels at their compression corners. There was only a 2.5% reduction in strength from that in 5P-A as compared to an average reduction of 11.8% for tests having 5 cycles of load at  $0.4 P_u$  and which had #10 sheet metal screws for intermediate sidelap connections.

Test 5Z. Fig. 4-10.  $P_u = 6750$  lbs. The fastener details were the same as those in Test 5R. This pulsating load test was made with 4 direct loads from the south jack which were from zero to 2900 lbs. and a final direct load from zero to failure. The load-deflection curves for the first five load applications up to 2900 lbs. were practically identical. The

comparison between the static load test 5P and this test can be made on the figure where the 5Z curve is plotted for the first direct load to 2900 lbs. and then for the fifth load from 2900 lbs. to failure. The first indication of failure was a slight deformation around the intermediate sidelap fasteners at  $0.74 P_u$ . End warping was first observed at  $0.83 P_u$ . The final failure was by tearing around the panel-to-panel fasteners.

#### Standard Corrugated Diaphragms of Various Thicknesses.

The following five statically loaded tests were made to investigate the effect of varying the panel thickness. Three different nominal thicknesses, 0.0299", 0.0179", and 0.0149" were used. The test panels were 12' long and had a cover width of 24". The nominal span across the purlins was 3' and no intermediate sidelap fasteners were used. Fastener details are given in Fig. 4-10 and the graphical comparisons of the test data are on Fig. 4-11. The average material properties and measured thicknesses are shown in Table 4-3.

Test 4P. Fig. 4-14.  $P_u = 4170$  lbs. 26 gage standard corrugated material with a measured thickness of 0.0188" was used and the diaphragm had no intermediate fasteners. No buckling of the panels was noted. Failure was by seam slip and splitting in the panel around the purlin sidelap fasteners. This test was identical to 5P except for the omission of intermediate fasteners. There was a 35% reduction in strength from that in 5P due to the omission of the inter-

mediate fasteners.

Test 4AP-2. Fig. 4-11.  $P_u = 5800$  lbs. This diaphragm was identical to 4P except that it was made from 22 gage material. Failure was by seam slip and tearing around the purlin sidelap fasteners at the purlins. The 23% increase in strength over that in 4P was apparently due to the use of 0.0310" thick panels over 0.0188" even though the thicker material had roughly a 40% lower yield point than the thinner material in Test 4P.

Test 4AP-3. Fig. 4-11.  $P_u = 6470$  lbs. This 22 gage diaphragm is identical to 4AP-2. Failure was due to seam slip in conjunction with tearing around the purlin sidelap fasteners at the purlins. There was a 37% strength increase over that in Test 4P.

Test 6AP. Fig. 4-11.  $P_u = 3700$  lbs. In this 28 gage diaphragm, failure was due to local buckling at the compression corners of the individual panels. There was an approximate 21% decrease in ultimate strength from that in 4P which is apparently due to the use of 28 gage material ( $t = 0.0162$ ").

Test 6AP-2. Fig. 4-11.  $P_u = 4100$  lbs. This was a duplicate of 6AP. Failure was due to tearing around the fasteners at the west marginal member and by local buckling of the diaphragm near the south-west corner. There was a 17% reduction in strength from the similar 26 gage test 4P.

#### Reversed Load Tests on Diaphragms Without Intermediate Fasteners

These tests were made on 26 gage standard corrugated diaphragms which were 144" long and 120" wide and having 4

spans of 3' nominal length as shown in Fig. 4-10. No intermediate fasteners were used. The expected ultimate load for the reversed load tests was taken from Test 4P in which  $P_u = 4710$  lbs. Material properties for these diaphragms are given in Table 4-3.

Test 4-R. Fig. 4-12.  $P_u = 4300$  lbs. The diaphragm was loaded for 5 cycles from zero to  $\pm 0.4 P_u = \pm 1880$  lbs. and the 6th load from zero to failure. Failure was by panel slip and tearing around the purlin sidelap fasteners on the second lap from the west marginal member. There was an approximate 8.5% ultimate strength reduction from that in 4P, due to load reversal.

Test 4R-2. Fig. 4-12.  $P_u = 4400$  lbs. This test was identical to 4-R except it was loaded for 29 cycles from 0 to  $\pm 0.3 P_u = \pm 1410$  lbs. and the 30th load application was from zero to failure. The failure mode was the same as in Test 4R. The strength reduction from that in 4P was only 6.5%.

Test 4L. Fig. 4-13.  $P_u = 2550$  lbs. This static load test had the special purlin connections shown in Fig. 3-8. No noticeable deformation of the diaphragm occurred prior to  $0.47 P_u$ . At this load a slight vertical separation was noted at laps between the purlins. At  $0.63 P_u$ , slight deformation was noted around the panel to panel screws. At  $0.86 P_u$ , pronounced tearing was observed around the purlin sidelap connections, mostly in the lower sheet of the lap. Final failure was by tearing of the panels around the panel-to-panel screws and some tearing around the screws in the end

marginal members.

Test 5L. Fig. 4-13.  $P_u = 4750$  lbs. This static load test had special purlin connections with intermediate fasteners at 18" o.c. The diaphragm showed no overall distortions until  $0.88 P_u$  at which time slight vertical separation was noticed between adjacent panels in regions between the purlins. At  $0.93 P_u$ , deformation was noted around the side lap fasteners. Failure occurred by tearing around the side lap fasteners and was restricted mostly to the lap between the first and second sheets from the east marginal member.

#### High Tensile Deep Corrugated Diaphragms

The next five tests were made using 26 gage high tensile deep corrugated diaphragms with two 5' spans and fastener details as shown in Fig. 4-27. The diaphragms had corrugations of 3" x 3/4". The material properties are given in Table 4-3.

Test 7P. Fig. 4-14.  $P_u = 3930$  lbs. In this statically loaded test, no intermediate fasteners were used. Failure was by buckling which caused vertical separation at the side-laps. This strut-like buckling along the panel edges was due to the absence of the intermediate fasteners over the 5' span. The diaphragm was very flexible near the ultimate load, allowing large deflections with very little increase in load resistance.

Test 7R. Fig. 4-14.  $P_u = 3300$  lbs. This test was identical to 7P except that it was loaded for 5 cycles from zero to  $\pm 0.4 P_u = \pm 0.4 \times 3930 = \pm 1570$  lbs. and a 6th load application from zero to failure. The expected ultimate load was

taken from Test 7P. The failure mode was different from that in 7P in that it occurred by splitting around the fasteners on the second lap from the south. There was a 16% strength reduction from that in Test 7P which was apparently due to load reversal effects.

Test 7R-2. Fig. 4-14.  $P_u = 3470$  lbs. This test was identical to 7P except that it was loaded for 25 cycles from zero to  $\pm 0.3 P_u = \pm 1180$  lbs. and the 26th load application was from zero to failure. There was an 11.7% reduction in strength from that in 7P.

Test 8P. Fig. 4-14.  $P_u = 6300$  lbs. This static load test was the same as Test 7P except that #10 sheet metal screws were added for intermediate sidelap fasteners. The intermediate fasteners were used at 30" c.c. as shown in Fig. 4-27. Failure was due to splitting in the panels around the sidelap fasteners. There was a 61% increase in the ultimate strength over that in 7P which was due to the addition of the intermediate fasteners.

Test 8R. Fig. 4-14.  $P_u = 5500$  lbs. This test was the same as 8P except that it was loaded for 5 cycles from zero to  $\pm 0.4 P_u = \pm 2500$  lbs. and on the 6th application from zero to failure. The failure mode was the same as in 8P. There was a 13% reduction in the ultimate strength due to reversal at  $0.4 P_u$ .

#### 26 Gage Box Ribbed Panels

The following four tests were made to study the joint influences of material tensile strength and reversed loading

on the ultimate load capacity of light gage steel diaphragms. Tests 20 and 20R were made with panels having an average yield strength at 0.2% offset of 54.5 ksi and an ultimate strength of 60.7 ksi while Tests 22 and 22R on full hard material had 101.4 ksi and 102.5 ksi respectively. The panel cover width of the panels was 36" and the 120" x 144" diaphragms had two 5' spans. Number 14 sheet metal screws were used for all connections as shown in Fig. 4-28. The sidelap fasteners did not pass into the purlins.

Test 20. Fig. 4-15.  $P_u = 3370$  lbs. In this statically loaded test, failure was due to overall panel buckling causing separation between adjacent panels in a direction normal to the diaphragm surface. Small localized buckling was also noted at the compression corners of each panel.

Test 20-R. Fig. 4-15.  $P_u = 3350$  lbs. This test was the same as 20 except that it was loaded for 5 cycles from zero to  $\pm 0.4 P_u = 1380$  lbs. and the 6th load was applied from zero to failure. Failure was by local buckling at panel corners in association with splitting along panel sidelap fasteners on the first lap from the north side. There was no appreciable reduction in strength from that in Test 20 due to load reversal.

Test 22. Fig. 4-15.  $P_u = 4400$  lbs. This static load test was identical to Test 20 except that full hard material was used. Failure was by the strut-like buckling along panel edges as described for Test 20. Violent snap through buckling was noted for the first time in this test. There was a 30%

strength increase over that in 20 due to the use of full hard material.

Test 22R. Fig. 4-15.  $P_u = 4000$  lbs. This test was identical to 22 except that it was loaded for 5 cycles from zero to  $\pm 0.4 P_u = \pm 1760$  lbs. and a final load from zero to failure. Failure was by local corner buckling on the individual panels. There was a 9% ultimate strength reduction from that in Test 22 due to load reversal.

#### 22 Gage Wide Rib Roof Deck

The following four tests were made to investigate the behavior of diaphragms having welded connections. The behavior of the welded intermediate fasteners was of particular interest in these tests. The diaphragms were 144" x 120" and had two spans of 6' each as shown in Fig. 4-29. The material properties are given in Table 4-3.

Test 24. Fig. 4-16.  $P_u = 3510$  lbs. No intermediate fasteners were used and the diaphragm was statically loaded in increments from zero to failure. At about  $0.51 P_u$ , yield zones were noted in the panels around the welds at the compression corners of the panels. Failure was by local corner buckling of the panels. No weld failures occurred.

Test 24R. Fig. 4-16.  $P_u = 3340$  lbs. This test was identical to 24 except that it was loaded for 5 cycles from zero to  $\pm 0.4 P_u = \pm 0.4 \times 3510 = \pm 1400$  lbs. and a 6th load application from zero to failure. Failure was initiated by a weld failure at a panel to frame connection and resulted in local panel buckling at the ultimate load. There was a strength reduction

of only 5% from the ultimate strength in Test 24 due to load reversal.

Test 26. Fig. 4-16.  $P_u = 4400$  lbs. This static load test was the same as Test 24 except that intermediate sidelap fasteners were added at 36" c.c. as shown in Fig. 4-29. The first weld failure occurred at  $0.8 P_u$  and final failure was by complete separation of all welds along the second panel side lap from the west. There was a strength increase over that in Test 24 of 25% due to the addition of intermediate fasteners.

Test 26R. Fig. 4-16.  $P_u = 4350$  lbs. This test was the same as 26 except that it was loaded for 5 cycles from zero to  $\pm 0.4 P_u = \pm 1760$  lbs. and a 6th load application from zero to failure. The first weld failure was in a panel to frame weld occurring at  $0.4 P_u$ . Final failure was sudden occurring by complete separation along the panel to panel connections in the second lap from the east. This was associated with a sudden drop in the load from 4350 lbs. to 3000 lbs. There was negligible ultimate strength reduction from that in Test 26 due to load reversal.

#### Standard Corrugated Diaphragms Without Intermediate Edge Fasteners

The following four tests were made on 26 gage standard corrugated diaphragms having intermediate sidelap fasteners but no intermediate edge fasteners. The diaphragms were 144" x 120" and had four spans of 3' nominal length. The first two tests had #10 sheet metal screws at the intermediate sidelaps

and the last two had 5/16" backed up fasteners. Fastener details and purlin spacings are shown in Fig. 4-25.

Test 28. Fig. 4-17.  $P_u = 4800$  lbs. This was a statically loaded diaphragm in which the intermediate sidelap fasteners were #10 sheet metal screws. Failure was by tearing around the fasteners in the marginal member on the east side. There was no apparent damage to the connections at the panel sidelaps.

Test 28R. Fig. 4-17.  $P_u = 4800$  lbs. This diaphragm test was identical to 28 except that it was loaded for 5 cycles from zero to  $\pm 0.4 P_u = \pm 1900$  lbs. and a final direct load from zero to failure. The expected ultimate load was taken from Test 28. Failure was identical to that in Test 28 occurring at the east marginal member with no apparent damage to the sidelap connections.

Test 30. Fig. 4-17.  $P_u = 5400$  lbs. This diaphragm had backed up type intermediate sidelap fasteners and was statically loaded to failure. Seam slip between panels and slight tilting of the intermediate sidelap fasteners was noted at  $0.93 P_u$ . Failure was by tearing around the edge fasteners on the west marginal member.

Test 30R. Fig. 4-17.  $P_u = 5300$  lbs. This diaphragm was identical to that in Test 30. It was loaded for 5 cycles from zero to  $\pm 0.4 P_u = \pm 2150$  lbs. The 6th and final direct load was applied directly from zero to failure. Failure was started by a local buckle at the southwest corner and the final failure resulted from tearing around the fasteners in

the west marginal member. At  $0.93 P_u$ , slip was observed along the panel side laps in conjunction with slight tilting of the intermediate sidelap fasteners. There was only a 2% strength reduction due to reversal at this intensity.

#### Standard Corrugated Diaphragms Without Sidelap Connections.

The results of a 12' long x 6' wide 26 gage standard corrugated diaphragm test are shown in Fig. 4-18. The panel-to-frame connections were made only across the panel ends as shown on the figure. Purlins were used at 3' centers but no panel-to-purlin connections were made.

Failure was due to overall buckling of the individual panels. At a relatively low average shear of 50 lbs/ft., the panel edges separated in a direction normal to the original midplane. From that point on, virtually all loads were resisted by diagonal tension action in the separate panels.

#### 26 Gage Box Rib Diaphragms.

The following five tests were made on box rib diaphragms which were made from panels having a cover width of 36". The diaphragms had two spans of 5' as indicated in Fig. 4-19. The material properties are given in Table 4-2.

Test 11P. Fig. 4-19.  $P_u = 2980$  lbs. In this static load test, there was no appreciable diaphragm distortion until  $0.87 P_u$  at which time the intermediate sidelap fasteners began to tilt and split the panels. At the same load, slight buckling on diagonally opposite corners of the individual panels occurred. The slip between the first and second panels

from the south was large enough to cause severe tilting of the panel-to-purlin fasteners which resulted in yielding around the fastener holes in the purlins.

Test 12P. Fig. 4-19.  $P_u = 5400$  lbs. This test was identical to 11P except intermediate sidelap fasteners were added at 20" c.c. At  $0.74 P_u$  approximately  $1/4$ " of seam slip was noted between panels in the midsection of the diaphragm. Final failure occurred by tearing around the panel-to-panel fasteners.

Test 11L. Fig. 4-19.  $P_u = 2940$  lbs. This diaphragm was statically loaded and had special purlin fasteners as shown in Fig. 3-8. No appreciable tearing was noted at the panel-to-panel fasteners in this test. Failure was by separation of the panels between the purlins and yielding around the fastener holes in the frame at the end marginal beams.

Test 12L. Fig. 4-19.  $P_u = 4800$  lbs. This test had the same type of connections as in 11L except that intermediate fasteners were added at 20" c.c. The test was statically loaded and slip was first observed between adjacent panels at  $0.50 P_u$ . Failure occurred by tearing in the panels around the sidelap fasteners. Bearing failures were observed in the panels around the end fasteners near the panel edges.

Test 12R. Fig. 4-19.  $P_u = 5400$  lbs. This test was identical to 12P except that it was loaded for five cycles from zero to  $\pm 2160$  lbs. ( $0.4 P_u$  from Test 12P) and a final direct load was applied from zero to failure. The diaphragm showed no failure tendencies below the maximum cyclic load intensity of

2160 lbs. Failure was by tearing around the panel-to-panel fasteners on the first lap from the south. As can be seen in Fig. 4-19, there was very little difference in the behaviors of Tests 12R and 12P.

#### 4.4 Small Diaphragm Tests.

Corrugated 26 gage diaphragms, varying in size from 17 3/4" x 24" to 72" x 120", were tested to study the variation in shear stiffness with the diaphragm size. The smaller 17 3/4" and 28" long diaphragms were tested in setups shown in Figs. 3-6 and 3-7. The larger sizes were tested on a frame having 6" cold formed channels as marginal members. A typical test is shown in Fig. 4-20.

The 72" x 120" and the 72" x 144" diaphragms had purlin spacing and fastener details as shown in Figs. 4-30 and 4-31. These diaphragms all failed in the same general manner by slip along the panel sidelaps, tilting of the intermediate sidelap fasteners, and tearing in the panel at the sidelap fasteners. In most cases, slight local buckling was noted at the compression corners of the panels. The failure modes were generally the same as in the large diaphragm tests with the same panel type.

The small diaphragms of 17 3/4" x 24" invariably failed due to excessive end deformation, local buckling, and tearing around the end fasteners near the tension corners of the diaphragms. The local buckling and end warping for a typical test is visible in Fig. 3-6.

The 28" x 24" diaphragms exhibited two types of failure.

In cases where the end fasteners were in every third valley (end pitch = 8"), failure was due to strut like buckling of the corrugations running between the end fasteners. These buckles are shown in the lower two pictures in Fig. 4-21. In other cases, where the end fasteners were in every first or every second valley, failure occurred by excessive end deformation, local buckling, and tearing around the end fasteners near the tension corners of the diaphragm. A typical test setup for a 28" x 24" diaphragm having end fasteners in every second valley, is shown in Fig. 3-7.

In some of the 17 3/4" and 28" long diaphragms, a single intermediate edge fastener was added on each longitudinal edge. No appreciable increase in the shear stiffness value was noted due to this addition although the ultimate strength was increased.

The test designation for the 17 3/4" and 28" long diaphragms is as follows. The first digit indicates that the end fasteners are in every nth valley, the second digit gives the series size where B denotes a 17 3/4 x 24" diaphragm and C denotes a 28" x 24" diaphragm, and the third digit gives the number of intermediate edge fasteners. The fourth digit is the test number.

The shear stiffness  $G'$  and the ultimate shear strength values for the small diaphragm tests are given in Table 4-4. The  $G'$  values are based on the relatively straight portion of the load-deflection curve below  $0.4 P_u$  in accordance with the formula:

$$G' = \frac{P}{\Delta} \cdot \frac{a}{b} \quad (4-1)$$

where  $P/\Delta'$  is the slope of the load-deflection curve and  $a/b$  is the ratio of the frame dimensions shown in Fig. 3-10.

The above equation is a modified form of equation 2-16 and always applies to the test results due to the way  $\Delta$  is measured. The influence of panel length is included in the measured value for  $\Delta$  which depends on whether the panels span in the  $a$  or in the  $b$  directions.

#### 4.5 Discussion and Conclusions.

##### a. Influence of Fasteners on Diaphragm Behavior.

The fasteners used in these tests include number 10 sheet metal screws, number 14 panel-to-frame screws, backed up screw type fasteners as shown in Fig. 3-11, and welded connections. The relative quality of these fasteners cannot be compared directly in all cases since they were used on various types of diaphragms. However, their performance can be discussed qualitatively. Test results pertaining to this discussion are given in Table 4-5.

I. Standard corrugated diaphragms without intermediate fasteners. This type of diaphragm which was attached to the frame with #14 screws as shown in Fig. 4-26, had a static ultimate strength of 4710 lbs. Under cyclic loading from zero to  $\pm 0.4 P_u$  for five cycles and then loaded to failure, there was an 8.5% reduction in ultimate strength. An identical diaphragm, loaded for 29 cycles from zero to  $\pm 0.3 P_u$  and then to failure, showed only a 6.5% reduction in strength.

This implies that only a small amount of damage is done to the diaphragm during the process of cyclic loading.

II. Standard corrugated diaphragms with intermediate fasteners. A comparison of Tests 4B and 5 in Table 4-1 where Test 5 had intermediate sidelap fasteners and 4B did not, shows that #10 screw type intermediate sidelap fasteners contribute strongly to the ultimate static strength. Their dependability under load reversal conditions is more questionable. The results from standard corrugated diaphragm tests having this type of intermediate sidelap fasteners and subjected to both static and reversed load loading, are shown in Figs. 4-7 and 4.8. The amount of damage sustained, due to load reversal at a particular intensity, may be taken as the deviation in behavior from that in Test 5P for each case. On this basis, the average ultimate strength reduction in diaphragms which were loaded for 5 cycles to  $\pm 0.4 P_u$  and then to failure was about 18.5% as can be seen in Table 4-5. Identical diaphragms, loaded for 29 cycles from zero to  $\pm 0.3 P_u$  and then to failure, showed an average strength reduction of about 11.8%. These comparisons show that the reduction in strength due to load reversal is more dependent on the intensity of load than on the number of cycles.

A further comparison can be made between the case where intermediate fasteners were used (Test 5P) and the case where they were not. The increase in static strength of 5P over that of 4P was about 53%, implying that this strong increase was due only to the addition of intermediate fasteners. By

comparing the reversed load tests with a 5 prefix and having intermediate fasteners (Table 4-5) to the comparably loaded tests with a 4 prefix and no intermediate fasteners, one finds that the former type averages about 35% stronger than the latter after 5 applications of cyclic loads to  $0.4 P_u$ . Similarly, when these diaphragms were loaded for 29 cycles from zero to  $\pm 0.3 P_u$ , the diaphragms having intermediate fasteners averaged about 44% stronger than those without intermediate fasteners. In the most extreme case where the diaphragms having intermediate fasteners and subjected to 5 cycles of reversed load at  $\pm 0.4 P_u$  are compared to the statically loaded Test 4P without intermediate sidelap fasteners, an increase in strength of 25% results.

The above leads to the conclusion that #10 sheet metal screws at the intermediate sidelap and #14 screw type intermediate edge fasteners will increase the static strength of corrugated diaphragms by about 50% or roughly 200 plf of diaphragm. These fasteners are also dependable under load reversal conditions and will increase the ultimate diaphragm strength over similarly loaded diaphragms without intermediate fasteners by about 130 plf of diaphragm under load reversal conditions at  $0.4 P_u$  for 5 cycles. Similar comparisons show that with cyclic loads up to  $0.3 P_u$  for 29 cycles, these fasteners will increase the strength by about 160 plf of diaphragm.

III. High strength deep corrugated diaphragms. Comparisons may be made between tests with an 8 prefix and those with a

7 prefix in Fig. 4-14. The former had intermediate fasteners at 36" c.c. while the latter did not have intermediate fasteners. The intermediate sidelap fasteners in 8P and 8R were #10 sheet metal screws and all other fasteners including the intermediate edge fasteners were #14 screws. The static strength of Test 8P was about 60% stronger than that of 7P which implies that this increase was due only to the addition of intermediate fasteners. The reversed load test 8R, which was loaded for 5 cycles to  $0.4 P_u$  and then to failure, was about 65% stronger than the similarly loaded test 7P without intermediate fasteners. These values are approximately in line with those in part II above and lead to the conclusion that #10 sheet metal screws for the intermediate sidelap fasteners, when used with intermediate edge fasteners, will increase the static strength in high strength deep corrugated diaphragms by about 60% or roughly 195 plf of diaphragm.

Comparing the statically loaded Test 7P to 7R-2 which was loaded for 25 cycles to  $0.3 P_u$  and then to failure, shows that an 11.7% strength reduction occurred due to reversal at this intensity (Table 4-5). Test 7R, which was loaded for 5 cycles to  $0.4 P_u$ , was 16% weaker than the statically loaded and identical diaphragm 7P. It may be concluded that diaphragms without intermediate fasteners which are loaded for 5 cycles from zero to  $\pm 0.4 P_u$  will be about 50 plf of diaphragm weaker than statically loaded identical diaphragms. After 25 cycles of reversed load, the same diaphragm would be only about 40 plf weaker. In diaphragms having intermediate fasteners,

strength reduction of about 65 plf of diaphragm from the static strength would result due to 5 cycles of reversed loading at  $0.4 P_u$ .

IV. Standard corrugated diaphragms with backed up type intermediate sidelap fastener. These diaphragms were identical to Test 5P in all respects except that they had 5/16" diameter backed up type intermediate sidelap fasteners as shown in Fig. 3-11. Since the failures in the standard corrugated diaphragms having #10 screws at the intermediate sidelaps were almost invariably associated with the tilting of and the tearing around these fasteners, two tests were run having special backed up fasteners. It was found that the mode of failure was completely changed, due to the use of backed up fasteners, from that in 5P where it occurred by tilting of the intermediate sidelap fasteners and tearing around the sidelap fasteners, to one of corner buckling in the individual panels. Fig. 4-9 shows the results of these tests; they are also in Table 4-5. The use of the special fastener increased the static diaphragm strength, over the 5P diaphragm having #10 intermediate sidelap fasteners, by only 2% but allowed only a decrease in strength of only 2.5% after 29 cycles of load to the rather severe level of  $0.4 P_u$ . This implies that if a fastener is used in which no tilting and loosening occurs, negligible damage will be incurred even at the intense cyclic load of  $\pm 0.4 P_u$  for large numbers of load cycles.

V. Welded fasteners. The results from tests on welded roof decks with and without intermediate sidelap fasteners and

under different types of loading are shown in Fig. 4-16. In the diaphragms having intermediate sidelap fasteners (Tests 26 and 26R), there was only a 1% reduction in the ultimate strength from the static strength due to 5 cycles of reversed loading at  $0.4 P_u$  as can be seen on the second page of Table 4-5. The strength reduction in roof deck diaphragms without intermediate fasteners (24 and 24R) under the same loading conditions was 4.8%, being a rather insignificant 14 plf of diaphragm. Since welded fasteners tend to remain tight or fail completely, these tests support the conclusions in part IV.

VI. Diaphragms without intermediate fasteners. In diaphragms without intermediate fasteners, all fasteners passed through the panels and into the frame with the exception of the ribbed panel diaphragms shown in Fig. 4-15. Since the panel to frame fasteners were well anchored in the frame, they acted somewhat as backed up fasteners and were very resistant to tilting. Consequently, they remained tight and would be expected to behave in accordance with the conclusion in part IV.

Comparison of the standard corrugated test 4P which was statically loaded and test 4R which was loaded for 5 cycles to  $0.4 P_u$ , shows only an 8.5% or roughly 34 plf of diaphragm reduction in strength (see Table 4-5). Test 4R-2, which was loaded for 29 cycles at  $0.3 P_u$ , showed a 6.5% or 26 plf reduction from the static strength of 4P due to reversal at this intensity.

The high strength deep corrugated diaphragms show an

ultimate strength reduction of 11.5% or 50 plf due to reversal at  $0.4 P_u$  for 5 cycles when tests 7P and 7R are compared (see Fig. 4-14). When test 7R-2 which was loaded to  $0.3 P_u$  for 25 cycles is compared to the statically loaded test 7P, a strength reduction of 12% or 38 plf results due to reversal at this intensity.

It may be concluded that diaphragms without intermediate sidelap fasteners and having screw type fasteners in other positions will sustain only small amounts of damage during load reversal of 5 cycles up to  $0.4 P_u$  and that the reduction from static strength will not usually be greater than about 50 plf of diaphragm.

In cases where the sidelap fasteners at the purlins were not anchored into the purlins such as in Tests 20, 20R, 22, and 22R on ribbed panel tests (Fig. 4-15), slightly more reduction in the static strength due to reversal at a particular intensity might be expected since the sidelap fasteners are subjected to tilting. However, the maximum strength reduction from that in the static tests cited was 9% or about 33 plf. This allows these diaphragms to fall into the same general category as above, i.e., sustaining little damage during load reversal at  $0.4 P_u$ .

VII. Diaphragms having intermediate sidelap fasteners but no intermediate edge fasteners. The results from these standard corrugated tests are shown in Fig. 4-17. Test 28, having intermediate sidelap fasteners of #10 sheet metal screws, was identical to 5P except in the omission of the intermediate

edge fasteners (see Fig. 4-25). It was 33% or about 200 plf of diaphragm weaker than 5P and only 2% or about 8 plf stronger than Test 4P which has no intermediate fasteners at all.

In Test 30, which had intermediate sidelap fasteners of the backed up screw type, the ultimate strength was somewhat increased over that in test 28 but was still about 27% or roughly 154 plf weaker than Test 5P-A which had the same type of intermediate sidelap fasteners but also having intermediate fasteners along the edges.

Under reversed loading conditions of 5 cycles at  $0.4 P_u$ , the diaphragms showed negligible reduction in strength from that in static tests. Thus, diaphragms having intermediate sidelap fasteners but no intermediate edge fasteners will sustain loads that are only slightly greater than diaphragms with no intermediate fasteners at all.

VIII. General. Suggestions have been made in the past that, since little damage seems to occur in diaphragms without intermediate fasteners when loaded for 5 cycles to  $\pm 0.4 P_u$ , these fasteners should be omitted in a manufacturer's test for strength even though they would be used in the structure. There are two objections to this suggestion. First, the shear strength and the stiffness values of the diaphragm would be completely changed, and second, the failure mode would be different. The first point is vividly illustrated by comparing tests with an 8 prefix to those with a 7 in Fig. 4-14. It is seen that the diaphragms having intermediate fasteners deflect much less for a given load than those with-

out the intermediate fasteners.

The fact that the failure mode will be changed due to the addition of intermediate fasteners is supported by tests whose results are shown in Figs. 4-14 and 4-15. Tests 7P and 20, having no intermediate fasteners, failed by strut like buckling along the panel edges. Test 8P, which had the intermediate fasteners was 60% stronger than 7P and the failure mode was changed from buckling to tearing around the sidelap fasteners.

On the basis of all the above conclusions, it can be stated in general that diaphragms having screw type intermediate fasteners will give dependable load resistance up to 30 cycles from zero to  $\pm 0.3 P_u$ . Diaphragms without intermediate fasteners will sustain loads up to 30 cycles from zero to  $\pm 0.4 P_u$  without appreciable damage. In each of the cases, the expected ultimate load  $P_u$  is taken from an identical and statically loaded diaphragm. The  $0.3 P_u$  value for the first case was greater than the  $0.4 P_u$  value for all diaphragms tested due to the static strength increase when intermediate sidelap fasteners were added.

b. Influence of Material Strength and Thickness.

Tests were made on diaphragms of various thicknesses and the results are given in Fig. 4-11. Fig. 4-22 shows the variation in shear load vs. the diaphragm thickness for specific deflections. The 28 gage ( $t=0.0162$ ") material had a tensile yield strength at 0.2% offset of 50.1 ksi while the 26 gage ( $t=0.0188$ ") had 58.7 ksi yield strength. The 22 gage

material had an actual thickness of 0.0310" and a yield strength at 0.2% offset of 33.4 ksi.

As shown on Fig. 4-22, the diaphragm shear capacity at a particular deflection varies almost linearly with the diaphragm thickness. The 22 gage diaphragms had an average ultimate shear strength that was 30% higher than the 26 gage diaphragm and the 26 gage diaphragm was 20% stronger than the 28 gage diaphragm. Thus, diaphragm strength and stiffness vary nearly linearly with the thickness being greater when the thickness is greater.

Four tests were made in an attempt to evaluate the effects of material strength on diaphragm behavior under load reversal conditions. The results are shown in Fig. 4-15. By using full hard material with a yield strength of 101.4 ksi as compared to a mild steel with a yield point of 54.5 ksi, an increase in ultimate diaphragm static strength of 31% resulted. Test 20R, on a mild steel diaphragm, showed no reduction in strength due to load reversal at  $\pm 0.4 P_u$  for 5 cycles whereas the full hard diaphragm (22R) showed a reduction of 9%. One may conclude that about the same behavior will result in full hard and mild steel diaphragms. Of course the cyclic load intensity will be greater in the former than the latter since the ultimate static strengths are different.

#### c. Shear Rigidity.

Warping occurs across the ends of corrugated diaphragms when they are shear loaded and the end fasteners are at discrete points. This type of warping is visible in Fig. 4-20. The

extension of the warped region into the diaphragm appears to be a function of the panel configuration and the end fastener spacing; it is independent of length along the corrugations. Thus, as the length is increased there is a relatively larger unwarped and rigid shear resisting area in the diaphragm. If the length is allowed to become large, it can be seen that the warped end portions of the diaphragms are less and less influential, accounting for variation in shear stiffness with corrugation length.

The shear stiffness  $G'$  which is defined by equation 2-16 can be determined from the slope of the load deflection curve from the test according to equation 4-1. Representative values of  $G'$  for various diaphragm types are shown in Table 4-7. Comparisons for light frame and heavy frame tests can be made by reading horizontally in the table.

The variation in  $G'$  with length is clearly shown in Fig. 4-24 for 26 gage standard corrugated diaphragms with a nominal thickness of 0.0179" and having end fasteners in every third valley (end pitch = 8"). There is an optimum point beyond which  $G'$  cannot increase and this upper limit is obviously controlled by the shear modulus of the material itself. Using equation 2-16 and letting the length become infinite,  $G'$  reduces to the following:

$$G'_{\max} = \frac{E_t}{2(1 + \nu)} \frac{L}{h} = 217,000 \text{ lb/in.} \quad (\text{a})$$

where  $\nu$  is 0.3,  $E$  is  $30 \times 10^6$  psi, and  $t$  is 0.0179". The unfolded corrugation width to pitch ratio is  $L/h = 2.813/2.667$ .

In plotting the theoretical values for  $G'$  of Fig. 4-24, equation 2-16 was used. The  $K_2$  value was determined from the known  $G'$  value for the 6' x 6' test shown on the figure by putting the known  $G'$  into the equation and solving for  $K_2$ . This resulted in a  $K_2 = 51.3$ . This value was put back into the equation and by allowing the length to vary, the smooth curve for  $G'$  v.s. length resulted. The theoretical values fit the experimental points quite well and the curve approaches the upper limit in the proper fashion. The theory thus extends the test data from one diaphragm test to cover all lengths of diaphragms which have the same panel types and fastener arrangements.

The shear stiffness is somewhat sensitive to the diaphragm width as can be seen by examination of the points for the 6' x 10', the 6' x 12' and the 6' x 6' diaphragms in Fig. 4-24. The second dimension in each case is the width perpendicular to the corrugations and is the only variable in the three tests. Width has a secondary influence on  $G'$  when compared to the diaphragm length. The variation in shear stiffness with length for box rib diaphragms is shown in Fig. 4-23. The 26 gage 36" wide diaphragm panels were identical to those used in Test 20 (see Fig. 4-28) and #14 panel-to-frame screws were used in each valley. The 6' x 6' diaphragm was tested on the small channel frame and had no intermediate purlins but it did have intermediate fasteners at 36" c.c. The smaller diaphragm was tested on a frame of the type shown in Fig. 3-4. From the two tests, the average  $K_2$  in equation 2-16 was

found to be 22.2. The smooth curve for  $G'$  resulted when  $K_2$  was put into equation 2-16 and the length allowed to vary.

The above leads to the conclusion that a moderate size diaphragm test say 6' x 6' can be used to predict the shear stiffness for all other diaphragms of that configuration when length is the only variable.

d. Influence of Frame Flexibility.

The influence of marginal member flexibility can be found for two extreme cases by comparing heavy frame and light frame tests. Tests 4B, 5, 11, and 12 are from the heavy frame group while 4L, 5L, 11P, and 12P are the corresponding identically connected diaphragms in the light frame group. It was found that the replacement of the heavy frame by the light frame resulted in the following shear strength reductions:

Comparing: a) 4B and 4L (no intermediate fasteners)	8.6%
b) 5 and 5L (intermediate fast. @ 18")	15.4%
c) 11 and 11P(no intermediate fasteners)	24.8%
d) 12 and 12P(intermediate fast. @ 20")	20.6%

The forces transferred from the diaphragm into the marginal members tend to cause bending of the edge members in the plane of the diaphragm. Cases b and d above are the more common type of diaphragm since they have intermediate sidelap fasteners. Comparing them and using weak axis moments of inertia of the frame members as a measure of the edge beam stiffness, an average reduction in strength of 18% is associated with a 98 + % decrease in marginal member flexibility.

A further influence of frame stiffness on diaphragm behavior can be determined comparing the shear stiffness values for the above mentioned tests. Referring to Table 4-7 and comparing the heavy frame test results to corresponding light frame results on the same line, it can be seen that the frame size has little influence on shear stiffness.

It is logical to conclude that shear strength and stiffness values for a diaphragm can be determined on a frame having members of moderate cross sections and the results will be applicable to practically all other similar diaphragms regardless of the edge beam sizes.

e. The Effect of Panel Cover Width.

Comparisons for this influence can be made from tests 11 through 14 in Fig. 4-6. Thirty-six inch cover widths were used in Tests 11 and 12 while 24" widths of the same material were used in Tests 13 and 14. The 24" panels were cut from the 36" widths. Comparing 11 and 13 where no intermediate fasteners were used, it was found that there was an ultimate strength increase of 24% due to the 50% increase in cover width. Similarly, there was a 17% increase in the case where intermediate fasteners were used.

This means that the wider panel is somewhat more desirable because it has fewer sidelap fasteners for a given area and thus, fewer failure regions plus the added strength.

f. "Lower Bound" Strength Tests.

When diaphragms are to have a specified number of panel-to-panel connections, it is meaningless to try to establish

a lower bound strength by testing a diaphragm having fewer than the specified fasteners or by testing single panel diaphragms.

The results from a 12' x 6' standard corrugated diaphragm test are shown on Fig. 4-18. The only fasteners were at the panel ends which allowed the panels to act essentially as individual units. At an average shear of 50 lb/ft., the panels began to separate along the entire length of the diaphragm. Failure was due to panel buckling and the maximum shear load was 125 lb/ft.

Suppose a load factor of say 2.7 were applied to the ultimate shear strength. The allowable shear would be:

$$S_a = \frac{125}{2.7} = 46 \text{ lb/ft} \quad (a)$$

The shear stiffness  $G'$  was found to be:

$$G' = 10,000 \text{ lb/in} \quad (b)$$

Since the primary function of the diaphragm is to give protection against weather, it becomes unservicable at 50 lb/ft when the laps open even though there might be considerable reserve strength. It is seen that  $S_a$  from (a) would provide almost no margin against loss of serviceability and that no more than about  $S_a = 40 \text{ lb/ft}$  could be allowed in such a diaphragm.

From Table 7-1, the comparable shear strength for a 12' long x 10' wide standard corrugated diaphragm having sidelap fasteners is:

$$S_u = 600 \text{ lb/ft} \quad (c)$$

Comparison of this value with  $S_u = 125$  lb/ft shows that the presence of sidelap fasteners has increased the strength about five-fold. With the same safety factor of 2.7, the allowable shear on a sidelap-connected diaphragm would be

$$S_a = \frac{600}{2.7} = 220 \text{ lb/ft} \quad (d)$$

while the above reasoning would allow only about 40 lb/ft for the unconnected diaphragm.

The shear stiffness  $G'$  per foot of diaphragm width perpendicular to the corrugations is, for the connected diaphragm,

$$G' = 47,200 \text{ lb/in} \quad (e)$$

compared to 10,100 lb/in for the unconnected diaphragm.

It appears that for a diaphragm of the tested dimensions the unconnected panels are about 1/5 as strong and 1/5 as stiff as the diaphragms having panel-to-purlin and panel-to-panel connections. It is evident, therefore, that tests of unconnected single panels cannot be used to estimate the strength and stiffness of connected panels. This is because of the different failure modes. In the single panel test failure was due to overall panel buckling while in the large diaphragm tests having sidelap fasteners it was due to tearing around the sidelap fasteners. Trying to determine the ultimate strength for the latter case from test results on the former is seen to be futile.

On this basis, it seems clear that the behavior of full size diaphragms of the types presently in use cannot be determined from single sheet tests with unfastened longitudinal edges.

## 5. DIAPHRAGM DEFLECTIONS

### 5.1 The Deflection Problem.

The deflection of a light gage steel diaphragm is a function of the shear loads, panel configuration, and method of connection. The total deflection is composed primarily of components due to shear distortion, seam slip, and local buckling.<sup>5</sup> For the purposes of structural analysis, it is only necessary to divide these into two groups: bending deflection and shear deflection. Deflections from seam slip and local buckling are functions of the diaphragm configuration and independent of frame size. They will be considered as part of the shear deflection.

Diaphragms may have very high shear strengths and yet be very flexible. Since they will be used in conjunction with other load carrying structural components, it is necessary that deflection compatibility exist between the component parts. Optimum use will be obtained when the diaphragm is carrying a maximum shear load while satisfying any limits imposed on load and deflection.

### 5.2 Deflection Analysis of Cantilever Tests.

Diaphragms will be used on structures having many different beam sizes. It is therefore, necessary to be able to remove the edge beam influence from the test results and arrive at the shear deflection only.

Considering the cantilevered diaphragm in Fig. 5-1, it

can be seen that the force in edge members C-D and G-E varies from zero to a maximum of  $P(a/b)$ . If the diaphragm were continuously connected, this variation would be linear. Since the connections in the edge member are closely spaced in relation to the length, linearity will be assumed. Examination of the member C-D freebody, with the origin at the right, shows that the differential elongation  $de$  of the member is:

$$de = \frac{Px}{b} \frac{dx}{AE} \quad (5-1)$$

where  $A$  is the cross sectional area of the member,  $E$  is the modulus of elasticity, and the other dimensions are shown on the figure. Referring to Fig. 5.1, this means that  $d\theta$  is:

$$d\theta = \frac{de}{b/2} = \frac{2Px}{b^2AE} dx \quad (5-2)$$

Taking the cantilever moment of inertia  $I_{eff}$  as  $2A(b/2)^2$  and neglecting any contribution of the diaphragm itself, equation (5-2) may be rewritten as:

$$d\theta = \frac{Pxdx}{EI_{eff}} \quad (5-3)$$

The moment of inertia of any additional member such as C'-D' about  $b/2$  is neglected since the member cannot transfer any appreciable force into the support due to the flexibility of member C-G. This is particularly true in light gage cold formed channel frameworks.

The deflection due to bending  $\Delta_\beta$  at E in the direction of the applied load will be:

$$\Delta_\beta = \int_0^a x d\theta = \int_0^a \frac{Px^2 dx}{EI_{eff}} = \frac{Pa^3}{3EI_{eff}} \quad (5-4)$$

which is the bending deflection of a cantilever having a moment of inertia of  $I_{\text{eff}} = Ab^2/2$ .

The shear deflection  $\Delta'$  is given by:

$$\Delta' = \Delta - \Delta_{\beta} \quad (5-5)$$

where  $\Delta$  is the total diaphragm deflection and  $\Delta_{\beta}$  is the deflection due to bending.

For a particular diaphragm,  $\Delta$  may be written as:

$$\Delta = P/k \quad (5-6)$$

where  $k$  is the slope of the load-deflection curve within the elastic range.

Equation 5-5 can now be expressed in more general terms to account for the bending deflection.

$$\Delta' = \left( P/k - \frac{Pa^3}{3EI_{\text{eff}}} \right) = \left( \frac{3EI_{\text{eff}} - a^3k}{3EI_{\text{eff}}k} \right) P$$

and:

$$P/\Delta' = \frac{P}{\Delta} \left[ \frac{1}{1 - \frac{a^3}{3EI_{\text{eff}}} \frac{P}{\Delta}} \right] \quad (5-7)$$

where  $P/\Delta'$  is the slope of the load-deflection curve after corrections for both support movement and cantilever bending have been made.

The shear stiffness  $G'$  is written so that it is independent of the diaphragm dimensions  $a$  and  $b$ .

$$G' = S/\delta'_c = (P/b)/(\Delta'/a) = \frac{P}{\Delta'} \frac{a}{b} \quad (5-8)$$

$S$  is the average shear per foot of diaphragm and is equal to  $P/b$ .  $\delta'_c$  is the shear deflection per foot of dimension  $a$ .

The diaphragm panels may be parallel or perpendicular to the loading direction. The influence of panel length will be accounted for in the measured value of  $\Delta$ . If the panels span the short direction,  $\Delta$  will be larger than if the span were over the greater dimension. Thus length is accounted for even though it does not appear directly in equation 5-8.

### 5.3 Diaphragm Deflections in Buildings.

The determination of deflections is a relatively straight forward procedure for diaphragms which act as simple beams. However, in applications such as roof diaphragms on multi-bay portal frame buildings, the deflection is not so easy to determine. This is because the interior frames will remove shear forces from the diaphragm in proportion to the frame stiffness. The deflection problem then becomes redundant in proportion to the number of interior frames. The additional equations which are required to solve the problem arise from the deflection compatibility relationships between the diaphragm and the frame.

Two cases and the assumptions involved in the solutions will be examined in the following two examples.

a. The Simple Beam Diaphragm. In the portal frame building shown in Fig. 5-2, it is assumed that half of the normal wall load due to a lateral pressure  $p$  is transferred into the roof diaphragm as a line load. This results in a load  $q$  per foot of diaphragm equal to:

$$q = ph/2 \qquad (5-9)$$

where  $h$  is the building height.

The interior columns are pinned at both ends and no lateral forces can be transferred from the diaphragm to the interior columns. The diaphragm problem reduces to that illustrated in Fig. 5-3.

The following assumptions will be made with respect to the diaphragm system in Figs. 5-2 and 5-3.

1. The diaphragm stiffness is given by Fig. 4-24.
2. Members AB and CD are continuous with an area A.  
Purlins are connected at their ends by light clip angles and cannot transfer longitudinal forces across member EF.
3. The diaphragm panels span the b dimension.
4. The building end walls are rigid in their plane but flexible normal to their plane.

Referring to Fig. 5-1 and using equation 5-8, the shear-deflection slope is constant and given by:

$$\frac{dy}{dx} = \frac{\Delta'}{a} = \frac{P}{G'b} \quad (5-10)$$

The slope of the shear-deflection curve for the uniformly loaded case under consideration is by similar analogy:

$$\frac{dy}{dx} = \frac{q(a-x)}{G'b} \quad (5-11)$$

The integration of the above equation between the limits of zero and a yields the shear deflection  $\Delta'$ .

$$\Delta' = \int_0^a dy = \frac{q}{G'b} \int_0^a (a-x)dx = qa^2 / 2G'b \quad (5-12)$$

In the above equations, no shape factor is used in computing

the shear deflections since  $G'$  has been defined as a function of the average shear on the section.

The purlins are unable to transfer forces longitudinally across the member EF and are disregarded in computing the effective moment of inertia  $I_{\text{eff}}$  for the framework. The diaphragm is thin and is corrugated such that most of it is out of the loading plane. It will not contribute much to bending resistance other than to maintain spacing between the edge members. The effective moment of inertia of the frame is therefore:

$$I_{\text{eff}} = 2 A \left(\frac{b}{2}\right)^2 = \frac{Ab^2}{2} \quad (5-13)$$

where  $A$  is the cross sectional area of the edge beams and  $b$  is the total length along the corrugations between the edge beams.

The midspan bending deflection is given by:

$$\Delta_{\beta} = \frac{5q (2a)^4}{384 EI_{\text{eff}}} = \frac{5 qa^4}{24 EI_{\text{eff}}} \quad (5-14)$$

where  $E$  is the modulus of elasticity for the edge beams.

The total deflection is

$$\Delta = \Delta' + \Delta_{\beta} = \frac{qa^2}{2b} \left[ \frac{1}{G'} + \frac{5a^2}{6bEA} \right] \quad (5-15)$$

The proper selection of shear stiffness from tests is indicated in the following two examples.

#### Example 1.

Given:  $b = 10'$ ,  $a = 20$

$E = 30 \times 10^6$  psi

panel length = 10'

$q = 1,000$  lb/ft. (a)

$A = 2$  in<sup>2</sup>

purlin spacing = 3 1/3'

Using Fig. 4-24 for a panel length of 10', G' is found to be:

$$G' = 39,000 \text{ lb/in} \quad (b)$$

The total deflection is:

$$\Delta = \frac{1000(20)^2}{2 \times 10} \left( \frac{1}{39,000} + \frac{5 \times 400 \times 12}{6 \times 10 \times 30 \times 10^6 \times 2} \right) = 0.64'' \quad (c)$$

### Example 2.

The diaphragm is similar to that in example 1 except that it is made from two 5 1/2' panel lengths which allow a total diaphragm length of 10' with a 1' overlap. As concluded in Chapter 4, the stiffness of this system will be determined on the basis of the 5 1/2' length. From Fig. 4-24, the shear stiffness is:

$$G' = 14,000 \text{ lb/in} \quad (d)$$

and the total deflection from equation 5-15 is:

$$\Delta = 20000 \left( \frac{1}{14,000} + \frac{2}{300,000} \right) = 1.56 \text{ in.} \quad (e)$$

These examples show how radically the deflection can change due to changes in stiffness even though the diaphragm type is constant and only the panel length is changed.

Another problem is raised when the roof panels are different in length. Suppose the roof in the previous example is made from 7' and 4' long panels with an end lap on the first interior purlin. For the longer section of the diaphragm, the shear stiffness would be 22,000 lb/in and for the shorter 7,500 lb/in. The longer section is much stiffer than the shorter and consequently, the shorter could not pick up any

appreciable shear loads until after the longer diaphragm has undergone considerable deformation. In an assembly of this type, the value for  $G'$  in equation 5-15 should be based on the longer panels and the relatively minor contribution of the short section should be ignored.

For cases when the panels span in the  $a$  direction on Fig. 5-3, no additional problem arises. The shear stiffness is independent of the span direction and the relationships in Fig. 4-24 still hold.

b. Two Bay Portal Frame Building with Rigid Knee Frames

The building has the same external dimensions and loads as in case a, the only difference being that the center frame in Fig. 5-4 is able to transfer forces  $F$  out of the diaphragm and into the foundation. Within the elastic range, the force  $F$  along the horizontal member in the interior frame can be related to the total eave deflection:

$$F = k\Delta \quad (5-16)$$

where  $k$  is a linear spring constant. The eave deflection problem is now reduced to that shown in Fig. 5-5 and is similar to case a except that a spring force is added. Between  $x = 0$  and  $x = a$ , the shear-deflection slope is given by:

$$\frac{dy}{dx} = \frac{q(a-x) - k\Delta/2}{G'b} \quad (5-17)$$

Integration yields the shear deflection:

$$\Delta' = \int_0^a dy = \frac{1}{G'b} \int_0^a [q(a-x) - \frac{k\Delta}{2}] dx = \frac{a}{2G'b}(qa - k\Delta) \quad (5-18)$$

The bending deflection for the diaphragm with uniform positive load and a concentrated negative midspan load is found to be:

$$\Delta_{\beta} = \frac{5qa^4}{24EI_{\text{eff}}} - \frac{1}{6} \frac{k\Delta a^3}{EI_{\text{eff}}} = \frac{a^3}{3EAb^2} \left( \frac{5qa}{4} - k\Delta \right) \quad (5-19)$$

And finally, the total eave deflection for the center frame is the sum of equations 5-18 and 5-19:

$$\Delta = \Delta' + \Delta_{\beta} = \frac{qa^2}{2b} \left( \frac{1}{G'} + \frac{5}{6} \frac{a^2}{EAb} \right) - \frac{k\Delta a}{b} \left( \frac{1}{2G'} + \frac{a^2}{3EAb} \right) \quad (5-20)$$

A simplification and rearrangement of 5-20 yields:

$$\Delta = \frac{\frac{qa^2}{b} \left( \frac{1}{2G'} + \frac{5}{12} \frac{a^2}{EAb} \right)}{1 + \frac{ka}{b} \left( \frac{1}{2G'} + \frac{a^2}{3EAb} \right)} \quad (5-21)$$

The above reduces to the simple beam solution of equation 5-15 when  $k = 0$ .

The last terms in both the numerator and denominator in 5-21 are about the same and they indicate the influence of bending deflection. It is of interest to investigate the magnitude of these terms and to compare them to  $1/2G'$ . If the edge beams were made from very heavy 36 WF 300 beams,  $A$  in equation 5-21 would be  $88.17 \text{ in}^2$  and if  $a = b = 10'$ ,  $G'$  would be  $36,000 \text{ lb/in}$ . The terms in the denominator would be:

$$\frac{a^2}{3EAb} = \frac{10 \times 12}{3 \times 30 \times 88.17} \times 10^{-6} = 1.5 \times 10^{-8}$$

$$\frac{1}{2G'} = \frac{1}{2 \times 36,000} = 1.4 \times 10^{-5}$$

Considering another extreme case, say when the edge beams are 8" x 2" - 10 gage channels with an  $A = 1.55 \text{ in}^2$  with all other dimensions are the same as before:

$$\frac{a^2}{3EAb} = \frac{10 \times 12}{3 \times 30 \times 1.55} \times 10^{-6} = 8.6 \times 10^{-7}$$

$$\frac{1}{2G'} = \frac{1}{2 \times 36,000} = 1.4 \times 10^{-5}$$

Similar comparisons arise for the numerator. In the first comparison, there are about three orders of magnitude of difference and in the latter, about one and one-half orders of difference. When the length of the diaphragm increases the difference becomes smaller, particularly when the edge members are small. For most cases, shear deflection will predominate. Equation 5-21 can be reduced to the following form for most cases when the edge beams are moderately heavy.

$$\Delta = \frac{qa^2/2G'b}{1+ka/2G'b} \quad (5-22)$$

#### 5.4 Conclusions.

Only two types of problems have been given detailed consideration. However, the procedure is perfectly general and applicable to any number of bay spaces with any size of diaphragm. The only difference for longer buildings having diaphragms of the type in case a is that shear and bending deflection equations are integrated over different lengths as dictated by the building dimensions. If the wall system is such that some of the loads are transferred into the diaphragm as concentrated loads, the problem is changed merely

as in any other simple beam problem.

The problem becomes more complicated if there is more than one interior rigid frame. Each interior frame increases the redundancy by one. Yet the basic concept is unchanged and the required equations arise from the deflection compatibility conditions at each frame.

Diaphragms on gable frame buildings pose yet another problem when the building is loaded laterally. The roof diaphragms may deflect by different amounts and the concepts in this chapter have to be modified somewhat to account for this. A gable frame mill building under various loading conditions and having a variable number of interior frames is considered in detail in the next chapter.

## 6. MILL BUILDING INVESTIGATION

### 6.1 Introduction.

It is common practice to design mill buildings as if the roof and wall loads on half the bay length to either side of a frame were transferred into that frame. This assumption does not take shear transfer by diaphragm action into account. Mill building end frames are usually braced in their plane by the end wall, resulting in a much stiffer assembly than at the interior frames. Due to the relative stiffness, in-plane roof forces which might otherwise be transferred into the foundation at the interior frames can be moved to the end wall and taken out of the system. This of course, would result in smaller stresses for the interior frames and consequently, in the use of smaller sections. In the following sections, mill buildings are investigated to determine the diaphragm influence on frame deflections and bending moments. This is to be done by theoretical means as well as by model analysis. Several different buildings having different lengths but constant frame sizes and constant bay spacing are studied to determine how the diaphragm bracing of the frames varies with the building length.

### 6.2 Prototype Building.

The prototype building frame which is constant in size for all the different lengths of buildings investigated was designed by conventional means which discounted any diaphragm action in the roof plane. The gable frames were assumed to

be pinned at the footing, resulting in a once redundant frame. The general shape of the structure is shown in Fig. 6-1 (only two bays are shown for clarity) and the dimensions are as follows:

Eave height:	H = 15'	
Rafter rise:	R = 10'	
Bay Length:	B = 20'	(6-1)
Span:	S = 40'	

Frame Size: 15" x 5 1/2" - 42.9 lb. Am. Std. beams.

Purlin Size: 8" x 2" - 10 gage cold formed channels.

The roof is 26 gage standard corrugated panels having purlin fasteners in every third valley and intermediate sidelap fasteners at approximately 18" c.c. The roof panels are 11.5' long and have one end lap on each roof surface. The shear stiffness is given by Fig. 4-24.

The purlins are spaced at approximately 3' c.c. and are connected between the webs of adjacent frames such that the top flanges of the purlin are in the same plane as the top flanges of the frames. This arrangement permits efficient shear interaction between the diaphragm and the building frames. The purlin-to-frame connections are light clip angles which are effectively hinged for small lateral frame deflections.

The building is loaded with wind loads, snow loads, or combinations of the two. The wind loads are taken from reference 9 and the snow load is assumed to be 30 psf of horizontal roof projection. The positive load sign convention

is shown in Fig. 6-2. Positive values indicate external pressure and the negative values are external suction.

Snow load:	$V = 30$ psf.
Wind-Windward wall:	$P_w = 14$ psf.
Windward roof:	$N_w = -6.7$ psf.
Leeward roof:	$N_l = -10.0$ psf.
Leeward wall:	$P_l = -8.0$ psf.

### 6.3 Structural Analysis.

Several different methods of analysis were considered. These included pure matrix formulation, conjugate frame analysis, the method of column analogy, and the slope deflection method. For illustrative purposes, it is desirable that the diaphragm and building frame interaction be clearly apparent. Typical matrix solutions tend to obscure the interaction and were discarded for this reason. The conjugate frame and column analogy methods are adequate for bending moment solutions but they are not readily useable for pin ended frame deflection solutions since there are generally no fixed tangents along any of the frame members. Since the primary problem is one of deflection compatibility between the building frame and the diaphragms, conjugate beam and column analogy methods were abandoned.

The slope deflection method seemed more desirable and was used because the bare frame solutions could be easily modified to account for diaphragm shear forces which act along the building frames in the plane of the roof. The diaphragm shear forces are easy to determine as functions of the eave deflections which come directly out of the slope deflection solution.

Even though the interior bare frames are only once redundant, they become multi-redundant when the roof diaphragms are attached. The problem is five times redundant for each frame when the frame column bases are pinned. However, since the solution will proceed by iterative steps which consider only two diaphragms at a time, the problem can be considered as three-fold redundant. The equations are formed in terms of five unknown rotations which are general enough to permit the solution if the column bases are fixed. The following formulation may be changed to account for end-of-column fixity by merely changing the initial fixed end moments.

The initial development of the solution is given on pages 495 to 500 of reference 10. SW and SL will be used to designate shear forces in pounds per foot for the windward and leeward diaphragms respectively.

Considering the intermediate frame, there are five unknown rotations in the problem which are of interest. These are the joint rotations  $\theta_i$  which are positive in the clockwise direction and  $\rho_{ij}$  which is the rotation of a line connecting the middle points of the column ends. The  $\rho_{ij}$  values are positive in the clockwise direction. The fixed end moments  $F_{ij}$  are positive if they tend to rotate the joints clockwise. The member stiffness is indicated by  $K_1$  and is the ratio of the section moment of inertia to the member length.  $K_1$  is the column stiffness and  $K_2$  is the rafter stiffness.

The first three equations arise from moment equilibrium conditions at each of the joints 2, 3, and 4 in Fig. 6-4.

$$F_{21} + F_{23} - (3EK_1 + 4EK_2)\theta_2 - 2EK_2\theta_3 + 3E(K_1 - K_2\frac{H}{R})\rho_{12} + 3EK_2\frac{H}{R}\rho_{45} = 0 \quad (6-2)$$

$$F_{32} + F_{34} - 2EK_2\theta_2 - 8EK_2\theta_3 - 2EK_2\theta_4 = 0 \quad (6-3)$$

$$F_{43} + F_{45} - 2EK_2\theta_3 - (3EK_1 + 4EK_2)\theta_4 + 3EK_2\frac{H}{R}\rho_{12} + 3(EK_1 - EK_2\frac{H}{R})\rho_{45} = 0 \quad (6-4)$$

The fourth equation is obtained by summing the moments about the center of moments in Fig. 6-4. This gives:

$$\begin{aligned} & [(-P_\ell H R + \frac{N_\ell}{2}(L^2 - 4R^2) + \frac{V}{4} S^2 + \frac{L^2}{2} N_w)] x_B + (1 + \frac{2R}{H})F_{21} + 2F_{34} + F_{43} \\ & - (1 + \frac{2R}{H})3EK_1\theta_2 - 10EK_2\theta_3 - 8EK_2\theta_4 + 3E(K_1 + 2K_1\frac{R}{H} + 3K_2\frac{H}{R})\rho_{12} - 9EK_2\frac{H}{R}\rho_{45} = 0 \quad (6-5) \end{aligned}$$

The fifth and final equation is found from the summation of horizontal forces equal to zero.

$$\begin{aligned} & [(P_w - P_\ell) \frac{H}{2} + (N_w - N_\ell)R] B + (F_{21} + F_{45})/H \\ & - \frac{3EK_1}{H} (\theta_2 + \theta_4 - \rho_{12} - \rho_{45}) = 0 \quad (6-6) \end{aligned}$$

If  $\theta_2$ ,  $\theta_3$ ,  $\theta_4$ ,  $\rho_{12}$ , and  $\rho_{45}$  are replaced by  $x_1$  through  $x_5$ , the set of equations can be written in the matrix form:

$$A X = B \quad (6-7)$$

where the A matrix is given by:

$$\begin{bmatrix} 3EK_1 + 4EK_2 & 2EK_2 & 0 & -3(EK_1 - EK_2\frac{H}{R}) & -3EK_2\frac{H}{R} \\ 2EK_2 & 8EK_2 & 2EK_2 & 0 & 0 \\ 0 & 2EK_2 & 3EK_1 + 4EK_2 & -3EK_2\frac{H}{R} & -3E(K_1 - K_2\frac{H}{R}) \\ 3EK_1(1 + \frac{2R}{H}) & 10EK_2 & 8EK_2 & -3E(K_1 + 2K_1\frac{R}{H} + 3K_2\frac{H}{R}) & 9EK_2\frac{H}{R} \\ 3EK_1/H & 0 & 3EK_1/H & -3EK_1/H & -3EK_1/H \end{bmatrix}$$

and the B vector is given by:

$$\left[ \begin{array}{c} F_{21} + F_{23} \\ F_{32} + F_{34} \\ F_{43} + F_{45} \\ B[-P_{\ell} x H x R + N_{\ell} (L^2 - 4R^2)/2 + \frac{V}{4} S^2 + \frac{L^2}{2} N_w] + (1 + \frac{2R}{H}) F_{21} + 2F_{34} + F_{43} \\ B [H(P_w - P_{\ell})/2 + (N_w - N_{\ell})R] + (F_{21} + F_{45})/H \end{array} \right]$$

The solution for x may be obtained by Gaussian elimination. The eave deflections of Fig. 6-3 can be found from  $x_4$  and  $x_5$  and the bending moments in the frame can be found by substituting the rotations back into equation 6-7 after A has been reduced to the upper triangular form.

It is now necessary to modify the above system to account for diaphragm shear forces. In Fig. 6-3, let TL and TW be the net shear forces on an interior frame due to the diaphragm action. For example,  $TW = SW_n - SW_f$ , the difference in the shear forces in the near diaphragm and the far diaphragm. Only TL will influence equation 6-5 for moment equilibrium about the center of moments. This will increase  $b_4$  by  $TL(R \times S)/L$ . The remainder of the equation is unchanged.

Both TL and TW enter into the equation for horizontal equilibrium. The component  $b_5$  will be increased by  $(TW+TL)\frac{S}{2L}$ .

The solution of any frame in the building is dependent on the influence of any other frame. It will be necessary to find the deflections in the first interior frame, the deflec-

tions in the second interior frame with respect to the first, and so on until the center of the building is reached. The problem is solved in the following steps:

1. Find the first interior frame deflections and the shear forces in the first diaphragms assuming that the end wall is rigid and that the diaphragms between the first and second interior frames are not yet in place.
2. Find the second interior frame deflections and the diaphragm shear forces assuming that the first interior frame is now fixed at the deflections found in step 1 and that the diaphragms in the next bay are not yet in place.
3. Repeat this procedure until the center of the building is reached. In this first cycle, it has been assumed that there is no carryover of shear from one diaphragm to the next.
4. The first three steps are now repeated except that the net diaphragm shear force on the frames will be changed by the amount of shear in the next diaphragm, e.g.,  $TL = SL_n - SL_f$ .  $TL$  and  $TW$  are the net diaphragm forces which tend to prevent lateral deflections of the frames.
5. The problem is now re-solved for the deflections and shear forces in the near diaphragms using the far diaphragm shear forces from the previous cycle. This gives improved values for  $SL_n$  or  $SW_n$ , the shear forces in the near diaphragms.
6. This procedure is repeated until the desired convergence is reached.

This is of course an iterative procedure and is best suited

to electronic computation. A computer program to do this is given in Appendix B. It is worth noting that convergence can be speeded by writing the diaphragm contribution to the  $b_4$  term in the following way:

$$TL(RxS) L = \frac{RxS}{L} (SL_n - SL_f) = \frac{RxS}{L} \left( \frac{G' xSxH}{2xB} \rho_{12} - SL_f \right) \quad (6-8)$$

by making use of equation 5-8 to define  $SL_n$  in terms of  $G'$ . The term multiplying  $\rho_{12}$  can now be shifted into the  $a$  matrix as part of the  $a_{44}$  term. Equation 6-8 applies to the first interior frame relative to the end frame where there is no lateral deflection. For other frames, the shear contribution from the diaphragm must be kept in terms of the relative frame deflections. Similar modifications can be made in equation 6-6 as can be seen by comparing the  $a_{5j}$  and the  $b_5$  terms in 6-7 to those following statement 1122 in the computer solution in Appendix B.

The solution above is adequate for the case when bending deflections of the diaphragms within the plane of the roof are small as compared to the shear deflections. When the edge beams are relatively light, bending deflections become significant and the shear solution is used only to determine preliminary deflections and diaphragm shear forces. Once preliminary values have been obtained for the diaphragm shear forces, the first approximation of the bending deflections can be found by placing the resultant diaphragm shear forces at each frame on the roof diaphragm and treating it as a simple beam. The total deflection consists of both the bending

and shear deflections. Therefore, the shear deflections and consequently the shear forces could not have been as great as those in the first approximation. The bending deflection influence on the forces is subtracted from the first approximate values to determine the second approximate values. The cycle is then repeated until the desired convergence is reached.

The convergence criterion is arbitrarily selected as being satisfied when the rate of change in the deflection of the interior frame nearest the end of the building is less than  $0.0001 \times H$  inches per iterative cycle. For most mill buildings, this means that the eave deflection is changing about 1/1000 in. per cycle when convergence is reached.

#### 6.4 Model Analysis.

The use of structural models to supplement theoretical solutions is an important application which can eliminate many tests on full sized structures. Models are especially useful in cases where no previous solutions exist as is the case for mill buildings with diaphragms.

The first concern in a shear diaphragm model study is the reproduction of the load-deflection characteristics of the prototype diaphragm. It is also desirable that the model be small and yet possess sufficient strength to allow for reasonably large loads and deflections. The model framework should be scaled so the system can be used directly to predict prototype behavior.

Assuming that a model diaphragm has been made which yields load-deflection curves which are geometrically similar

to those in the prototype, the problem may be approached as follows.

Assume a linear scale factor  $n$ :

$$n = \ell / \ell_m \quad (6-9)$$

where  $\ell$  is a prototype length and  $\ell_m$  is the corresponding model length. The subscript  $m$  is used to denote model quantities and prototype quantities have no subscripts. A second factor  $k_1$  may be established which relates the slope of the prototype diaphragm load-deflection curve to that in the model:

$$k_1 = \frac{(P/\Delta)}{(P/\Delta)_m} \quad (6-10)$$

where  $P$  denotes the total shear force and  $\Delta$  the total deflection. It is important to note in the above equation that any model diaphragm, regardless of panel configuration, can be used to represent any prototype diaphragm so long as  $k_1$  can be established.

The frame moments of inertia  $I$  will be related by:

$$I_m = \frac{I}{k_2} \frac{E}{E_m} \quad (6-11)$$

where  $E$  is the modulus of elasticity and  $k_2$  is an arbitrary constant to control the section size.

Shear forces may be considered as line loads or as concentrated loads at corner of the diaphragms. Since the shear-deflection relationship between the model and prototype has been established in equation 6-10, concentrated loads are related by:

$$P_m = P k_1 \frac{\Delta_m}{\Delta} \quad (6-12)$$

The frame deflection will be proportional to  $P\ell^3/EI$ . The deflection prediction equation will be:

$$\Delta = \Delta_m \frac{P\ell^3}{EI} \frac{E_m I_m}{P_m \ell_m^3} = \Delta_m \frac{n^4 k_1}{k_2} \quad (6-13)$$

Making the substitution into equation 6-12, concentrated model loads are given by:

$$P_m = P/nk_1 \quad (6-14)$$

Uniform loads per square area are related by:

$$P_m = np/k_1 \quad (6-15)$$

The bending moments are proportional to  $P \times \ell$  and the prediction equation is:

$$M = n^2 k_1 M_m \quad (6-16)$$

The bending stress prediction equation for the frame is:

$$\sigma = \sigma_m \frac{My/2I}{(My/2I)_m} = \frac{My}{M_m y_m} \frac{I_m}{I} \sigma_m \quad (6-17)$$

where  $M$  is the bending moment and  $y$  is the distance from the neutral axis to the point in question. Substituting for  $M$  and  $I$ , the bending stress is given by:

$$\sigma = \sigma_m \left[ \frac{n^2 k_1}{k_2} \frac{E}{E_m} \frac{y}{y_m} \right] \quad (6-18)$$

The  $y$  terms are left in equation 6-18 since the depth of the frame cross section is often distorted relative to other length dimensions in the model.

### 6.5 The Model Materials.

Three diaphragm types were investigated in an attempt to obtain a value of  $k_1$  in equation 6-10 which was close to the

assumed scale factor of  $n = 20$ . This was desirable in order to control the model loads. Brass diaphragms with thicknesses of 0.001" and 0.002" were tested but the most suitable material was found to be 0.002" tin coated steel.

The diaphragms were corrugated by using the corrugator shown in Fig. 6-5. This produced diaphragms having a nominal corrugation pitch of 1/4" and a nominal depth of 1/16". No attempt was made to scale the model corrugations in accordance with equation 6-9 since any distortions were automatically accounted for when model test results were placed in equation 6-10 to determine the value of  $k_1$ .

The model frames and purlins were made from plexiglass. The modulus of elasticity was determined from flexure tests on a 21" beam having a nominal cross section of 1/2" x 5/8" which was equipped with both dial gages and foil gages. The average value was:

$$E_m = 461,000 \text{ lb/in}^2 \quad (6-19)$$

The continuous eave and crown frame connections were made with CD-18 cement which is recommended for plexiglas joints.

The purlins were connected between the adjacent frames so that their top edge was in the same plane as the top of the frames. The purlin-to-frame connections were made with 1/2" brass butt hinges using aluminum rivets and number 3 screws. A typical purlin end connection is shown in Fig. 6-7.

The diaphragm-to-purlin connections were made along every third valley with small spots of an epoxy cement, EPON 907. Spots of the cement are visible in Fig. 6-8.

## 6.6 The Model Buildings.

Several different buildings having different numbers of interior frames were investigated. The model study was restricted to mill buildings having from 2 to 5 bays of constant length and loaded with combinations of lateral and vertical loads. The scale factor  $n$  was chosen as 20. This resulted in a model having the following dimensions:

Eave height:	$H = 9''$
Rafter rise:	$R = 6''$
Bay length:	$B = 12''$
Span:	$S = 24''$

A general view of a 5 bay model is shown in Fig. 6-10.

The prototype frames had constant section properties with a major axis moment of inertia of  $441.8 \text{ in}^4$ . The model frames had nominal cross sections of  $1/2'' \times 1''$ . The actual dimensions were  $0.481'' \times 1.004''$  which resulted in a moment of inertia of:

$$(I_x)_m = 0.0406 \text{ in}^4 \quad (6-20)$$

Assuming an  $E$  for steel of  $30 \times 10^6 \text{ lb/in}^2$  and making use of equations 6-11, 6-19, and 6-20, the distortion factor on  $I_x$  is found to be:

$$k_2 = EI/(EI)_m = 708,000 \quad (6-21)$$

The prototype purlins were  $8'' \times 2''$  -10 gage channels with a major moment of inertia of  $12.9 \text{ in}^4$ . By equation 6-11, the purlin moment of inertia is:

$$(I_{\text{purlin}}) = 11.85 \times 10^{-4} \text{ in}^4 \quad (6-22)$$

Fixing the small dimension of the rectangular cross section at  $1/8''$ , the section depth  $h$  is found to be:

$$h = 0.485" \quad (6-23)$$

This value was rounded off to 1/2" without introducing any appreciable error. The 1/2" x 1/8" purlins were used in the model building and in the model shear panel tests.

The building frame was cut to the centerline dimensions shown in Fig. 6-9a. The pinned frame supports were made by inserting 7/64" diameter pins through a double angle arrangement as can be seen on the first frame in Fig. 6-6. The holes in the frame were about 0.0005" oversize and the support provided negligible rotational restraint.

Loads were applied to the building frames at the points indicated in Fig. 6-9a. A photograph of the loading system is shown in Fig. 6-6. Normal outward loads were applied through pivot bars by means of gravity loading. Vertical loads were imposed by hanging weights directly on the frames as indicated by the weight  $W_3$  in Fig. 6-9a. Lateral loads were applied by cords which passed over rollers as can be seen in Fig. 6-6 or  $W_1$  in Fig. 6-9a.

In the analysis, the building was assumed to have a rigid end wall. The end wall of the model was made from 1/2" plywood which was clamped to the end frame at several points. This gave almost total restraint against deflections in the plane of the end frame.

### 6.7 The Model Tests.

The diaphragm shear test is used to establish the relationship  $k_1$  between the prototype and model diaphragms. The frame details are shown in Fig. 6-7. The frame duplicates one

section of the model building roof. The test setup is shown in Fig. 6-9. Loads were applied in 5 lb. increments from zero to failure on the three different test panels. Failure occurred in the diaphragm-to-purlin connections near the pinned support at the upper left corner.

The test results were reduced in the same manner as outlined in 3.2 of Chapter 3. The results of the three tests are shown on a large scale in Fig. 6-11. The solid curve is a composite of all the data and is used for the model load-deflection slope:

$$(P/\Delta)_m = 2830 \text{ lb/in} \quad (6-24)$$

From Fig. 4-24, the value of  $G'$  which applies to the prototype is:

$$G' = 43,000 \text{ lb/in} = \frac{P}{\Delta'} \frac{a}{b} \quad (6-25)$$

where  $a/b = (11.5)/20$ . Whence

$$P/\Delta' = 74,800 \text{ lb/in} \quad (6-26)$$

Solving for  $k_1$  in equation 6-10 gives:

$$k_1 = 26.45 \quad (6-27)$$

The  $k_1$  value is now used in equation 6-15 to determine the model building loads. This results in:

$$\text{Vertical load: } V = 22.65 \text{ psf}$$

$$\text{Wind-Windward wall: } P_w = 10.29 \text{ psf}$$

$$\text{Wind-Windward roof: } N_w = -5.06 \text{ psf}$$

$$\text{Wind-Leeward roof: } N_\ell = -7.56 \text{ psf}$$

$$\text{Wind-Leeward wall: } P_\ell = -6.04 \text{ psf}$$

These uniform loads were replaced by equivalent concentrated

loads at the frame load points indicated in Figs. 6-6 and 6-9a. The buildings were loaded both before and after the roof diaphragms were applied. The recorded eave deflections gave a measure of the diaphragm influence on the building frames. Knowing the eave deflections, it was possible to solve for the column rotations and in turn for the frame bending moments.

The results for the model mill building tests are shown in Figs. 6-12 and 6-13 for 2, 3, 4, and 5 bay buildings. The horizontal lines represent values determined for the building frames prior to attaching the roof diaphragms. The lower curves show the comparable values after the diaphragms have been attached. Solid curves give the measured test results and the dashed curves indicate analytical values from the computer solution in Appendix B. In Figs. 6-12 and 6-13, all values can be compared to the bare frame results shown by the horizontal lines in the left side of Fig. 6-12. It can be seen that the analytic and measured values are very close for the cases when diaphragms were on the buildings. However, the measured values were lower than the computed values for the bare frame tests. This might have been due to applying the roof wind loads through the pivot bars shown in Fig. 6-6. Since the frame deflections were larger in the bare frame tests, the bar rotations were larger and consequently the roof loads were slightly different in the bare frame tests from those in the roofed buildings.

On the basis of the good agreement between the measured model deflections and those from the computer solution, the method of analysis proved to be valid. The computer program was

then used to solve 4 different mill buildings under the wind load conditions at the top of page 72. The results are shown in Figs. 6-14 and 6-15. The maximum eave moment  $M_2$  is shown for each building along with the maximum eave deflections  $\Delta_2$  and  $\Delta_4$  which are the horizontal deflections for the windward and leeward sides respectively. The diaphragm influence is clearly shown in the following table where the percent reduction indicates the reduction from the bare frame values due to the use of diaphragms.

Number of Bays	Quantity	Percent Reduction from Bare Frame Values	
		First Int. Frame	Second Int. Frame
5	$\Delta_2$	75	52
	$\Delta_4$	80	65
	$M_2$	70	43
4	$\Delta_2$	78	61
	$\Delta_4$	85	75
	$M_2$	72	48
3	$\Delta_2$	86	
	$\Delta_4$	96	
	$M_2$	79	
2	$\Delta_2$	87	
	$\Delta_4$	98	
	$M_2$	82	

It can be seen that the diaphragm action is much more pronounced in the shorter buildings but that it is still very significant in the 5 bay building. The general trend in the above table seems to indicate that the diaphragm bracing influence

could be considerable even in much longer buildings, say up to 10 bays in length.

## 7. LOAD FACTORS AND STANDARD TEST PROCEDURES

### 7.1 Introduction.

The essential points in regard to load and safety factors are examined in the first part of this chapter. The second part is concerned with the procedures to be considered in the standardization of diaphragm shear tests. The conclusions are based on the test data in chapter 4.

### 7.2 Load Factors for Light Gage Steel Shear Diaphragms.

Scope. This discussion is limited to those light gage steel roof and wall diaphragms in which the steel diaphragm is the only shear resisting element. This means that diaphragms having concrete fill or other shear resisting materials are not considered. The diaphragm loads considered herein are those applied in and parallel to the plane of contact between the diaphragm and its supporting framework.

Types of Diaphragm Loading. The shear forces which arise in a diaphragm may result from dead loads, snow loads, wind loads, earthquake loads, or combinations thereof.

a) Dead Loads. Careful consideration must be given to the use of diaphragms to resist dead loads. Since the roof or the walls of a light gage steel building or the surfaces of shells and folded plates do not constitute diaphragms until the final panels are in place and connected, they are not capable of resisting shear forces which arise prior to completion. Consequently, the diaphragm is totally ineffective as

a dead load shear resisting device unless special erection techniques are employed. For example, the dead load shear forces which would result in the roof of a mill building would be due to the weight of the diaphragm and supporting framework. Unless some special device such as pretensioned guy wires spanning between the eaves is used, all dead load frame deflections will have occurred prior to completion of the roof diaphragm and as a result no dead load shear forces will act in the completed diaphragm.

b) Live Loads. Wind and snow loads should be taken as those recommended by local codes. In the absence of local codes, wind loads of the type recommended in "Wind Forces on Structures: Final Report of the Task Committee on Wind Forces of the Committee on Loads and Stresses of the Structural Div., ASCE" II: 1124:3269 by J. M. Biggs<sup>9</sup> should be considered.

Earthquake loads should be calculated on the basis of the Seismic Probability Map for the United States in accordance with the Uniform Building Code, 1961 Edition, Section 2313 or local codes.

Load Factors. The real loads applied to a structure are never known with certainty nor can the strength of the structure be absolutely determined. With this in mind, load factors are established to account for the possibility of combinations of overload and understrength.

To make the proposed approach consistent with other pertinent safety provisions of the AISI Specifications<sup>11</sup>, the load testing provisions of the Specifications will be utilized

as a starting point.

According to the AISI Specification 6.2(b), a structure must be able to withstand test loads equal to  $1.5 \times$  (dead load) +  $2.0 \times$  (live load). If a 10% overload is allowed on the calculated dead load, the implied understrength allowance must be:

$$1.50/1.10 = 1.36 = 1.00/0.735 \quad (7-1)$$

Thus, in the extreme case, the dead loads may be 110% of their estimated value and the structure's strength only 73.5% of the expected value since  $1.10(1/0.735) = 1.50$ .

If the same understrength allowance of 1.36 is permitted on the live loads, then the live load overload allowance must be:

$$2.00/1.36 = 1.47 \quad (7-2)$$

a) Modifications. The understrength allowances in equations 7-1 and 7-2 will be modified for light gage steel diaphragms in accordance with the type of connections used in the diaphragm, since failure is almost invariably associated with fastener failure.

In welded connections for light gage construction, the AISI Specifications imply an increase in the safety factor from 1.65 to 2.50. It is proposed that this increase be applied to welded steel diaphragms; this is related to welding in thin material. Considerable experience is required on the part of the welder to produce a suitable weld without "burn-through" in the material. Even under very closely controlled laboratory conditions, some welds appear perfect and yet have

insufficient fusion to give proper carrying capacity. It is logical to modify the understrength allowance for a welded diaphragm in accordance with its weakest part, the connection.

If the understrength allowances are modified in accordance with the ratio  $2.50/1.65 = 1.52$ , the new understrength factor is  $1.36 \times 1.52 = 2.06$  and the load factors for welded diaphragms will be:

$$\text{Dead load factor: } 1.10 \times 2.06 = 2.27 \quad (7-3)$$

$$\text{Live load factor: } 1.47 \times 2.06 = 3.03 \quad (7-4)$$

On this basis, it can be recommended that a welded diaphragm should be designed to withstand test loads of about  $2.2 \times$  (dead load) +  $3.0 \times$  (live load).

Similar to the safety factors implied for welds, the AISI Specifications imply a safety factor of about 2.2 for bolted connections. The screw connected diaphragms in the tests were not bolted but the screws were generally anchored such that the behavior under load was similar to that for bolts. Diaphragms having spreading backed fasteners, i.e., fasteners having some device which will expand and provide anchorage after the fastener is inserted in the hole (see Fig. 3-11), will be considered in this category. Based on a safety factor of 2.2, the understrength allowance will be  $(2.2/1.65) \times 1.36 = 1.81$ . The load factors for screw connected diaphragms and those having backed up fasteners will be:

$$\text{Dead load factor: } 1.10 \times 1.81 = 1.99 \quad (7-5)$$

$$\text{Live load factor: } 1.47 \times 1.81 = 2.66 \quad (7-6)$$

b) Diaphragms with Load Reversal. Light gage steel diaphragms will often be used in situations where there will be stress reversal or, at least, pulsating stresses. The testing of a diaphragm under reversed load conditions is a slow and tedious process and many tests would be required to determine accurately the effects of load reversal at a particular intensity.

The recommended load factors for reversed loading conditions are developed in equations 7-7 through 7-12, below, by considering one aspect at a time and modifying each successive set of values until the final factors are obtained.

On the basis of 26 tests (See Table 4-5), reductions in the static strength will be recommended in order to account for the effects of load reversal.

(In the first section in Table 4-5, Tests 5R and 5R-3 are considerably out of line with other reversed load tests. Certainly they do not satisfy the test requirement as outlined in the AISI Specification 6.2(b) which states that no one test of three should deviate from the average of the three by more than  $\pm 10\%$ . However, the general trend of all tests, and in particular the repeats of the two mentioned tests, seems to indicate that something was inherently wrong with these two diaphragms. However, because there is no ready explanation of why they deviated from the average by as much as they did, their results are included in the average values of test results.)

Table 4-6 shows the average reduction in static strength

due to the reversal regimes indicated. The first two entries are average reductions from all tests which were loaded to either 0.3 or 0.4 of the expected ultimate loads. The remainder of the table shows average percent reductions for diaphragms having particular types of connections and loaded to either 0.3 or 0.4 of the expected ultimate loads with the number of indicated load reversals. From this table, it may be concluded that the ultimate strength for a diaphragm under fully reversed load conditions can be taken as the following fractions of the ultimate static test strength:

<u>Screw Connected Diaphragms:</u>	$0.85 \times P_u$	
<u>Diaph. w/Backed up Seam Conn.:</u>	$0.95 \times P_u$	(7-7)
<u>Welded Diaphragms:</u>	$0.95 \times P_u$	

where  $P_u$  is the ultimate static test load. The second entry refers to diaphragms in which the intermediate sidelap fasteners, i.e., those sidelap seam fasteners not anchoring into the purlins, have mechanical back up devices such as in spreading backed fasteners, pop rivets, lock rivets, and the like.

On the basis of conditions 7-7, together with 7-4 and 7-6, the live load factors to be applied to the static strength for conditions of load reversal should be:

<u>Screw Connected Diaphragms:</u>	RLF: $2.66/0.85 = 3.13$
<u>Diaph. w/Backed up Seam Conn.:</u>	RLF: $2.66/0.95 = 2.80$ (7-8)
<u>Welded Diaphragms:</u>	RLF: $3.03/0.95 = 3.19$

where RLF is the load factor for load reversals.

According to AISI Specification 3.8.1, an increase in the allowable stresses of 33 1/3% is permitted if the stress

reversals are due to wind or earthquake. If for example, the allowable stress is taken as the yield stress divided by the load factor  $S_y/L.F.$ , then an increase of 33 1/3% means (1.33)  $S_y/L.F.$  or:

$$\text{Allow. Stress} = 1.33 S_y/L.F. = S_y/(0.75 \times L.F.) \quad (a)$$

Thus increasing the allowable stress by 1/3 is the same as decreasing the load factor by 1/4. Then equation 7-8 may be further refined according to the above, to account for wind or earthquake loads:

<u>Screw Connected Diaphragms:</u>	RLF: 3.13 x 0.75 = 2.35
<u>Diaph. w/Backed up Seam Conn.:</u>	RLF: 2.80 x 0.75 = 2.10 (7-9)
<u>Welded Diaphragms:</u>	RLF: 3.19 x 0.75 = 2.39

The test investigations on which equation 7-7 is based have been limited to reversed load tests of either 0.3  $P_u$  or 0.4  $P_u$  and consequently this limitation must be reflected on equation 7-9 such that the load factors are within the scope of investigated load intensities. That is, the factors in 7-9 should not be less than:

<u>Screw Connected Diaphragms:</u>	RLF: (1/0.3) x 0.75 = 2.5
<u>Diaph. w/Backed up Seam Conn.:</u>	RLF: (1/0.4) x 0.75 = 1.87
<u>Welded Diaphragms:</u>	RLF: (1/0.4) x 0.75 = 1.87

Due to the limitations imposed by the range of reversed load tests on which this information is based, the load factors must be taken as the larger of the values in equations 7-9 or 7-10.

c) Gravity Loads. For gravity live loads and dead loads, the load factors may be taken from equations 7-3 through 7-6

with no reduction of the type in 7-9.

<u>Screw Connected Diaphragms:</u>	GLLF: 2.66	
<u>Diaph. w/Backed up Seam Conn.:</u>	GLLF: 2.66	(7-11)
<u>Welded Diaphragms:</u>	GLLF: 3.03	
<u>Screw Connected Diaphragms:</u>	DLF: 1.99	
<u>Diaph. w/Backed up Seam Conn.:</u>	DLF: 1.99	(7-12)
<u>Welded Diaphragms:</u>	DLF: 2.27	

GLLF is the gravity live load factor and DLF is the dead load factor.

#### Conclusions and Recommendations on Load Factors.

The tests on which the load factors in this section are based include standard corrugated, deep corrugated, box ribbed, and roof deck configurations. These configurations seem to be typical of diaphragms used in light gage steel construction and any recommendations based on this investigation should apply equally to all types of light gage steel diaphragms.

From equations 7-8 through 7-12, the final recommended load factors are as follows:

#### Final Recommended Values for Load Factors

<u>Diaphragm Type</u>	<u>Wind or Earthquake Load Factor</u>	<u>Gravity Live Load Factor</u>	<u>Dead Load Factor</u>
Screw Connected Diaphragm:	2.5	2.7	2.0
Diaph. w/Backed up Seam Conn.:	2.1	2.7	2.0
Welded Diaphragms:	2.4	3.0	2.3

The factors in the first column also can be applied to structural loads such as those which arise from movement of overhead

cranes.

Diaphragms have been used quite extensively on the West Coast with wind and earthquake load factors of about 3. This makes the recommended values above appear somewhat low. However, the development which has been followed to arrive at these values seems entirely consistent with other safety measures contained in the AISI Specs. There is no reason to penalize a diaphragm to an arbitrary load factor of 3 when lower values are acceptable for other parts of the structure.

### 7.3 Standard Test Procedure for Light Gage Steel Diaphragms.

The use of light gage steel diaphragms to resist in-plane shear loads is a feasible and apparently economical undertaking. However, because of the complexities of typical roof and wall diaphragms, including the variations in panel configuration, fastener types, material properties, etc., it is at present not possible to predict their behavior by purely theoretical means. This makes tests necessary for each type of diaphragm in order to establish reliable results.

In writing a specification to control such tests on shear diaphragms, the following points should be considered:

a) Feasible Test Arrangements. At least two possibilities exist, one being a cantilever type test in which the loads are applied at one corner of a cantilevered diaphragm and the other a simple beam test representing a multi-bay diaphragm with loads at several interior points. In his paper, "Shear Diaphragms of Light Gage Steel", A. H. Nilson<sup>5</sup> has shown that a simple cantilever test can be used to predict

the behavior of the more complicated multi-bay type simple beam test. Since the cantilever test is easier, faster, and more economical to perform, it should be considered as the standard test.

b) Diaphragm Size. The discussions with regard to diaphragm size are based on standard corrugated diaphragms having screw type connections. However, the conclusions are of a general nature and should be expected to apply to all light gage steel diaphragms.

The investigation has not included diaphragms of extremely large areas where direct comparison can be made with smaller diaphragms. However, several 26 gage standard corrugated diaphragms having dimensions of 12' and less have been tested. From these tests, it is possible to conclude that the average ultimate shear strength  $S_u$  per foot of diaphragm is relatively independent of diaphragm size. This can be noted from Table 7-1 where the range on  $S_u$  is from 587 plf to 675 plf. If strength were the only criterion, almost any reasonable size diaphragm would be acceptable in a standard test.

It was pointed out in Chapter 4, Section 4.5c that the shear stiffness is strongly dependent on the diaphragm length. This is because the accordion-like end warping and low load resisting part of the diaphragm becomes relatively larger as the diaphragm is shortened. Any test on a short diaphragm will result in a smaller shear stiffness than if the test diaphragm were longer. The short test is not necessarily conservative for if short test  $G'$  values are used in a longer diaphragm

application then the higher degree of stiffness may result in shear overloads.

Very narrow diaphragms should also be avoided for tests since there is some warping between the fasteners along the panel edges. However, due to the beam action of the corrugation, edge warping is much less pronounced than that across the corrugation ends.

The test diaphragm should be approximately square with nominal dimensions of about 6' x 6'. However, it should be large enough to have at least one interior purlin with the panel manufacturer's recommended purlin spacing. From a test diaphragm of this size, the shear strength can be determined directly and the load-deflection curve slope can be used to determine the  $K_2$  value for equation 2-16. Shear stiffnesses for other diaphragms can then be determined as on page 52.

The recommended diaphragm test size above is for diaphragms having "open" panel shapes similar to those indicated in Fig. 3-1. It is of interest to determine whether or not shear stiffness and shear strength are functions of diaphragm length for other diaphragms such as those having cellular type panels. Nilson<sup>6</sup> has given numerical test results for cellular panel diaphragms ranging in size from 12' x 10' to 30' x 30' (The panels were designated as type 9). The original load-deflection curves for these tests were available. Although no direct comparisons could be made from the data, it is possible to show that the shear strength and the stiffness are relatively insensitive to the depth of the cell as long as other parameters do not vary. Treating variations in cell depth as a secondary

influence, it can be shown that the shear strength is insensitive to the diaphragm length. It was further noted that the shear stiffness varies with length of panel but not as much as it does in open section diaphragms. This is most likely due to the nearly continuous flat plate element along the cell bottoms and in the plane of attachment between the diaphragm and the frame. The flat element transfers a large portion of the shear forces which results in small shear forces across the out-of-plane diaphragm components. This leads to less panel end warping and less stiffness variation with length.

The cellular flat plate element is not accounted for in the theory of Chapter 2 even though it is apparent that stiffness for cellular diaphragms varies with length. In the absence of more extensive test data, this type of diaphragm should be tested as a full sized specimen.

c) Test Frame. The discussion of the influence of frame stiffness on the diaphragm strength in Section 4.5d of Chapter 4, indicates that rather extreme variations in frame stiffness have only mild effects on the shear strength. The diaphragm characteristics should be established on a framework composed of members with minimal practical stiffness. Any heavier framework in actual use will cause the diaphragm to be slightly stronger.

It is necessary that the test frame have purlins or girts of approximately the same spacing as in the prototype. These serve two purposes; to prevent out-of-plane buckling of the entire diaphragm and to supply anchorage for the sidelap

fasteners at the purlins. Fasteners which anchor into a relatively thick material such as the purlins resist tilting, tearing, and are generally stronger than if there were no such anchorage. In regard to the latter point, several early tests were made in which the purlins prevented out-of-plane buckling but had no direct connection to the diaphragm (See for example Figs. 3-6 and 4-3). From these tests, it can be concluded that the presence of purlin connections may increase the shear strength by as much as 80% and may double the stiffness.

Since it is necessary to know the load-deflection characteristics with as much accuracy as possible, the framework should have members of minimum practical stiffness and all purlins and connections should be spaced approximately as in the prototype.

d) Frame Supports and Connections. The diaphragm frame should be attached at one corner with a pinned connection which transfers the horizontal forces from the diaphragm-to-frame contact plane into the support and thus preventing warping the diaphragm surface. A roller or doubly pinned link should be provided at the opposite corner depending on whether or not reversed load tests are desired. (Refer to Figs. 3-2 and 3-3 for schematic drawings and for typical corner details.) Supports must be supplied to prevent frame deflections normal to the diaphragm surface. This can be done by testing the diaphragm in a horizontal position and supporting the corners of the frame with a series of rollers.

All internal connections should be pinned, allowing no shear stiffness in the bare frame itself. Clip angle connections between the purlins and the edge members may be considered as pinned connections within the range of diaphragm deflections. The pinned corner connections, which are more difficult to make, require the cutting away of webs at the ends of the edge members and fitting with thin end plates such that bolts can be passed through the corners permitting an effective hinge (See Fig. 3-2).

e) Diaphragm Connections. The diaphragm should be attached to the test frame in the same manner as it will be attached to the prototype frame. The test connections should include any closure angles which might be used across panel ends.

f) Loading and Instrumentation. Loads should be applied in increments from zero to failure parallel to and in the plane of contact between the diaphragm and the frame at the corner indicated in Fig. 3-2. Minimum instrumentation should consist of dial gages located as shown in Fig. 3-9. Deflections should be recorded after each application of incremental load.

g) Interpretation of Test Data. Since the frame is rectangular prior to testing and since only small deflections relative to the overall dimensions occur, a small deflection theory is adequate to correct for support movement. The true diaphragm deflection at E parallel to the loading direction is given by:

$$\Delta = E - \left( A + \frac{a}{b} (B + G) \right) \quad (7-13)$$

where A, B, G, and E are the dial gage readings at the respective points indicated in Fig. 3-9 and a/b is the ratio of the frame dimensions in the figure.

The deflection given by 7-13 includes both shear and bending deflections. The latter should be corrected for as shown in Chapter 5, resulting in the shear deflection only. Then the shear stiffness  $G'$  can be determined from the nearly linear portion of the load-deflection curves up to about 0.4  $P_u$  as:

$$G' = S/\delta'_c = \frac{P}{\Delta'}, (a/b) \quad (7-14)$$

where  $P/\Delta'$  is the slope of the load-deflection curve after corrections for bending have been made.

#### Conclusions and Recommendations on a Standard Test Procedure.

In light gage steel construction, a particular type of roof or wall panel is commonly used in a somewhat restricted manner. The manufacturer usually recommends a maximum purlin or girt spacing and the type and arrangement of connections. The maximum recommended spacing should be used in tests. On this basis and considering the points outlined in this section, the standard test should satisfy the following requirements:

1. It should be a cantilever type test having marginal members of the minimal stiffness expected in construction.
2. Test diaphragms for panels having the general shapes shown in Fig. 3-1 should be nominal in size, say about 6' x 6' but large enough to have at least one interior purlin. Cellular

diaphragm tests for long span prototypes should be larger (See page 95).

3. The test frame should have purlins (or girts) at the maximum spacing recommended by the manufacturer.
4. Diaphragm connections should be identical with those used in the prototype since appreciable change in type or spacing of connections can result in an entirely different mode of failure.
5. Frame details, loading methods, instrumentation, and interpretation of data should be as outlined in other parts of this chapter.

## 8. SUMMARY

### 8.1 General Diaphragm Behavior.

Sixty tests on 120" x 144" light gage cold formed steel diaphragms were made to investigate the general behavior of roof and wall diaphragms as they are currently fabricated. The test variables included panel configuration, fastener arrangement, material properties, and span lengths. A few tests were made on diaphragms having unusual types and arrangements of fasteners but the majority of the diaphragms were assembled according to manufacturer's recommendations. Two different test frames were used, one having rather heavy marginal frame members made of 10 WF 21# beams and the other having marginal members of light gage cold formed channels. The effects of static, pulsating, and reversed loading were investigated and compared. In addition, the influence of various types of fasteners were compared.

A second series of smaller diaphragm tests was made using either light gage channel frames or equal leg light angle frames. This series was primarily for the investigation of shear strength and stiffness variation with diaphragm size.

A brief list of the conclusions is given below.

I. Frame Flexibility. It was found that the frame flexibility had a moderate influence on the ultimate strength of the diaphragms. Taking the marginal member moment of inertia about the axis normal to the diaphragm, i.e., the weak axis, as a

measure of the flexibility, it was found that a 98% increase in flexibility only reduced the diaphragm shear strength by about 18%. Similarly, the frame flexibility has only a moderate influence on the diaphragm shear stiffness  $G'$ .

II. Intermediate Fasteners. No constant relationship exists between the number of fasteners along a panel side lap and the shear strength. However, in most tests, the strength increased about twofold when the number of side lap fasteners was doubled.

III. Effect of Panel Cover Width. Four tests which were made on ribbed panel diaphragms showed that the static ultimate strength increased on the average by 20% when 36" panels were used to replace 24" panels of the same material.

IV. Thickness Influence. Standard corrugated diaphragms of three different thicknesses and having identical fastener arrangements were tested. The diaphragms had thicknesses of 0.0162", 0.0188", and 0.0310". It was found that the diaphragm shear strength at a particular deflection varied almost linearly with the panel thickness, being greater for the thicker diaphragms.

V. Effect of Pulsating Loads. A 26 gage standard corrugated diaphragm was loaded from zero to  $0.4 P_u$  for five cycles. When compared to an identical statically loaded diaphragm, it was found that the pulsating load reduced the strength by about 6%. Pulsating loads within this limit of intensity seem to do little damage to the diaphragm.

VI. Effect of Reversed Cyclic Loading. Reversed loads up to about  $\pm 0.3 P_u$  will cause a reduction from the static shear strength of 5 to 10% in diaphragms which have no intermediate fasteners. Similar loads on diaphragms having intermediate screw type fasteners cause relatively larger strength reductions. For large numbers of cycles, the reduction may be as much as 30% but it is usually less than 20%. However, the ultimate strength in the latter case where intermediate fasteners are used is still higher than the former.

VII. Fastener Type. If intermediate fasteners are used in which very little tilting and loosening can occur, negligible damage in the diaphragm will result even after the very intense cyclic loading of  $\pm 0.4 P_u$  for 29 cycles. Welded diaphragms and those having backed up intermediate fasteners fall in this category.

VIII. Material Strength. Tests on mild steel and full hard diaphragms with identical configurations show that their test behavior is about the same. The shear stiffness is unaffected by the change in material strength but the ultimate strength for the full hard diaphragms is up to 20% greater.

IX. Shear Stiffness. The shear stiffness is dependent primarily on the panel length, the panel configuration, and the spacing of the panel end fasteners. Additional fasteners across the panel ends tend to reduce warping and increase the stiffness. The stiffness for a particular type of diaphragm is very strongly dependent on the panel length even though the shear strength is not.

## 8.2 Diaphragm Deflections.

The diaphragm stiffness and deflection is mildly dependent on the size of the marginal members used in the test frame. However, this influence is considered in the analysis in Chapter 5 where the shear stiffness can be determined independently of any bending stiffness which the frame members possess. This allows standard tests to be made on rather light test frames and does not require tests with all possible frame member sizes.

Diaphragm shear deflections in buildings are relatively easy to determine when the roof is flat and the interior frames are pinned at the eaves. The problem is more complicated for rigid frames but can be solved by treating the diaphragm-frame interaction forces as if they arose from spring supports. Other shear deflection problems in pitched roof buildings are more complicated but can be solved by using deflection compatibility conditions between the building frames and the roof diaphragms.

## 8.3 Load Factors.

Load factors for light gage steel diaphragms were developed depending on the type of diaphragm connections. The development was within the framework of the AISI Specifications and resulted in the following recommended values:

Diaphragm Type	Wind or Earthquake Load Factor	Gravity Live Load Factor	Dead Load Factor
Screw Connected Diaphragm:	2.5	2.7	2.0
Diaph. w/Backed up Seam Connections:	2.1	2.7	2.0
Welded Diaphragms:	2.4	3.0	2.3

#### 8.4 Diaphragm Influence in Mill Buildings.

Diaphragms may be used to brace interior building frames against lateral loads and in some cases, against vertical loads. The moderately stiff standard corrugated diaphragm may reduce eave deflections in mill buildings by as much as 4 or 5 times from those determined when the diaphragm action is discounted. Similar reductions in bending moment are obtained when the diaphragm action is considered. This of course can lead to considerable reduction in the size of the interior building frames.

#### 8.5 Possibilities for Future Investigations.

The shear stiffness is probably the single most important parameter in light gage steel diaphragms for it is this that determines the diaphragm shear loads in all cases where deflection compatibility conditions must be met.

The variation in shear stiffness with length has been studied in considerable detail for the standard corrugated shape and the variation is predictable by the developed theory. However, diaphragms in large roofs will normally consist of more than one panel length and there is some question as to how the stiffness varies for the assembly. If both panels in a two panel length diaphragm are equal, it is reasonable to base the stiffness on one panel length since there can be little restraint against corrugation warping across most of the commonly used end laps. However, if one of the panels is somewhat different in length, the stiffness is different and the shorter section may never come under appreciable shear

load. The problem of shear stiffness of the overall assembly might be resolved by model tests of the type outlined in Chapter 6 where different combinations of panel lengths can be used.

The shear stiffness equation 2-16 establishes the stiffness variation with length of diaphragm. It is quite accurate for the various sizes of standard corrugated diaphragms tested and applies equally well to two square box rib diaphragms. The development of the equation is such that it should apply to any corrugation shape. However, it would be of interest to extend tests to other panel configurations for further verification.

## APPENDIX A - NOTATIONS

$a$	= test frame dimension perpendicular to loading direction
$b$	= frame dimension parallel to loading direction
$B$	= mill building bay length
$e$	= total fiber elongation
$E$	= modulus of elasticity
$F_{1j}$	= fixed end moment
$G'$	= shear stiffness
$h$	= corrugation pitch
$H$	= mill building eave height
$I_{eff}$	= effective moment of inertia of diaphragm frame
$K_1$	= member stiffness
$K, K_2$	= constants in shear deflection solution
$k_2$	= moment of inertia distortion factor
$L$	= developed corrugation width or rafter length
$l$	= diaphragm length parallel to corrugations
$M$	= bending moment
$n, k_1$	= scale factors for model building
$p(x)$	= distributed load
$P$	= concentrated shear load
$P_u$	= ultimate concentrated shear load
$R$	= rafter rise
$S$	= frame span
$S_a$	= allowable diaphragm shear in plf
$S_u$	= ultimate diaphragm shear in plf

SL	= shear force in leeward diaphragm
SW	= shear force in windward diaphragm
t	= diaphragm thickness
U	= bending energy
w	= diaphragm width perpendicular to corrugations
RLF	= load factor for reversed loads
DLF	= load factor for dead loads
GLFF	= gravity live load factor
$\Delta'$	= shear deflection
$\Delta_{\beta}$	= bending deflection
$\Delta$	= total deflection = $\Delta' + \Delta_{\beta}$
$\delta_w$	= warping deflection parallel to corrugation edge
$\delta'(x)$	= warping deflection normal to corrugation edge
$\delta'_c$	= shear deflection per foot of diaphragm dimension a
$\theta_i$	= joint rotation
$\rho_{ij}$	= member rotation
$\sigma$	= bending stress

## APPENDIX B

### Mill Building Computer Analysis.

The program is written in CORC, a computer language described in the Manual "CORC - The Cornell Computing Language" by R. W. Conway and W. L. Maxwell of the Department of Industrial Engineering, Cornell University, Ithaca, New York.

The definition of terms is contained in statements 0010 through 0059.

SOLUTION OF UNIFORMLY LOADED GABLE FRAME BY SLOPE  
DEFLECTION

DICTIONARY OF VARIABLES

VARIABLE			DESCRIPTION
0010 N			NUMBER OF TYPES OF LOADS
0011 SP			SPAN LENGTH IN FEET.
0012 EH			EAVE HEIGHT (FEET)
0013 R			RISE IN RAFTER (FEET)
0014 PW			WIND LOADS
0015 NW			IN
0016 NL			POUNDS
0017 PL			PER SQ.FT.
0018 VL			VERTICAL LOAD
0019 L			RAFTER LENGTH (FEET)
0020 F	5	5	FIXED END MOMENTS, FRAME CONV.
0022 K	2		REL. STIFF I/L IN <sup>4</sup> /FT.
0023 MW	5		WINDWARD DIAPH B. MOM FT LB
0024 A	5	5	COEF IN MATRIX
0025 ML	5		LEE DIAP BEND MOM FT LB
0026 AA	5	5	TEMP COEF IN MATRIX
0027 DW	5		WINDWARD BEND DEFL. IN.
0028 R	5		RIGHT SIDE OF MATRIX EQNS.
0029 DL	5		LEE SIDE BEND DEFL IN.
0030 BR	5		TEMPORARY B VALUES.
0031 IEFF			GIRDER MOMENT OF INERTIA
0032 X	5		UNKNOWN QUANTITIES
0034 E		30,000	\$10 <sup>6</sup> (6) FRAME MODULUS OF ELASTICITY
0036 IX	2		MAJOR MOM OF INERTIA IN <sup>4</sup> (4)
0037 P			COUNTER
0038 I			INDICES OR TEMP VARIABLE
0040 J			INDICES OR TEMP VARIABLE
0042 S			REDUCTION MULTIPLIER
0044 M			INDICES OR TEMP VARIABLE
0045 CHEK			THMPORARY CHECK CONST.
0046 MOM	4	5	BENDING MOMENTS FT-LB.
0047 G			SHEAR STIFFNESS (LR/IN.)
0048 DELH	4	5	HOR. EAVE DEFLN. (INCHES)
0049 Y			TEMP. VALUE FOR SW(1)
0050 BAY			BAY LENGTH (FEET)
0051 SW	8		WINDWARD DIAPH SHEAR LB.
0052 YY			TEMP. VALUE FOR SL(1)
0053 SL	8		LEEWARD DIAPH SHEAR LBS.
0054 GPM			SHEAR MODULUS LB/INCH
0055 NF			NUMBER OF INTERIOR FRAMES
0056 TL			CONSTANT * GPM (FT.-LB./FT.)
0057 C			VARIABLE COUNTER
0058 Q			COUNTER
0059 U			TEMPORARY CONSTANT

PROGRAM STATEMENTS

LABEL	STATEMENT
0060	READ N, SP, EH, R, IX(1), IX(2), BAY, IEFF, G
0070	LET DELH(2,1) = 0
0080	LET DELH(4,1) = 0
0100	REPEAT PROGRAM N TIMES
0110 PROGRAM	BEGIN
0120	READ PW, NW, NL, PL, VL, NF

```

0130          LET I = SQRT((SP/2)*S(2) + (R)*S(2))
0150          LET Q = I
0160 TEST     IF Q EQL I
0170                                     THEN GO TO GEQLZERO
0180                                     ELSE GO TO GNOTZERO
0190 GEQLZERO LET GPM = 0
0200          LET C = 2
0205          GO TO XAGAIN
0207 GNOTZERO LET GPM = G
0209          LET U = NF
0212          IF U EQL 1
0214                                     THEN GO TO ODD
0216                                     ELSE GO TO FVODD
0222 FVODD   REPEAT EVENODD UNTIL U LFO 1
0223 FVFNODD BEGIN
0225          LET U = U/2
0227 EVENODD END
0230          IF U EQL 1
0232                                     THEN GO TO EVEN
0234                                     ELSE GO TO ODD
0236 EVEN    LET C = NF/2 + 1
0238          GO TO XAGAIN
0240 ODD     LET C = NF/2 + 3/2
0244          NOTE FIRST 4 EQNS ARE IN FT-LBS. 5TH IN LBS.
0246          NOTE USE PROPER UNITS F.G. 1/144 ETC.
0248 XAGAIN  REPEAT XLOOP 1 TIMES
0260 XLOOP  BEGIN
0290          LET F(1,2) = 0
0300          LET F(5,4) = 0
0310          LET F(2,1) = -(PL*EH*EH*BAY)/B
0320          LET F(4,5) = (PW*EH*EH*BAY)/B
0330          LET F(2,3) = BAY*(NL*PL + VL*SP*SP/4)/12
0340          LET F(3,2) = -F(2,3)
0350          LET F(3,4) = BAY*(NW*PL + VL*SP*SP/4)/12
0360          LET F(4,3) = -F(3,4)
0370          NOTE K(1)=MEMBER STIFFNESS = MOM.INERTIA/LENGTH
0380          LET K(1) = IX(1)/LH
0390          LET K(2) = IX(2)/L
0400          LET A(1,1) = + (3*E*K(1) + 4*F*K(2))/144
0410          LET A(3,3) = A(1,1)
0420          LET A(1,2) = 2*F*K(2)/144
0430          LET A(2,3) = A(1,2)
0440          LET A(2,1) = A(1,2)
0450          LET A(3,2) = A(1,2)
0460          LET A(1,3) = 0
0470          LET A(2,4) = 0
0480          LET A(2,5) = 0
0490          LET A(3,1) = 0
0500          LET A(4,2) = 0
0510          LET A(2,2) = 3*F*K(2)/144
0520          LET A(4,3) = A(2,2)
0530          LET A(4,2) = 12*F*K(2)/144
0540          LET A(5,1) = (3*E*K(1))/(144*EH)
0550          LET A(5,3) = A(5,1)
0570          LET TL = (GPM*EH*SP)/(2*BAY)
0600          LET A(1,5) = - 3*E*K(2)*LH/D/144
0610          LET A(3,4) = A(1,5)
0620          LET A(1,4) = (-3*E*K(1) - K(2)*LH/D)/144
0630          LET A(3,5) = A(1,4)
0640          LET A(4,5) = 6*E*K(2)*LH/(144*D)

```

```

0641          LET A(4,1) = 3*E*K(1)*(1+2*R/EH)/144
0642          LET B(1) = F(2,1) + F(2,3)
0643          LET B(2) = F(3,2) + F(3,4)
0644          LET B(3) = F(4,3) + F(4,5)
1070 NEWBEND  REPEAT SOLVBEND 1 TIMES
1075          REPEAT YLOOP FOR P = (2,1, C)
1080 YLOOP    BEGIN
1102          IF P EQL C
1104                                THEN GO TO ODCHK
1106                                ELSE GO TO NFEVNTWO
1108 ODCHK    IF U EQL 1
1110                                THEN GO TO NFEVNTWO
1112                                ELSE GO TO NFODDTWO
1114 NFODDTWO LET B(4) = (- (PL)*EH*R + (L*L*NW)/2 + VL*SP*SP/4 + NL*(L*L
1116 C          - 4*R*R)/2)*BAY + (1+2*R/EH)*F(2,1) +
1118 C          F(4,3) + 2*F(3,4) - 2*R*SP*(TL*DELH(2,P-1)
1120 C          /EH + GPM*L*DL(P)/BAY)/L
1122          LET B(5) = ((PW-PL)*EH/2 + (NW-NL)*R)*BAY + (F(2,1) + F(4,5)
1124 C          )/EH - TL*SP*(DELH(2,P-1) + DELH(4,P-1))
1126 C          / (L*EH) - GPM*SP*(DL(P) + DW(P))/BAY
1130          LET A(5,4) = -(3*E*K(1)/EH + 3456*TL*SP/(2*L))/144
1132          LET A(5,5) = A(5,4)
1134          LET A(4,4) = (-3*E*K(1) - 3*E*K(1)*2*R/EH - 9*E*EH*
1136 C          K(2)/R - 3456*TL*R*SP/L)/144
1150          GO TO SOLVTWO
1155 NFEVNTWO LET B(4) = (- (PL)*EH*R + (L*L*NW)/2 + VL*SP*SP/4 + NL*(L*L
1160 C          - 4*R*R)/2)*BAY + (1+2*R/EH)*F(2,1) +
1165 C          F(4,3) + 2*F(3,4) - (TL*R*SP*DELH(2,P-1))/
1170 C          (L*EH) - SL(P)*R*SP/L
1175 C          - R*SP*GPM*DL(P)/BAY
1180          LET B(5) = ((PW-PL)*EH/2 + (NW-NL)*R)*BAY + (F(2,1) + F(4,5)
1185 C          )/EH - TL*SP*(DELH(2,P-1) + DELH(4,P-1))
1190 C          / (2*L*EH) - (SL(P) + SW(P))*(SP/(2*L))
1195 C          - GPM*SP*(DW(P) + DL(P))/ (2*BAY)
1196          LET A(5,4) = -(3*E*K(1)/EH + 1728*TL*SP/(2*L))/144
1197          LET A(5,5) = A(5,4)
1198          LET A(4,4) = (-3*E*K(1) - 3*E*K(1)*2*R/EH - 9*E*EH*
1199 C          K(2)/R - 1728*TL*R*SP/L)/144
1200 SOLVTWO  REPEAT SOLVE 1 TIMES
1210          NOTE X(1) THRU X(3) = THETA2 THRU THETA4 - JOINT ROTAT
1220          NOTE X(4) AND X(5) = MEMB ROT. OF MEMB 1-2 AND 4-5 RESP
1230          LET I = 3*E*K(1)/144
1240          LET J = 4*E*K(2)/144
1250          LET M = 2*E*K(2)/144
1260          LET S = 3*E*K(2)*EH/(144*R)
1270          LET MOM(2,P) = F(2,1) - I*X(1) + I*X(4)
1280          LET MOM(3,P) = F(3,2) - M*X(1) - J*X(2) + S*(X(5) - X(4))
1282          LET MOM(4,P) = F(4,3) - M*X(2) - J*X(3) + S*(X(4) - X(5))
1336          LET SW(P-1) = (TL/EH)*(X(5)*EH*12 - DELH(4,P-1))
1337 C          - GPM*L*(DW(P))/BAY
1338          LET SL(P-1) = (TL/EH)*(X(4)*EH*12 - DELH(2,P-1))
1339 C          - GPM*L*(DL(P))/BAY
1340          NOTE HOR DEFL AT EAVES TO RIGHT IS POSITIVE
1342          LET DELH(2,P) = EH*X(4)*12
1344          LET DELH(4,P) = EH*X(5)*12
1357 YLOOP    END
1362          IF GPM EQL 0
1363                                THEN GO TO XLOOP
1364                                ELSE GO TO ABLE
1365 ABLE     IF ABS(CHEK - DELH(4,2)) GTR (EH/75000 )

```

```

1366                                     THEN GO TO BAKER
1367                                     ELSE GO TO XLOOP
1368 BAKER                               LET CHEK = DELH(4,2)
1370                                     NOTE TEMPORARY CHECK ON CONTROL
1372                                     IF ABS(CHEK) GTR 100
1374                                     THEN GO TO XLOOP
1376                                     ELSE GO TO NEWRFND
1378 XLOOP                               END
1380                                     LET CHEK = 0
1381                                     TITLE
1382                                     TITLE
1383                                     TITLE
1384                                     TITLE SHEAR + BENDING SOLUTION
1386                                     TITLE RESULTS ARE FOR THE FOLLOWING BAY SIZE AND LOADS
1388                                     WRITE BAY, GPM, TL, PW, NW, NL, PL, VL, NF
1390                                     REPEAT WLOOP FOR P = (1,1,C-1)
1400 WLOOP                               BEGIN
1410                                     WRITE MOM(2,P+1), MOM(3,P+1), MOM(4,P+1)
1420                                     WRITE SL(P), SW(P)
1430                                     WRITE DELH(2,P+1), DFLH(4,P+1)
1431                                     LET MOM(2,P+1) = 0
1432                                     LET MOM(3,P+1) = 0
1433                                     LET MOM(4,P+1) = 0
1434                                     LET SL(P) = 0
1435                                     LET SW(P) = 0
1436                                     LET DELH(2,P+1) = 0
1437                                     LET DFLH(4,P+1) = 0
1440 WLOOP                               END
1445                                     REPEAT ZEROLOOP FOR I = (1,1,5)
1450 ZEROLOOP                             BEGIN
1455                                     LET MW(I) = 0
1459                                     LET ML(I) = 0
1465                                     LET DL(I) = 0
1470                                     LET DW(I) = 0
1475 ZEROLOOP                             END
1480                                     TITLE
1481                                     TITLE
1510                                     LET Q = Q+1
1520                                     IF Q GTR 2
1530                                     THEN GO TO RESET
1540                                     ELSE GO TO TEST
1545 RESET                               LET NF = NF - 1
1550                                     IF NF EQL 0
1555                                     THEN GO TO PROGRAM
1560                                     ELSE GO TO TEST
1630 PROGRAM                             FND
1635                                     NOTE GAUSSIAN ELIMINATION SUBROUTINE
1809 SOLVE                               BEGIN
1810                                     NOTE RETAIN A(I,J) AND B(I)
1820                                     REPEAT SUBSTUTE FOR I=(1,1,5)
1830 SUBSTUTE                             BEGIN
1840                                     REPEAT SUBSUB FOR J = (1,1,5)
1850 SUBSUB                               BEGIN
1860                                     LET AA(I,J) = A(I,J)
1870 SUBSUB                               END
1880                                     LET BB(I) = B(I)
1890 SUBSTUTE                             END
1900                                     NOTE SOLVE SYSTEM BY GAUSSIAN ELIMINATION
1910                                     REPEAT HLOOP FOR I = (1,1,4)
1920 HLOOP                               BEGIN

```

```

1930 REPEAT PLOOP FOR J = (1+1,5)
1940 PLOOP BEGIN
1950 IF AA(J,1) EQL 0
1960 THEN GO TO PLOOP
1970 ELSE GO TO CALCULAT
1980 CALCULAT LET S = -AA(J,1)/AA(1,1)
1990 REPEAT AJM FOR M=(1,5)
2000 AJM BEGIN
2010 LET AA(J,M) = AA(J,M) + S*AA(1,M)
2020 AJM END
2030 LET BB(J) = BB(J) + S*BB(1)
2040 PLOOP END
2050 MLOOP END
2060 LET J=5
2070 REPEAT QRI FOR I=(5,-1,1)
2080 QRI BEGIN
2090 LET M = BB(I)
2100 JEQL1 IF J EQL I
2110 THEN GO TO JN
2120 ELSE GO TO MTERM
2130 MTERM LET M = M - AA(1,J)*X(J)
2140 LET J=J-1
2150 GO TO JEQL1
2160 JN LET J=5
2180 LET X(1) = M/AA(1,1)
2190 QRI END
2191 SOLVE END
2195 NOTE BENDING DEFLECTION SUBROUTINE
2200 SOLVBEND BEGIN
2210 LET Y = 0
2220 LET YY = 0
2288 REPEAT MLOOP FOR I = (1,1,(-1)
2289 MLOOP BEGIN
2290 LET Y = Y + SW(I)
2291 LET YY = YY + SL(I)
2292 LET MW(I) = BAY*Y
2293 LET ML(I) = BAY*YY
2294 MLOOP END
2300 LET DW(2) = 1728*(BAYS(2))*(5*MW(1)/6 + MW(2) + MW(3)
2301 C + MW(4))/(E*I*EFF)
2302 LET DW(3) = 1728*(BAYS(2))*(MW(1)+1*MW(2)/6 + 2*MW(3)
2304 C + 2*MW(4))/(E*I*EFF)
2306 LET DW(4) = 1728*(BAYS(2))*(MW(1)+2*MW(2)+17*MW(3)/6
2308 C + 3*MW(4))/(E*I*EFF)
2310 LET DW(5) = 1728*(BAYS(2))*(MW(1)+2*MW(2)+3*MW(3) +
2312 C 27*MW(4)/6)/(E*I*EFF)
2322 LET DL(2) = 1728*(BAYS(2))*(5*ML(1)/6 + ML(2) + ML(3)
2324 C + ML(4))/(E*I*EFF)
2326 LET DL(3) = 1728*(BAYS(2))*(ML(1) + 11*ML(2)/6
2328 C + 2*ML(3)+2*ML(4))/(E*I*EFF)
2330 LET DL(4) = 1728*(BAYS(2))*(ML(1)+2*ML(2)+17*ML(3)/6
2332 C + 3*ML(4))/(E*I*EFF)
2332 LET DL(5) = 1728*(BAYS(2))*(ML(1)+2*ML(2)+3*ML(3)
2334 C + 27*ML(4)/6)/(E*I*EFF)
2340 SOLVBEND END
2600 STOP

```

## TYPICAL DATA SET

VARIABLE	INITIAL VALUE
----------	---------------



## BIBLIOGRAPHY

1. Timoshenko, S. P. and Gere, J. M., Theory of Elastic Stability, McGraw-Hill, New York, 1961.
2. Smith, G. E., "Elastic Buckling in Shear of Infinitely Long Corrugated Plates with Clamped Parallel Edges", M.A.E. Thesis, Cornell University, 1957.
3. McKenzie, K. I., "The Shear Stiffness of a Corrugated Web", Aeronautical Research Council Reports and Memoranda No. 3342, London, 1963.
4. Shimizu, E. S., "Optimum Design of Corrugated Panels in Shear", M.S. Thesis, University of California, Los Angeles, 1959.
5. Nilson, A. H., "Deflections of Light Gage Steel Floor Systems Under the Action of Horizontal Loads", M.S. Thesis, Cornell University, 1956.
6. Nilson, A. H., "Shear Diaphragms of Light Gage Steel", Journal of the Structural Division, ASCE, Vol. 86, Nov., 1960.
7. Godfrey, D. A. and Bryan, E. R., "The Calculated and Observed Effects of Dead Load and Dynamic Crane Loads on the Framework of a Workshops Building", Inst. of Civ. Engr., Vol. 13, June, 1959.
8. Bryan, E. R. and El-Dakhakhini, W. M., "Shear of Thin Plates with Flexible Edge Members", Proceedings of the ASCE, Vol. 90, No. ST4, August, 1964.
9. Biggs, J. M., "Wind Forces on Structures: Final Report of the Task Committee on Wind Forces of the Committee on Loads and Stresses of the Structural Div., ASCE", Transactions, ASCE, Vol. 126 II, 1961.
10. Kinney, J. S., Indeterminate Structural Analysis, Addison-Wesley, Reading, Mass., 1957.
11. Light Gage Cold-Formed Steel Design Manual, American Iron and Steel Institute, New York, 1962.
12. Luttrell, L. D., "Structural Performance of Light Gage Steel Diaphragms", Ph.D. Thesis, Cornell University, Sept., 1965.

Table 4-1. Summary of Heavy Frame Tests.

Test No.	Panel Type & Cover Width	Gage <sup>+</sup> S.or G.	Span (ft.)	End Conn. Panel-Frame No./Panel	Intermediate Fasteners <sup>++</sup>	Max.Load (plf)	
1	18" Narrow Rib Roof Deck	22/S	6	3 Puddle Welds	None	310	] F
2	"	"	"	"	F.W.@ 36"	414	
3	24" Wide Rib Roof Deck	22/S	6	"	None	285	] F
3A	"	"	"	"	F.W.@ 24"	475	
4*	24" Standard Corrugated	26/G	3	3-#14 Screws	None	177	
4A	"	22/G	"	"	None	467	] F } G
4B	"	26/G	"	"	None	232	
5	"	"	"	"	#10 Screws @ 18"	467	
6	"	29/G	"	"	None	222	
7**	24" Deep Corrugated	26/G	5	"	None	316	
7A	"	"	"	"	None	229	] F
8	"	"	"	"	#10 Screws @ 30"	375	
9*	24" Box Rib	26/G	"	"	None	107	] F
10	"	"	"	"	#10@ 36"	246	
11	36" Box Rib	"	"	6 Lock Rivets	None	330	] F } C.W.
12	"	"	"	"	L.R. @ 20"	567	
13	24" Box Rib	"	"	"	None	267	] F } C.W.
14	"	"	"	"	L.R. @ 20"	485	

+ S- Steel; G- Galvanized

++ F.W. - Fillet Weld; L.R. - Lock Rivet.

\* No panel-to-panel connections anywhere along the side lap.

\*\* Panels had longitudinal cracks prior to testing. Did not use the special panel-to-frame connections as in 7A.

Brackets along the right column indicate comparisons for the influence of: F - panel-to-panel connections; G - thickness; and C.W. - cover width.

Table 4-2. Diaphragm Material Properties.\*

Panel Type	Used for Tests No.	Gage	Tensile Strength (ksi)		Elong. per 2" (%)
			Yield at 0.2% off.	Ult.	
Narrow Rib Roof Deck	1 and 2	22	32.8	45.3	25
Wide Rib Roof Deck	3 and 3A	22	35.5	49.1	37
Standard Corr.	4	26	53.3	66.5	20
Standard Corr.	4A	22	43.3	54.7	35
Standard Corr.	4B	26	64.3	69.6	24
Standard Corr.	5, 4L, 5L, 5Z	26	56.5	61.8	25
Standard Corr.	6	29	50.9	65.3	27
Deep Corrugated (Full Hard)	7	26	153.0	154.5	3.5
Deep Corrugated (Full Hard)	7A and 8	26	116.7	116.8	3.0
Box Rib Panels	9 and 10	26	48.3	59.7	28
Box Rib Panels	11, 12, 13, 14 11L thru 12L 12R	26	50.0	61.1	28

\*Based on random samples from each shipment of material.

Table 4-3. Diaphragm Material Properties.\*

Panel Type	Used For Tests No.	Galvanized Thickness (in.)	Uncoated Thickness (in.)	Tensile Strength (ksi)		Elong. per 2" %
				Yield at 0.2% off.	Ult.	
26 ga. std. corrugated	4P, 5P, 5R	0.02035	0.01875	58.7	63.3	25
26 ga. std. corrugated	4R, 4R-2	.02052	.01865	60.2	64.8	27
26 ga. std. corrugated	Small Diaphragms, 5PA, 5PA-R	.02238	.02008	48.1	51.0	29
26 ga. std. corrugated	5R-2, 5R-3, 5R-4, 5R-5, 5R-6	.02117	.01940	57.4	62.3	23
26 ga. High St. Deep Corrugated	7P, 7R, & 7R-2	.02264	.01933	107.4	107.7	3.2
26 ga. High St. Deep Corrugated	8P, 8R, & 8R-2	.02186	.01884	128.6	128.6	3.0
22 ga. std. Corrugated	4AP, 4AP-2, 4AP-3	.03260	.03100	33.4	45.4	30
26 ga. std. corrugated	1-10x12-1, 28, 28R 1-10x12-2, 30, 30R	.02133	.01829	48.2	56.8	24
28 ga. std. Corrugated	6AP, 6AP-2	.02000	.01617	50.1	54.9	20
26 ga. Box Rib (Mild)	20, 20R	.02227	.02026	54.5	60.7	25
26 ga. Box Rib (Full Hard)	22, 22R	.02217	.02002	101.4	102.5	3.0
22 ga. Galv. Roof Deck	24, 24R, 26, 26R	.03181	.03032	49.2	57.6	26

\* Based on random samples from each shipment of material.

Table 4-4. Small Diaphragm Tests on 26 Gage Corrugated Panels

Series Description	Test No.	Ultimate Strength (plf)	G' (lb/in)	Avg. G' (lb/in)	Comments
B Series 17 3/4" x 24" Std. Corr. Loaded Parallel to 17 3/4" dim. See Fig. 3-6.	3B0-1	*	2260	2000	#14 screw fasteners used except as indicated. First digit indicates the nth valley fastener spacing. The third digit gives the number of intermediate edge fasteners.
	3B0-2	785	1830		
	3B1-1	1095	1920		
	2B0-1	1300	3150	3280	
	2B1-1	1600	3410		
	1B0-1	1890	11250		
	1B1-1	2640	21000		
	C Series 28" x 24" Std. Corr. Loaded Parallel to the 28" dim. See Fig. 3-7.	3C0-1	515	3120	
3C0-2		625	3120		
3C1-1		815	3120		
2C0-1		960	4880	5300	
2C1-1		1140	5720		
1C0-1		1630	11350		
1C1-1	1990	18200			

\* Not loaded to failure.

Table 4-5. Summary of Light Frame Tests.

Test Type, Number and Loading Cond.*	Type Conn.	Intermediate Fasteners	Ult. Str. (lbs)	% Reduction From Static Strength**	Ave. Red. (%)
26 Gage Standard Corrugated					
5P (S.L.)	Screw	Yes	7200	-	-
5Z (5 P.L. to $.4P_u$ )	"	"	6750	6.2	
5R (5 Cy to $0.4P_u$ )	"	"	5000	30.6	
5R-2 (5 Cy to $0.4P_u$ )	"	"	6300	12.5	18.5
5R-4 (5 Cy to $0.4P_u$ )	"	"	6300	12.5%	
5R-3 (29 Cy to $.3P_u$ )	"	"	5000	30.6%	
5R-5 (29 Cy to $.3P_u$ )	"	"	6800	5.5	12
5R-6 (29 Cy to $.3P_u$ )	"	"	7250	0.0	
26 Gage Standard Corrugated					
4P (S.L.)	Screw	no	4700	-	
4R (5 Cy to $.4P_u$ )	"	"	4300	8.5	
4R-2 (29 Cy to $.3P_u$ )	"	"	4400	6.5	
26 Gage Standard Corrugated					
5P-A (S.L.)	Backed Up Fastener	Yes	7350	-	
5PA-R(29 Cy to $.4P_u$ )	"	"	7170	2.5	
26 Gage Box Rib Panels					
12P (S.L.)	Lock Rivet	Yes	5400	-	
12R (5 Cy to $.4P_u$ )	"	"	5350	0	
26 Gage High Strength Deep Corr.					
8P (S.L.)	Screw	Yes	6300	-	
8R (5 Cy to $.4P_u$ )	"	"	5500	13.0	
26 Gage High Strength Deep Corr.					
7P (S.L.)	Screw	no	3930	-	
7R (5 Cy to $.4P_u$ )	"	"	3300	16	
7R-2 (25 Cy to $.3P_u$ )	"	"	3470	11.7	

\* S.L.: Static Load; P.L.: Pulsating Load; Cy: Fully reversed cyclic Load.

\*\* The static strength is given as the first entry in each frame.

Table 4-5. Continued.

Test Type, Number and Loading Cond.*	Type Conn.	Intermediate Fasteners	Ult. Str. (lbs)	% Reduction From Static Strength**	Ave. Red. (%)
26 Gage Box Rib (Soft)					
20 (S.L.)	Screw	No	3370	-	
20R (5 Cy to $.4P_u$ )	"	"	3350	0	
26 Gage Box Rib (Full Hard)					
22 (S.L.)	Screw	No	4400	-	
22R (5 Cy to $.4P_u$ )	"	"	4000	9	
22 Gage Roof Deck					
24 (S.L.)	Weld	No	3510	-	
24R (5 Cy to $.4P_u$ )	"	"	3340	5	
22 Gage Roof Deck					
26 (S.L.)	Weld	Yes	4400	-	
26R (5 Cy to $.4P_u$ )	"	"	4350	0	
22 Gage Standard Corrugated					
4AP (S.L.)	Screw	No	6150	-	
4AP-2 (S.L.)	"	"	5800	-	
4AP-3 (S.L.)	"	"	6470	-	
28 Gage Standard Corrugated					
6AP (S.L.)	Screw	No	3700	-	
6AP-2 (S.L.)	"	"	4100	-	

\* S.L.: Static Load, P.L.: Pulsating Load, Cy: Fully reversed cyclic load.

\*\* The static strength is given as the first entry in each frame.

Table 4-6. Average Decrease in Static Strength Due to Load Reversals in the Indicated Regime.

<u>Diaphragm Type</u>	<u>Average Reduction (%)</u>
<u>All Tests Having:</u>	
25 or more cycles at 0.3 $P_u$	10.9
5 cycles at 0.4 $P_u$	10.7
<u>Screw Connected Diaphragms:</u>	
25 or more cycles at 0.3 $P_u$	10.9
5 cycles at 0.4 $P_u$	12.8
<u>Diaphragms w/Backed up Conn.:</u>	
5 cycles at 0.4 $P_u$	1.3
<u>Welded Diaphragms</u>	
5 cycles at 0.4 $P_u$	2.5

Table 4-7. Shear Stiffness for Full Sized Diaphragms.

Diaphragm Type (lxw)	Light Frame		Heavy Frame	
	Test No.	G'(lb/in)	Test No.	G'(lb/in)
Box Rib Panels (10' x 12')	11L	6,970		
	12L	9,600		
	11P	4,730	11	5,125
	12P	12,430	12	12,880
	12R	10,800		
Standard Corr. (12' x 10')	4L	20,750	4B	18,900
	5L	15,430	5	26,000
Welded Roof Deck (12' x 10')			3	5,210
			3A	5,730
	24	9,750		
	26	16,680		
High Strength Deep Corrugated Panels (10' x 12')	7A	5,600		
	8	9,200		
			7P	9,000
			8P	15,000

Table 7-1. Ultimate Shear Strength and Stiffnesses of  
26 Gage Standard Corrugated Diaphragms.

Diaphragm Size (ft.)	Frame	Ultimate Shear $S_u$ (plf)	$P/\Delta'$ (lb/in)	Stiffness $G'$ (lb/in)
$l \times w$	a/b			
12 x 10	10/12	600	56,800	47,200
10 x 6	10/6	600	16,100	26,900
6 x 12	6/12	587	38,600	19,300
6 x 10	10/6	600	11,600	19,370
6 x 6	6/6	600	15,700	15,700
-----				
4 x 4*	4/4	---	8,000	8,000
1.48 x 2	2/1.48	675	1,670	2,260

\* The last two tests were made on a 1 1/2" x 1 1/2" angle frame while the first 5 tests were made on a 6" x 1 1/2" channel frame.

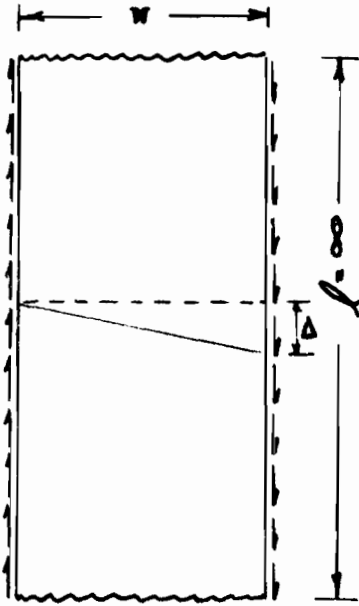


Fig. 2-1. Infinite sheet in shear.

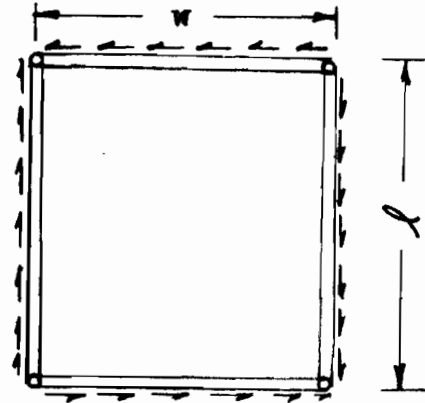


Fig. 2-2. Finite diaphragm with pin-ended rigid edge members.

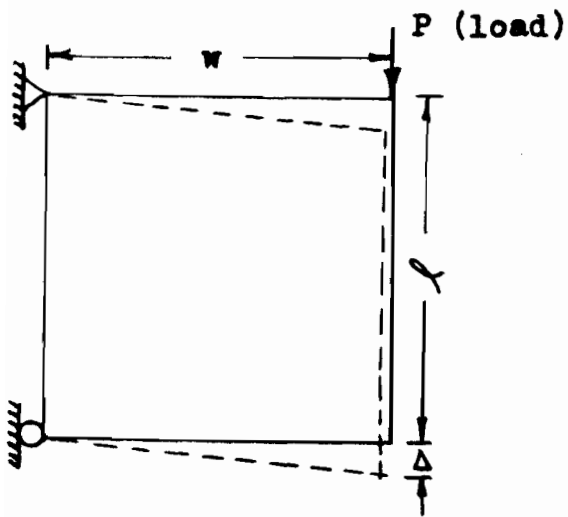


Fig. 2-3. Diaphragm with shears applied through edge beams.

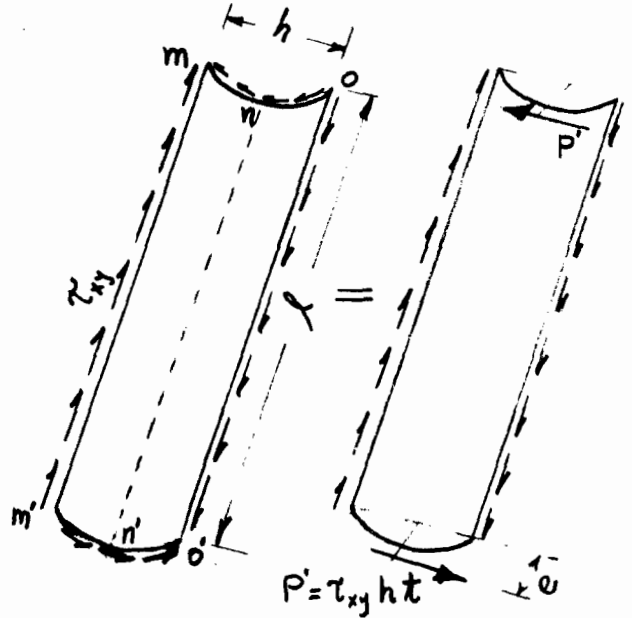


Fig. 2-4. Idealized single corrugation in pure shear.  $e$  locates the shear center.

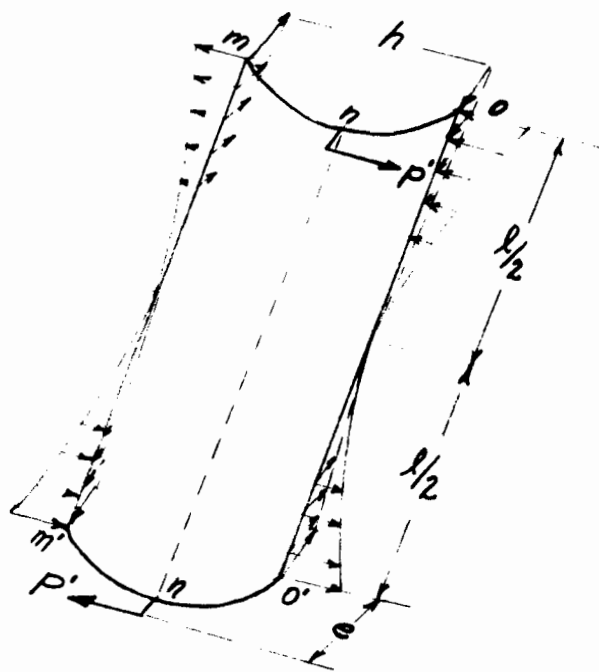


Fig. 2-5. Idealized corrugation loaded through shear center.

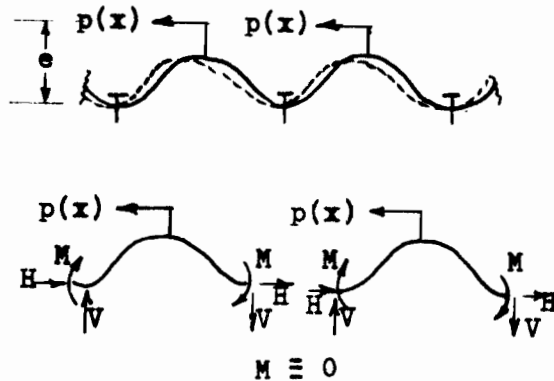


Fig. 2-6. End view of warped corrugations.

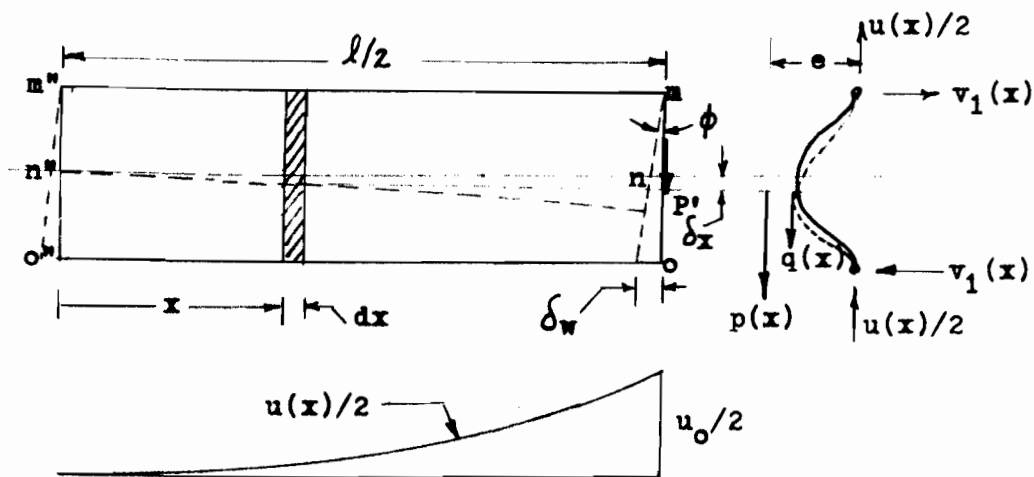


Fig. 2-7. Half-length corrugation freebody.

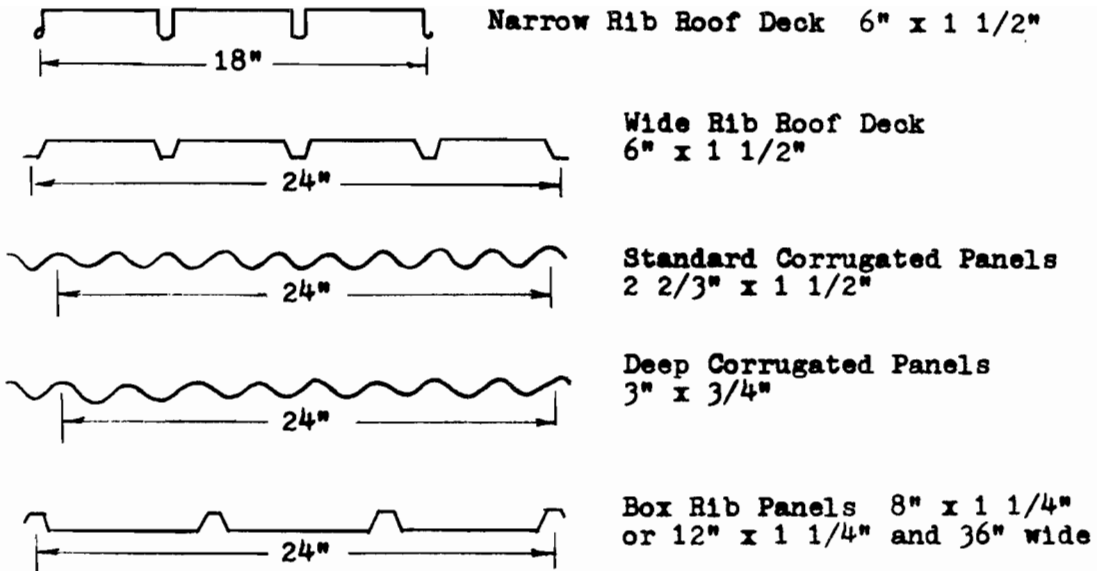


Fig. 3-1. Panel Configurations showing nominal dimensions.

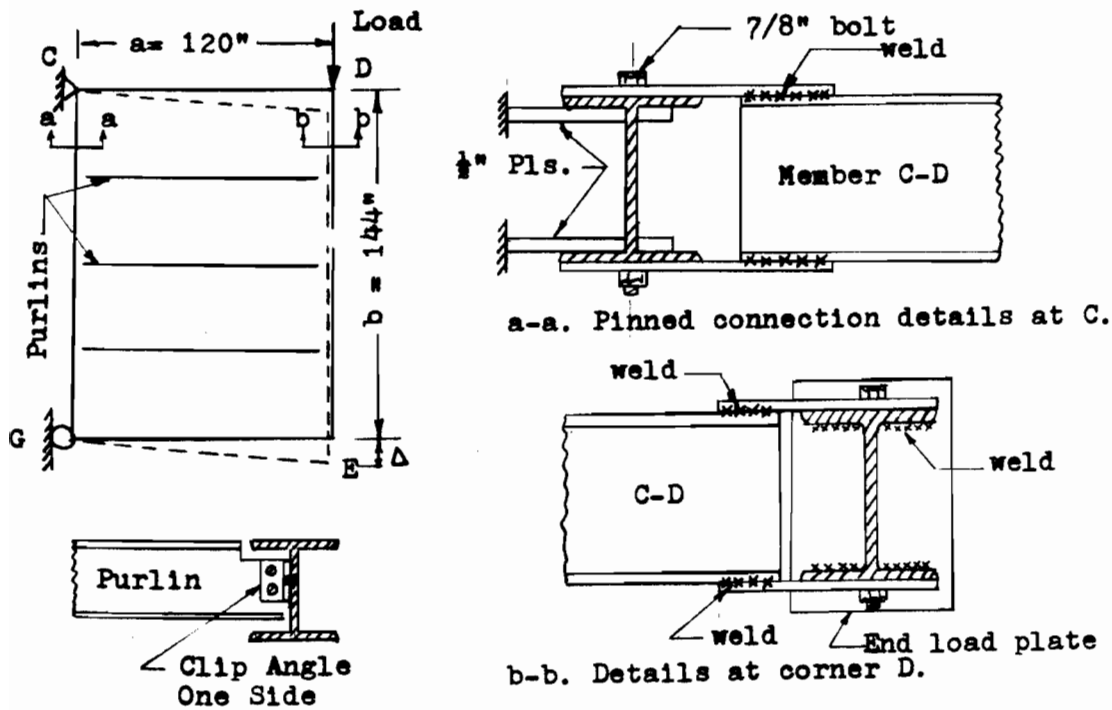
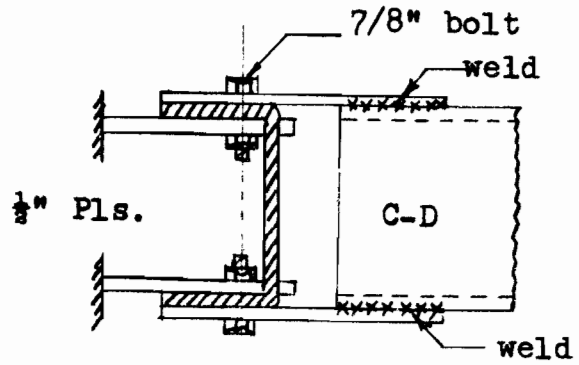
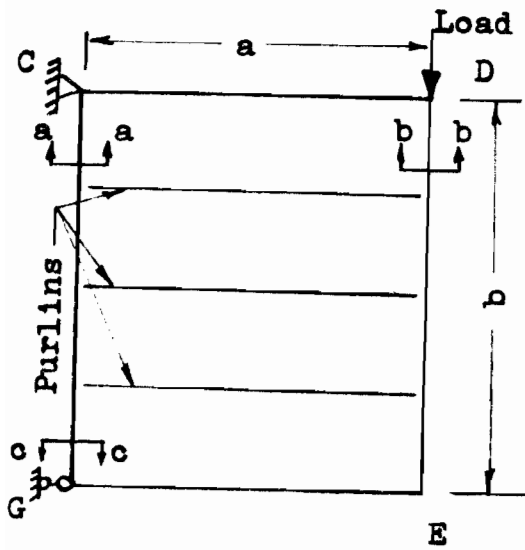
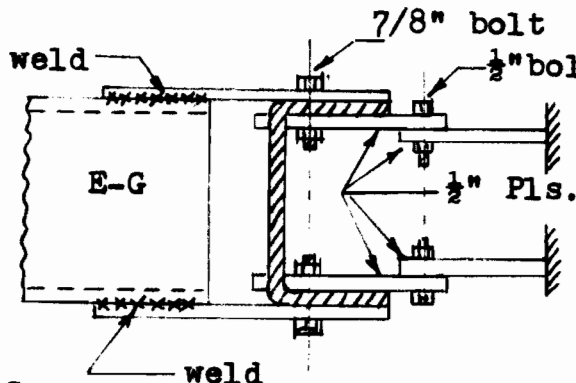


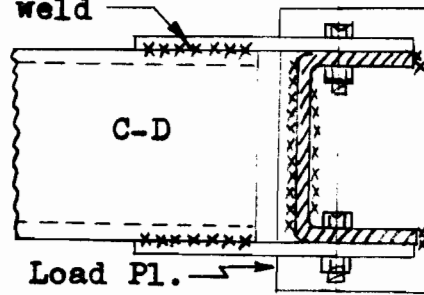
Fig. 3-2. Heavy frame details. Purlin spacing is variable and they may span either direction.



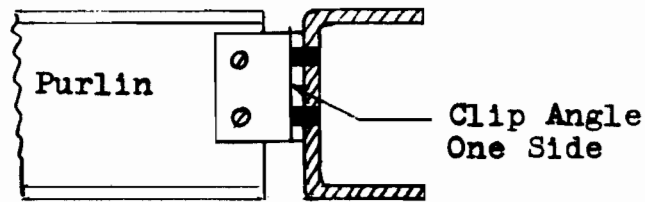
Section a-a. Details of pinned corner support at C.



Section c-c. Double link details at corner G.



Section b-b. Pinned corner details at D.



Typical purlin-to-edge beam connection.

Fig. 3-3. Light frame details. Purlin spacing is variable and the purlins may span either direction.

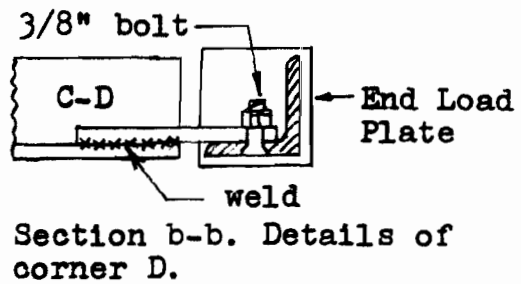
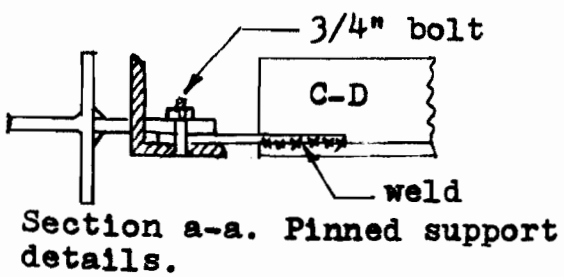
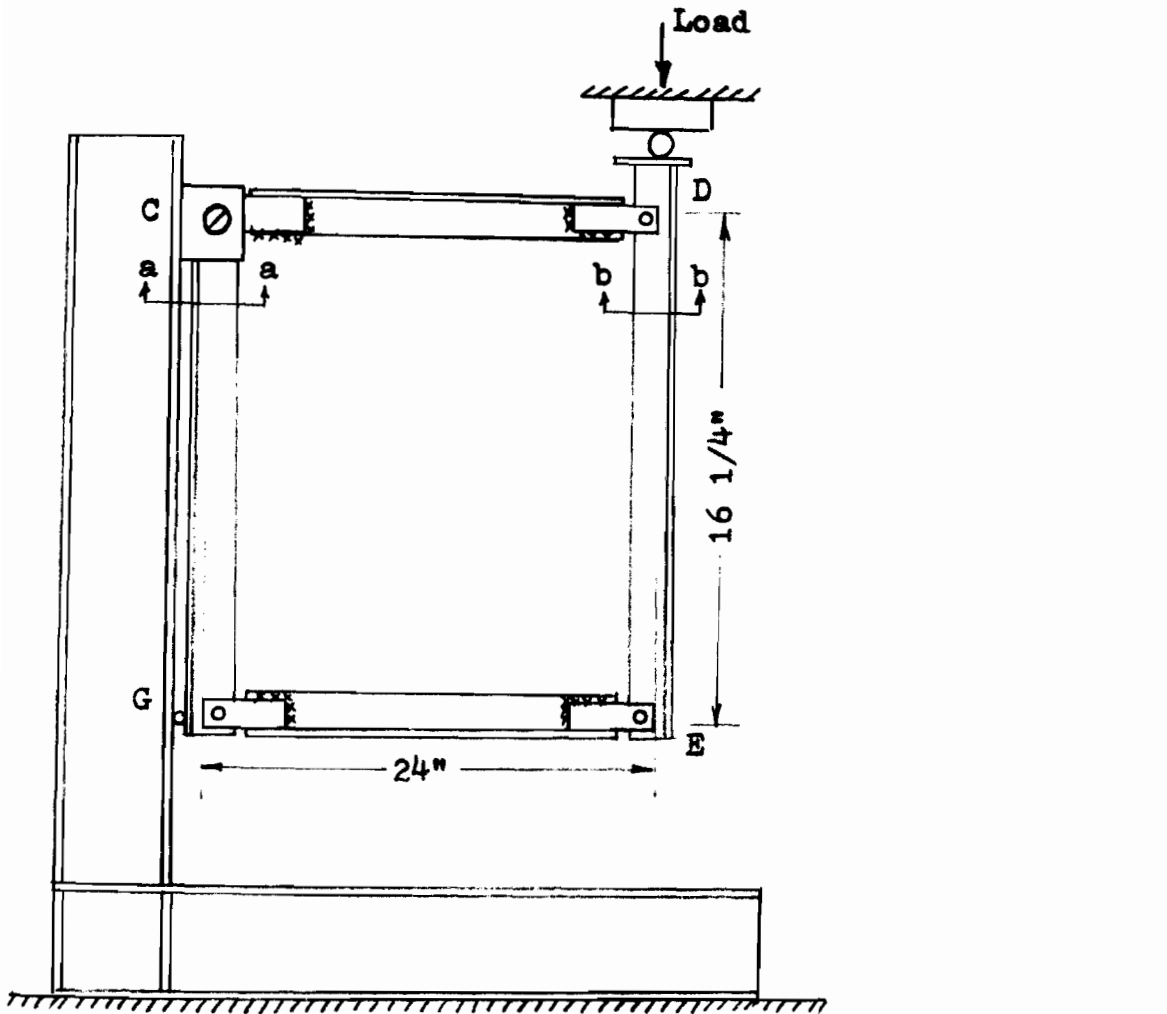


Fig. 3-4. Equal leg angle test frame details. Diaphragm is attached to far side.

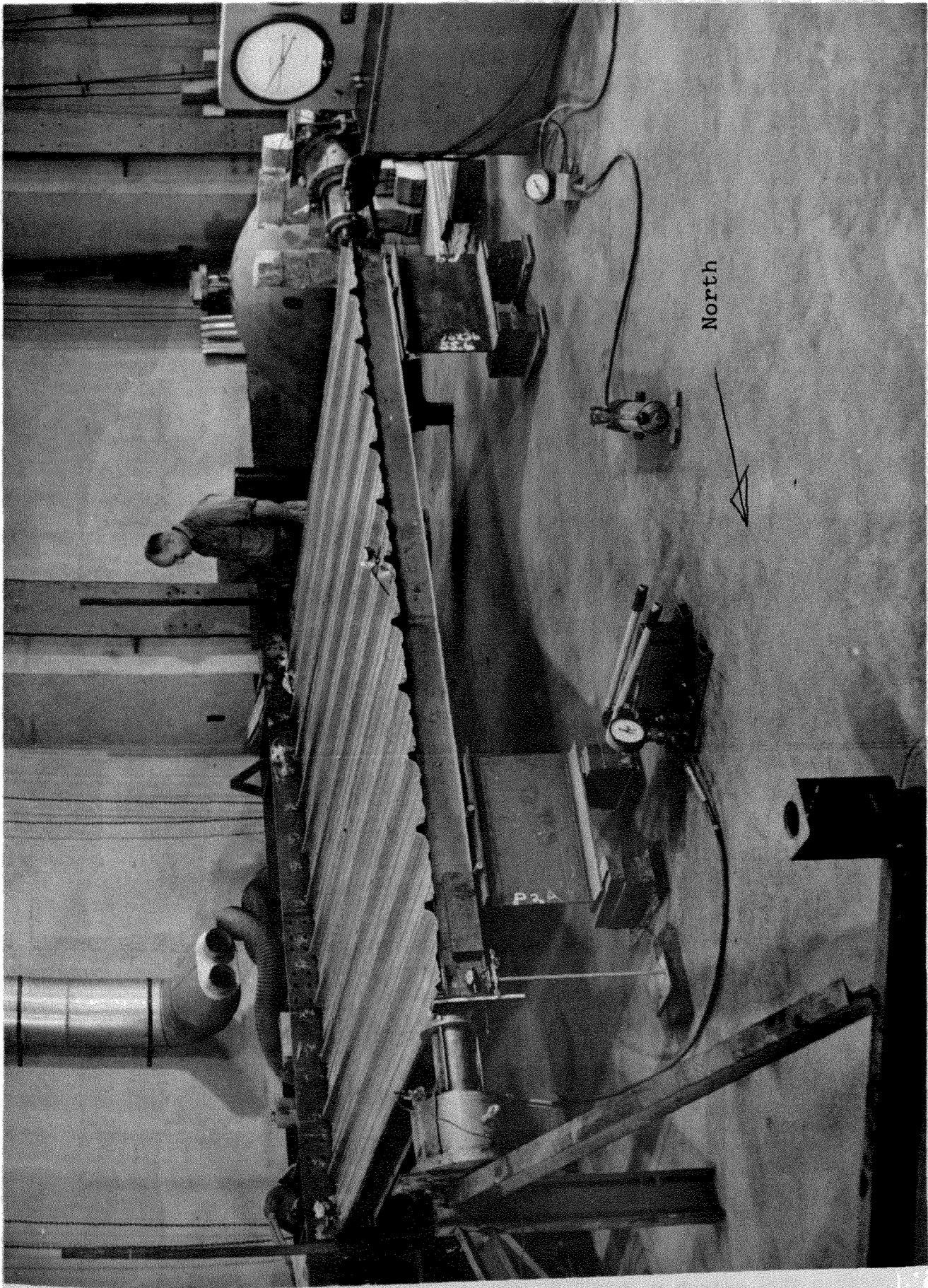
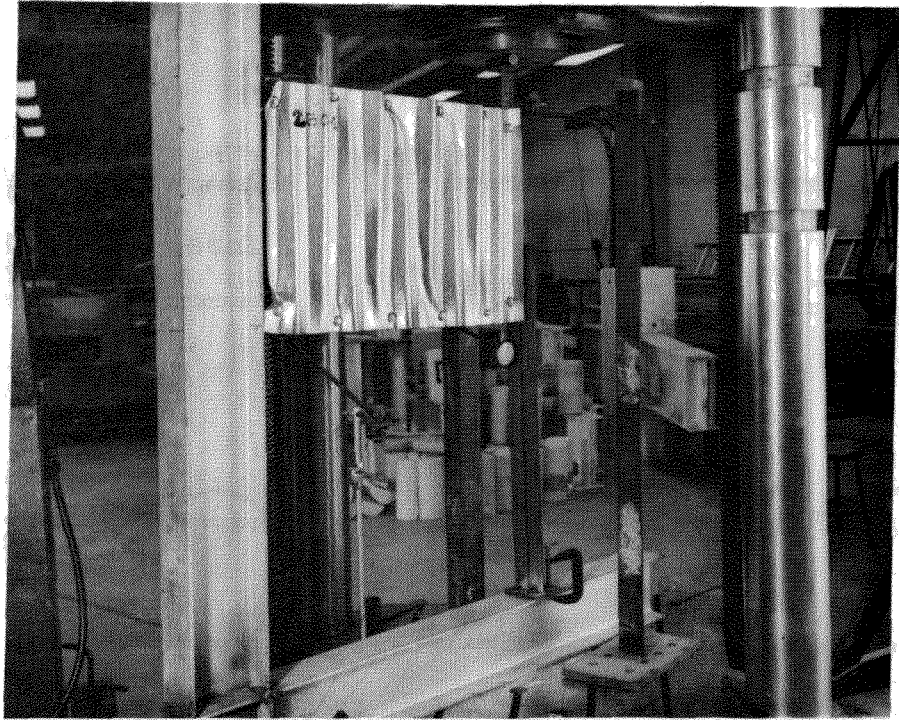
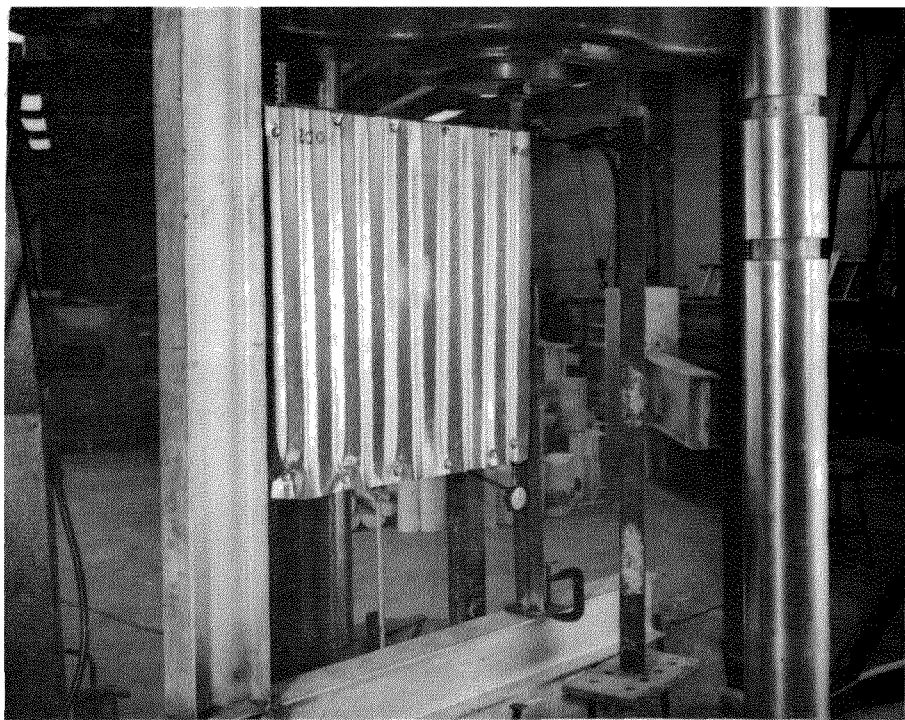


Fig. 3-5. Typical Diaphragm Test Setup.



280-1

Fig. 3-6. 26 Gage Standard Corrugated B Series (17 3/4" x 24").



2C0-1

Fig. 3-7. 26 Gage Standard Corrugated C Series (28" x 24").

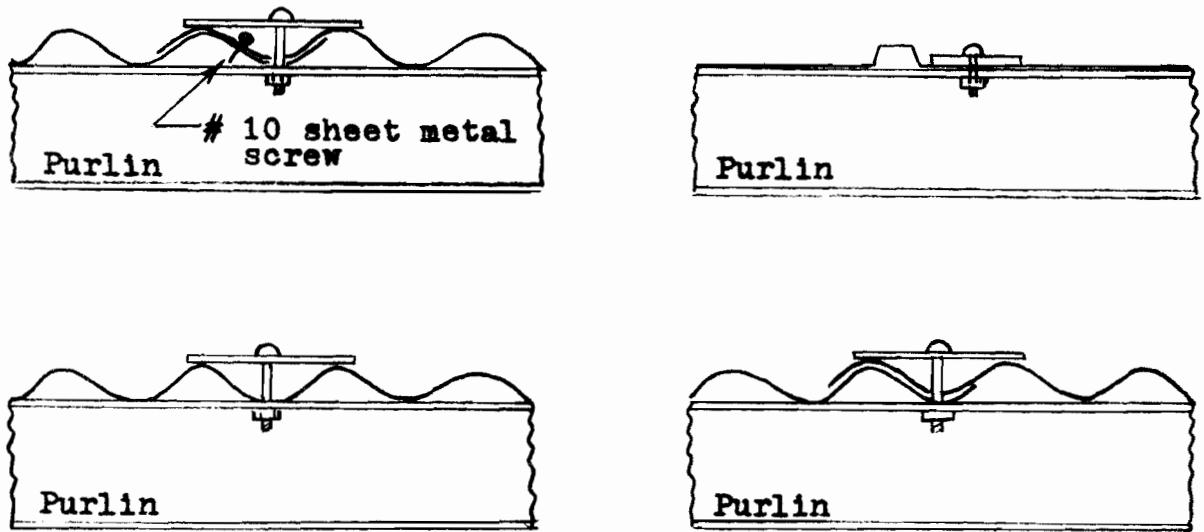


Fig. 3-8. Special purlin connections using 4" x 4" greased plates. The hole in the panel was 3/4" and the bolt was 3/16" diameter.

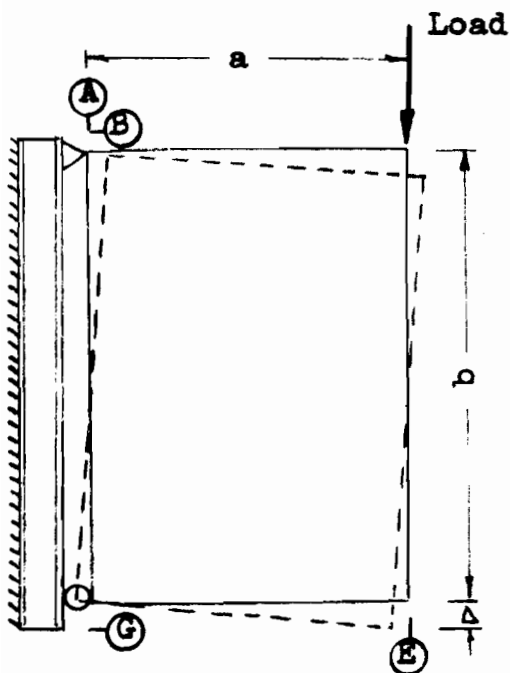


Fig. 3-9. Corner movement in horizontal diaphragms.

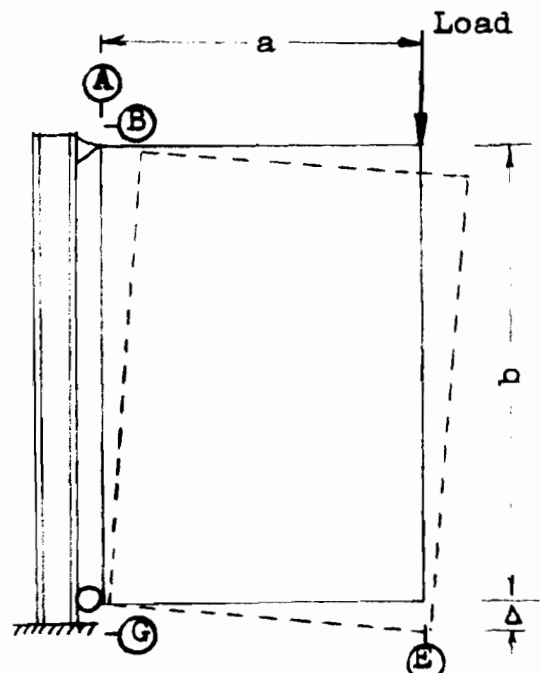
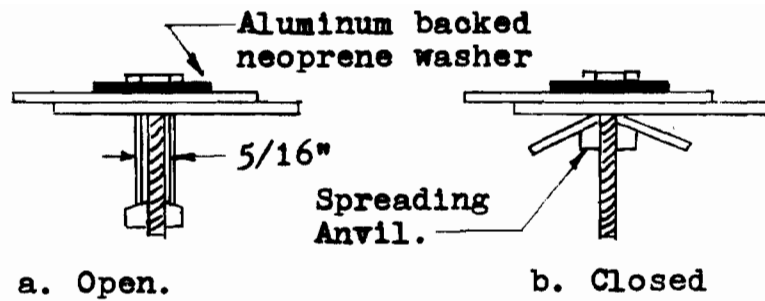
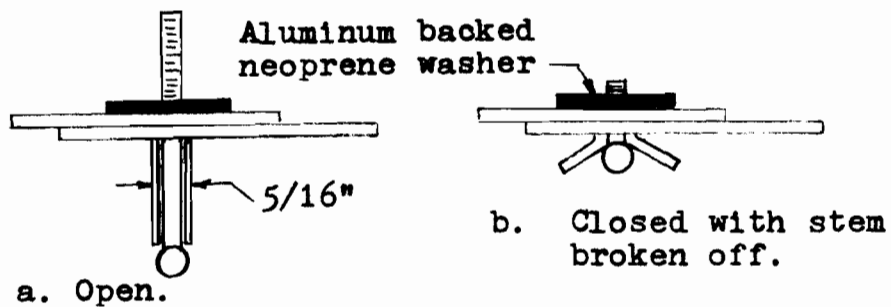


Fig. 3-10. Corner movement in vertical diaphragms.

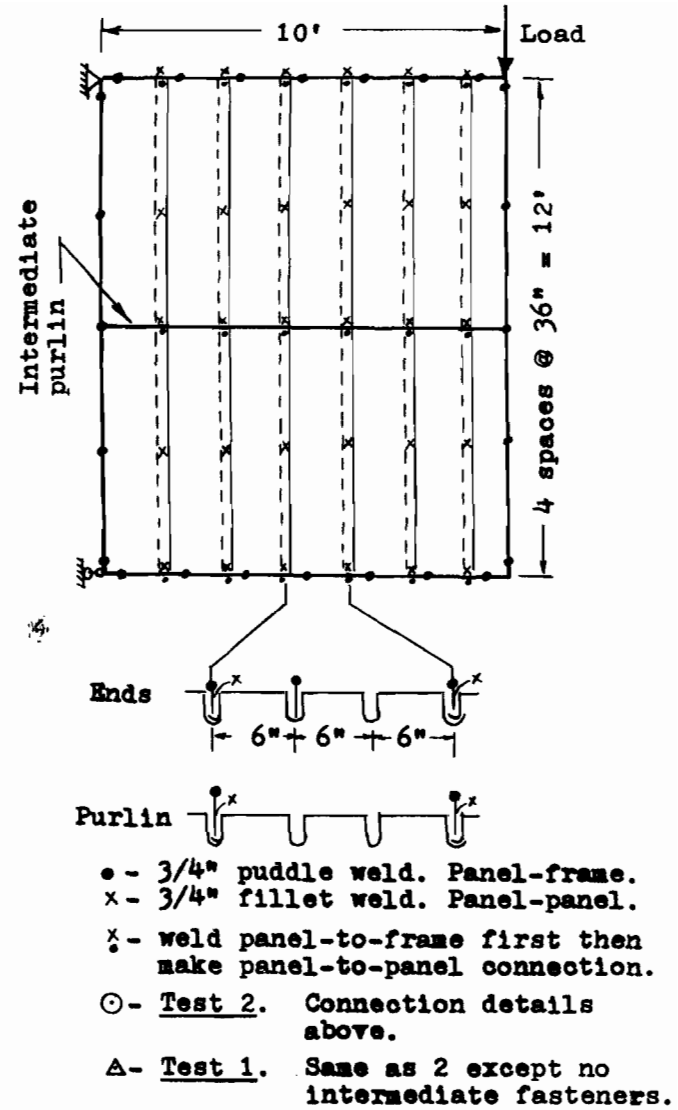
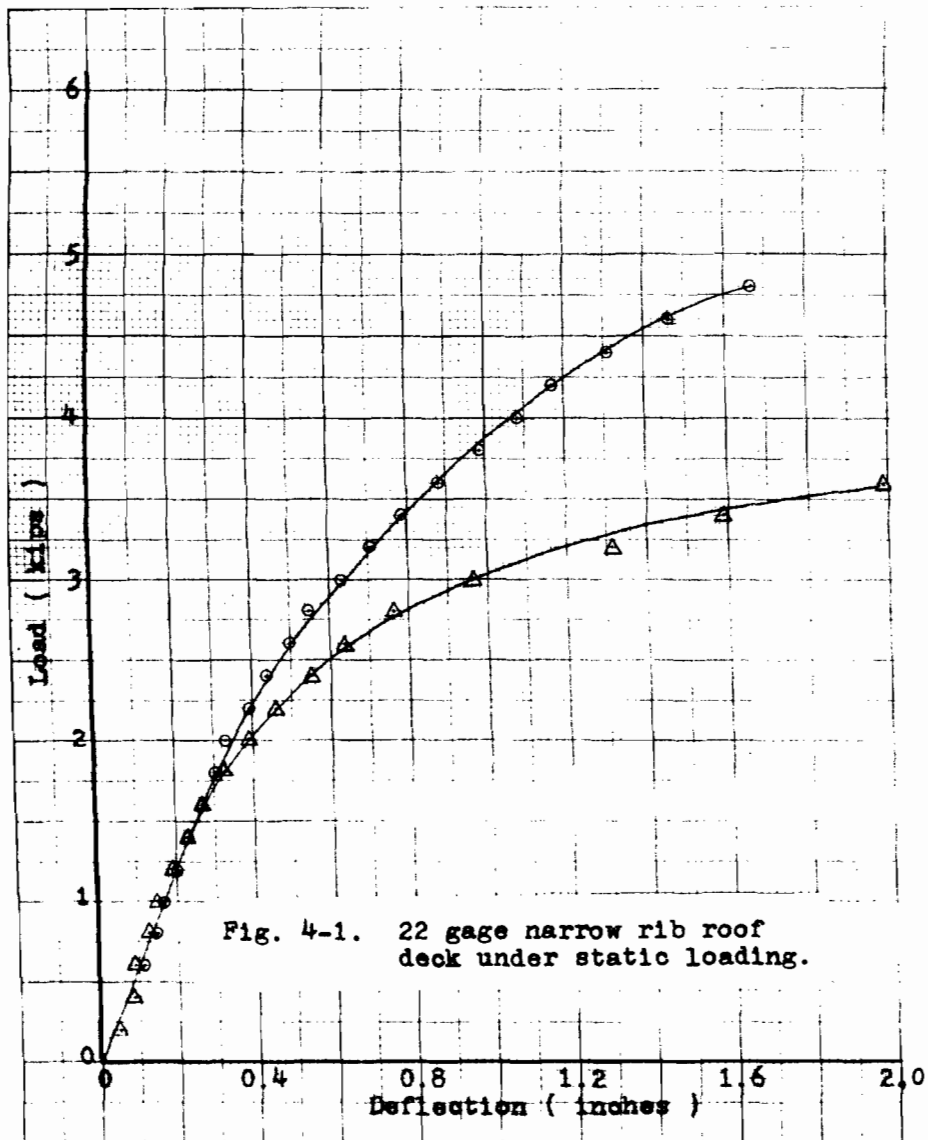


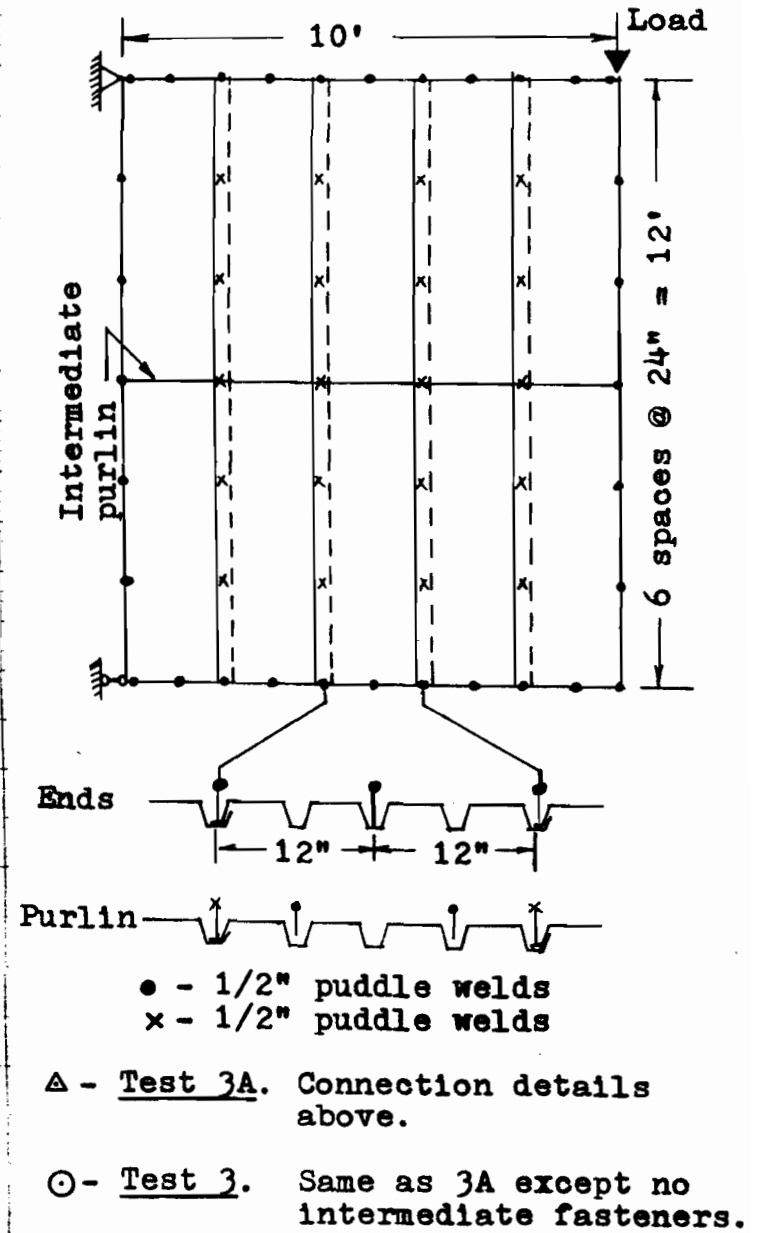
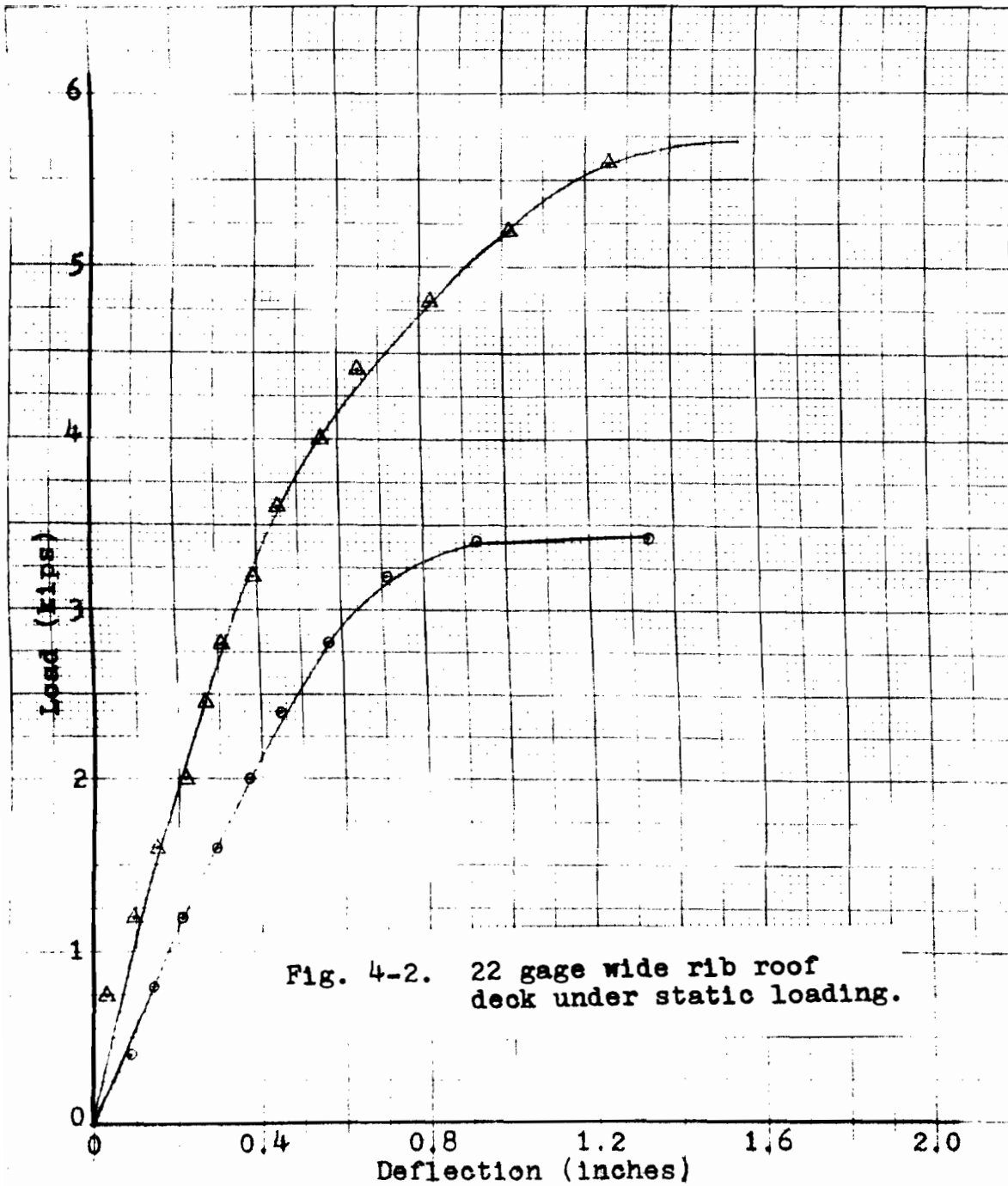
The screw type fastener was used in tests 5P-A and 5PA-R.

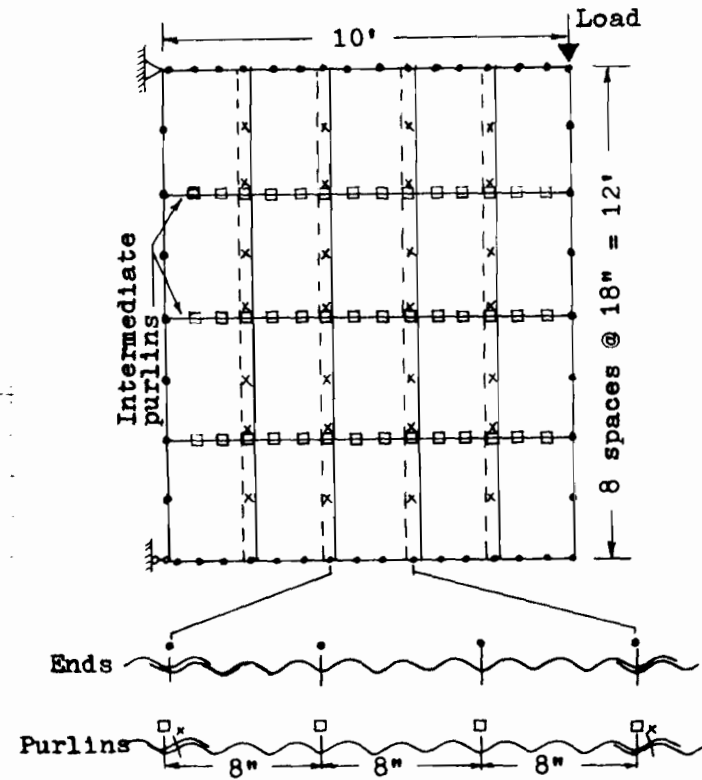
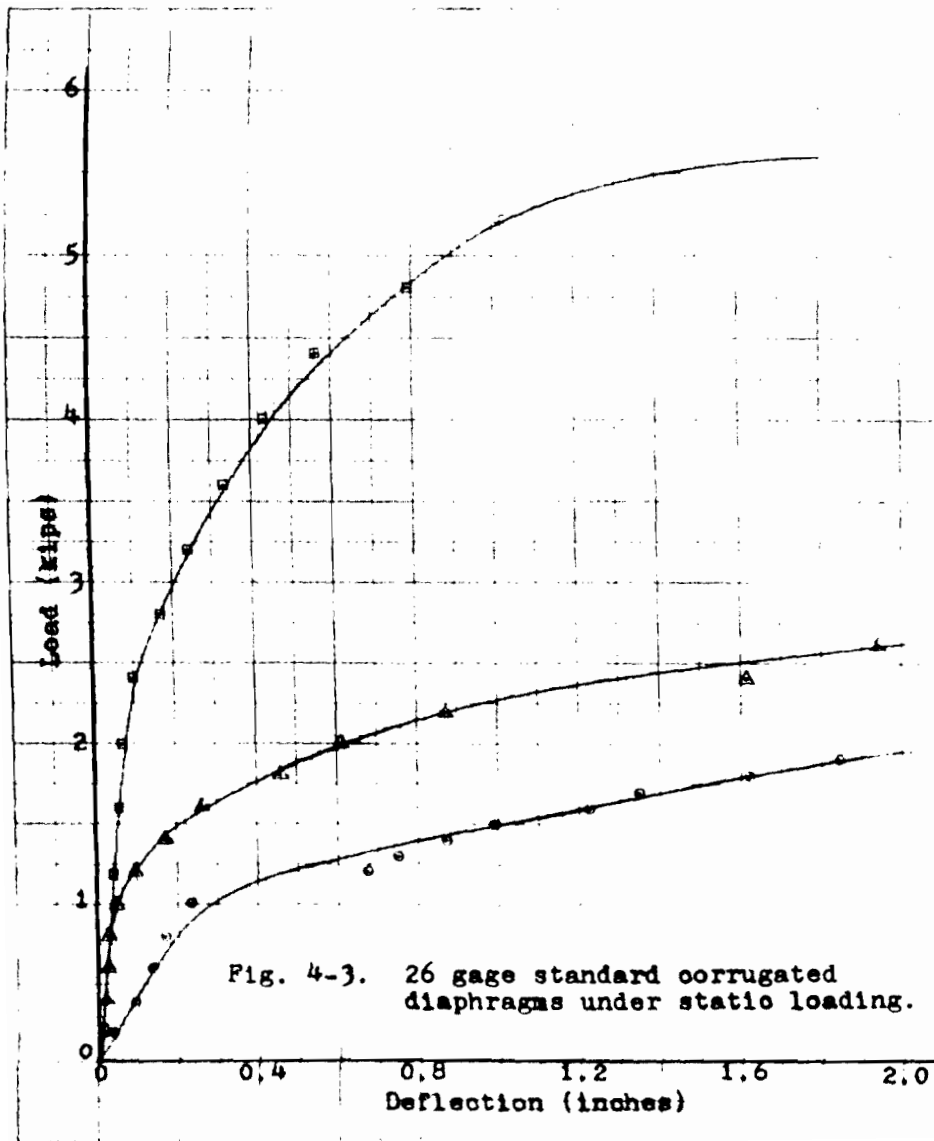


The above fasteners were used in box rib panel tests 11, 12, 13, 14 and on other tests having these prefixes.

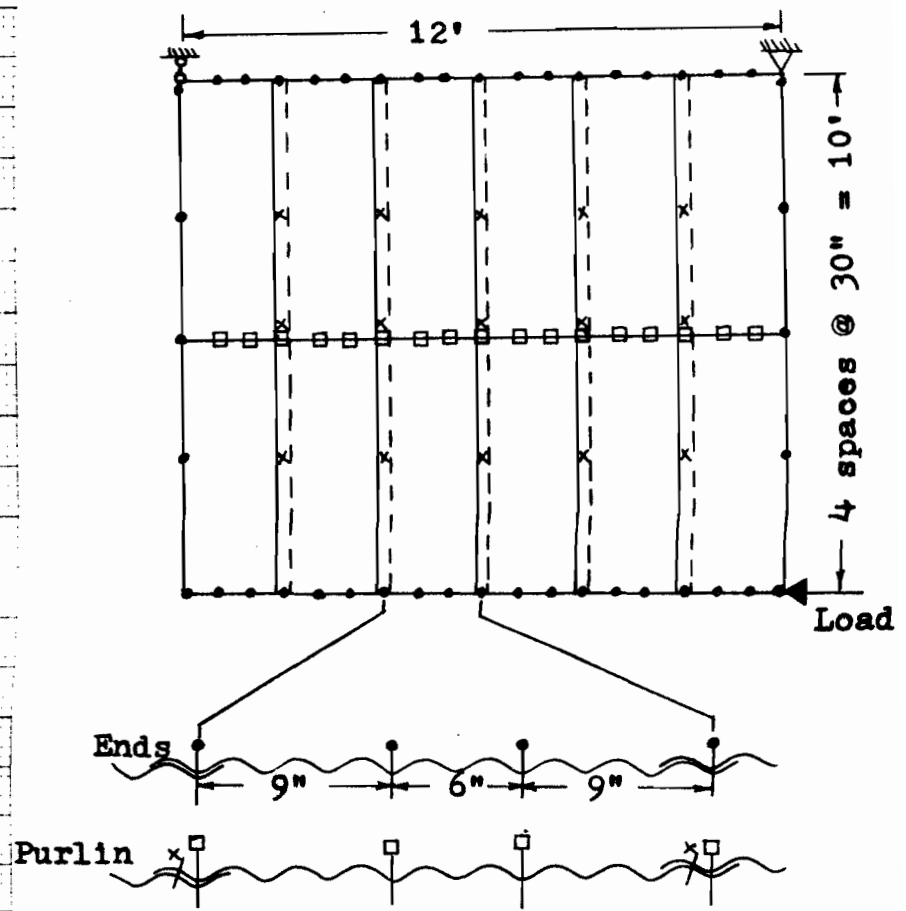
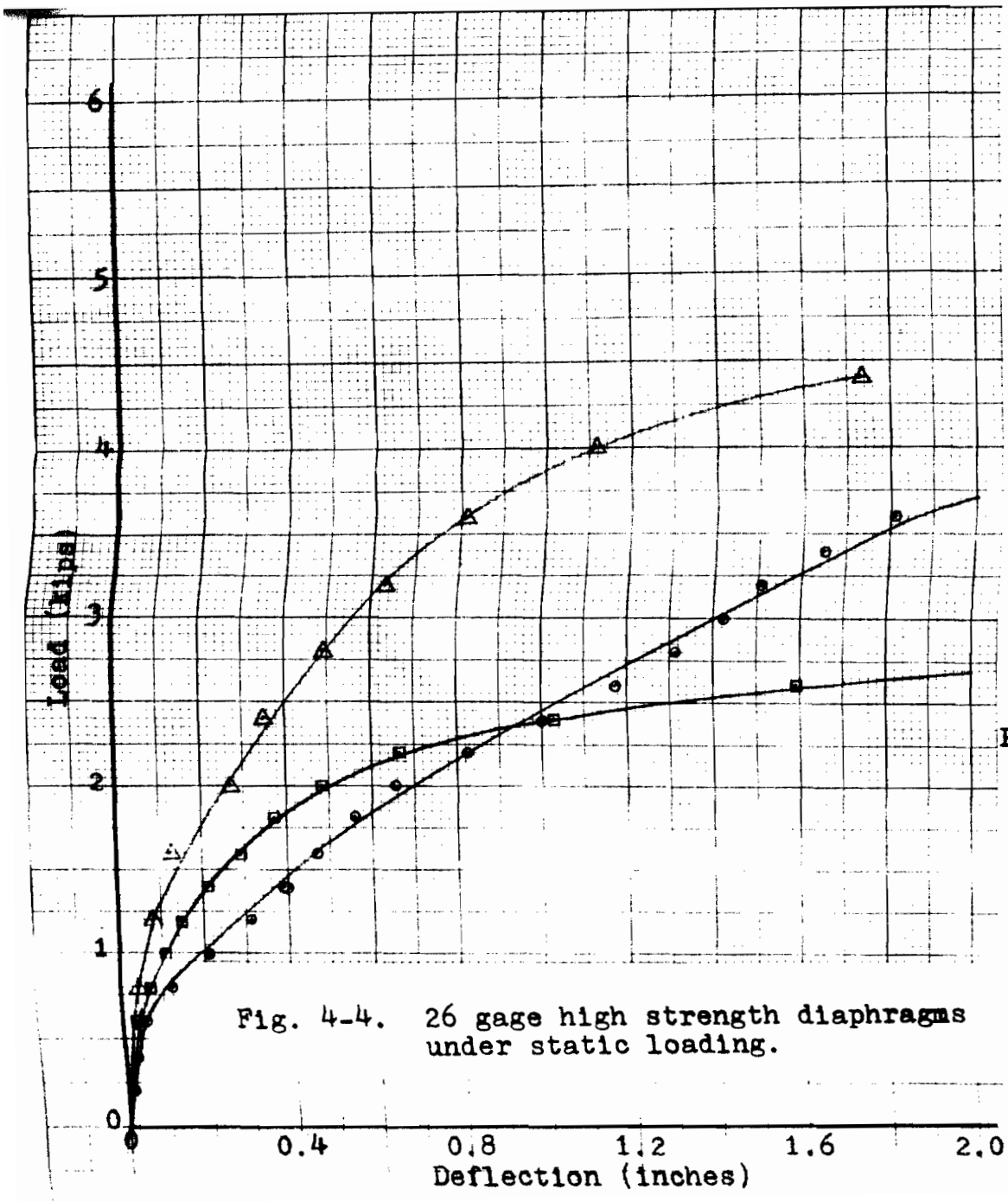
Fig. 3-11. Spreading back fasteners.



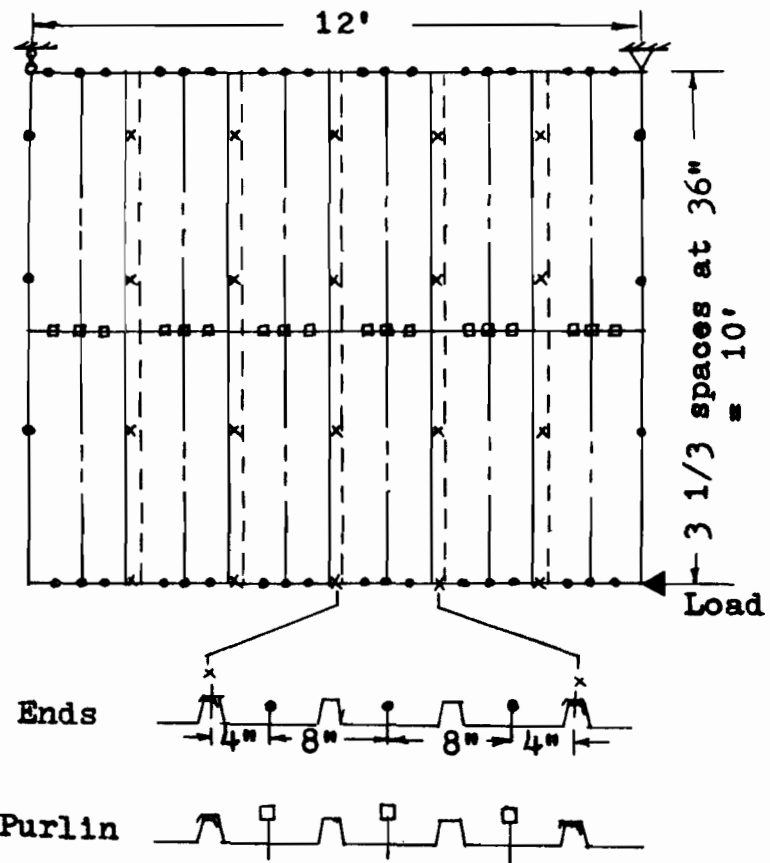
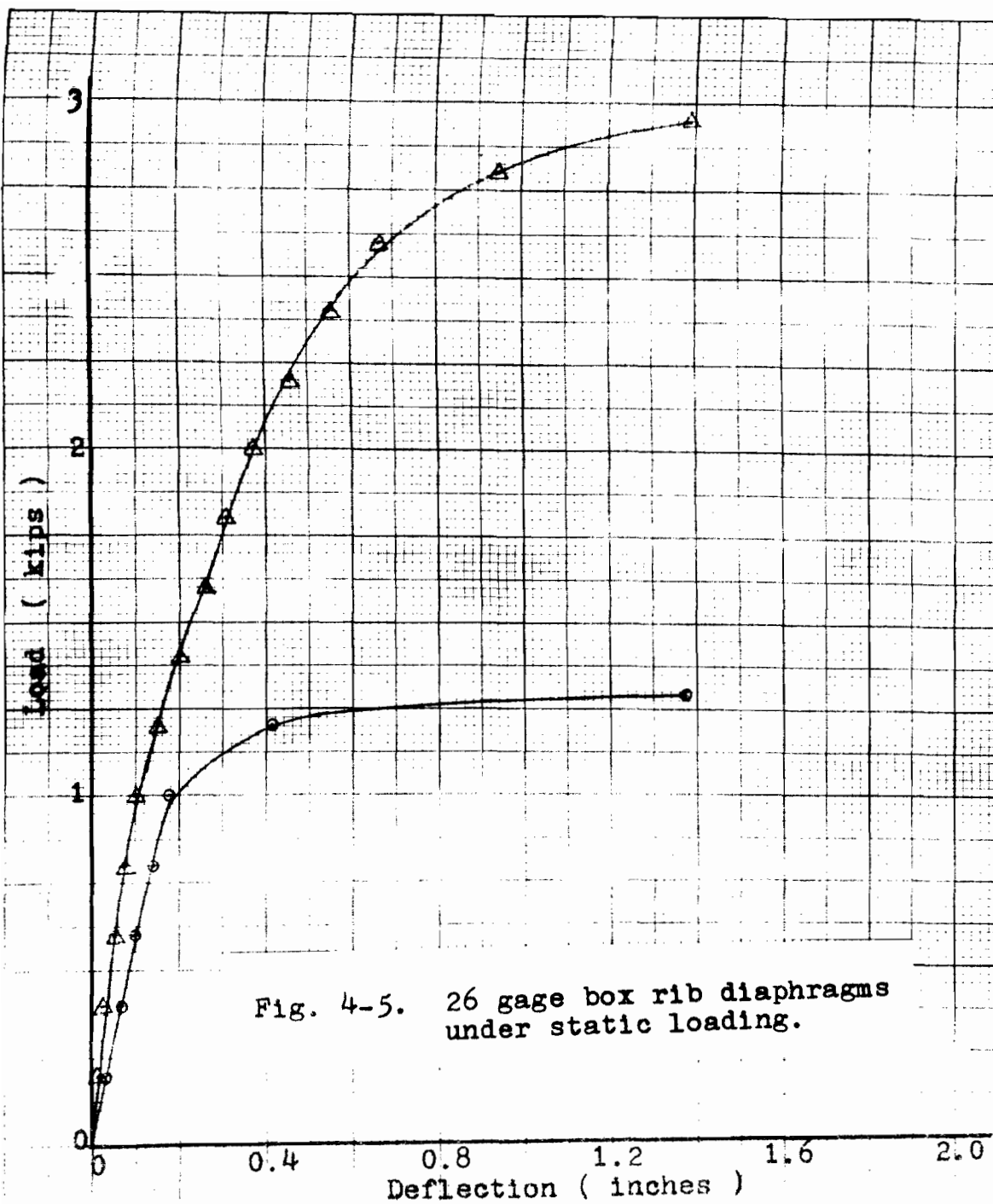




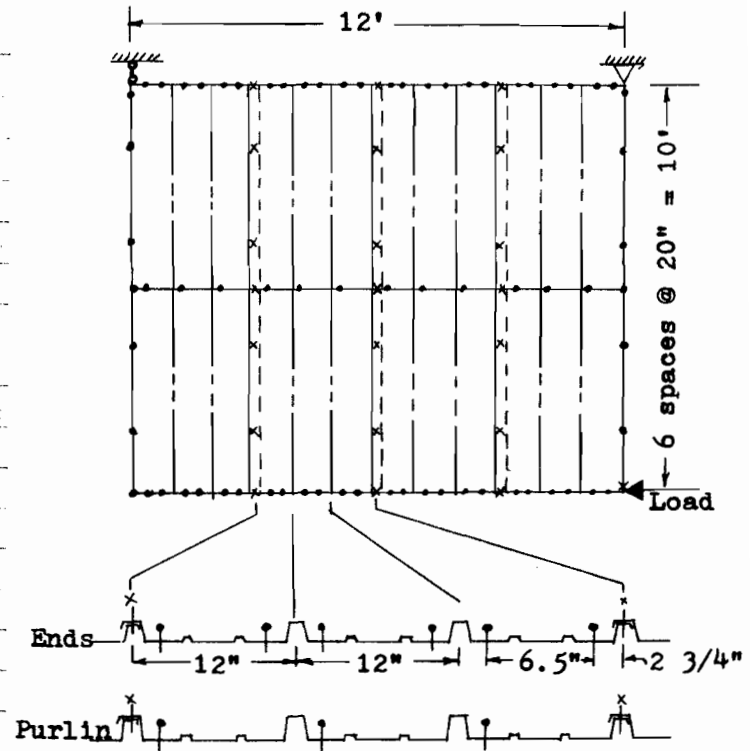
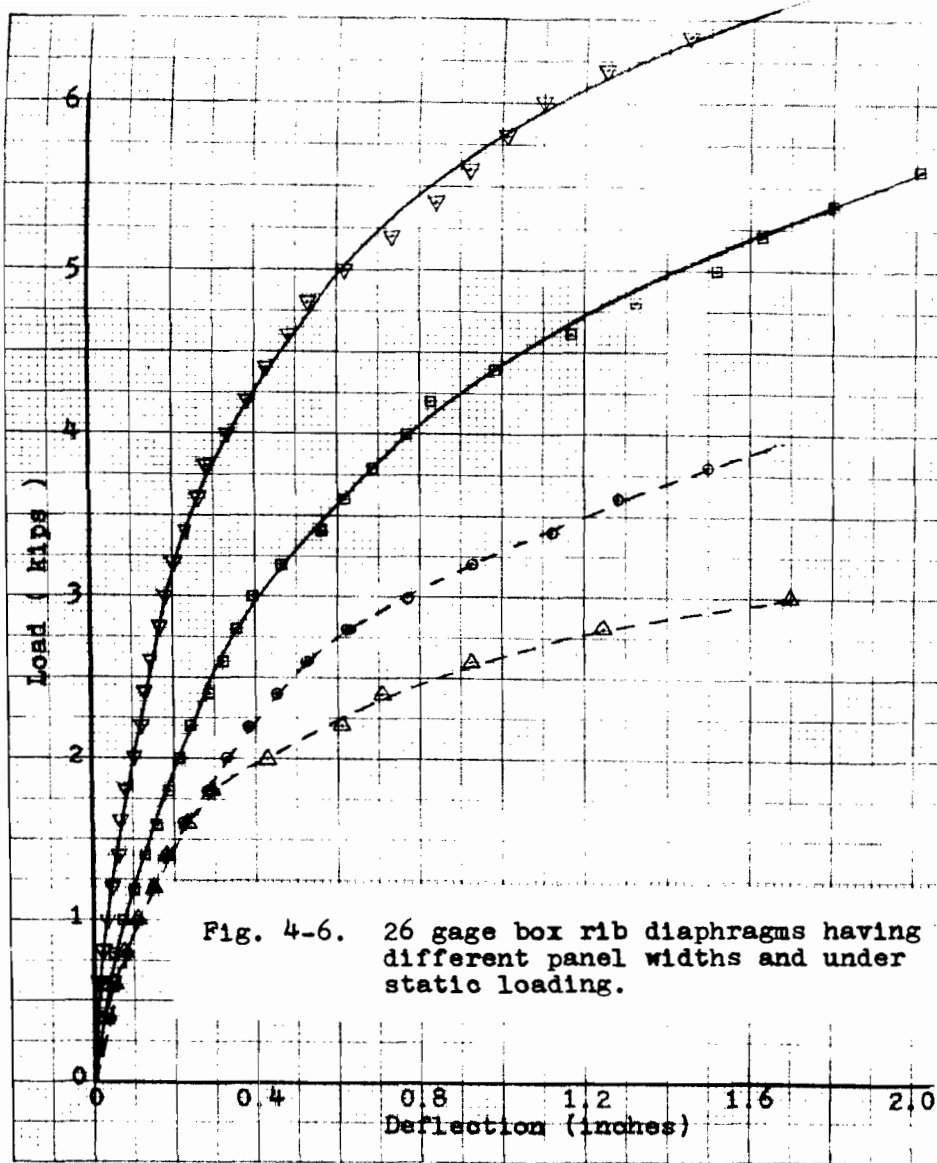
- - # 14 Screws. Panel-to-frame.
- - Non load resisting connection.
- × - # 10 Screws. Panel-to-panel.
- - Test 5. Connection details above.
- △ - Test 4B. Same as 5 except no intermediate fasteners.
- - Test 4. Same as 4B except no #10 screws at purlins.



- - # 14 Screws. Panel-to-frame.
  - - Non load resisting connection.
  - × - # 10 Screws. Panel-to-panel.
- Δ - Test 8. Connection details above.
  - - Test 7A. Same as 8 except no intermediate fasteners.
  - - Test 7. Same as 7A but replaced non load resisting conn. with # 14 screws.



- x - # 10 Screw. Panel-to-panel.
  - - # 14 Screw. Panel-to-frame.
  - Non load resisting connection.
- Panel-to-panel screws at 36" c.c. in prepunched holes.
- △ - Test 10. Connection details above.
  - - Test 9. Same as 10 except no panel-to-panel screws nor intermediate conns. on marginal members.



- x - Panel-to-panel lock rivet.
- - Panel-to-frame lock rivet.
- ▽ - Test 12. Connection details above.
- - Test 11. Same as 12 except no intermediate fasteners.
- - Test 14. Corresponds to 12 except sheet width is 24".
- △ - Test 13. Corresponds to 11 except sheet width is 24".

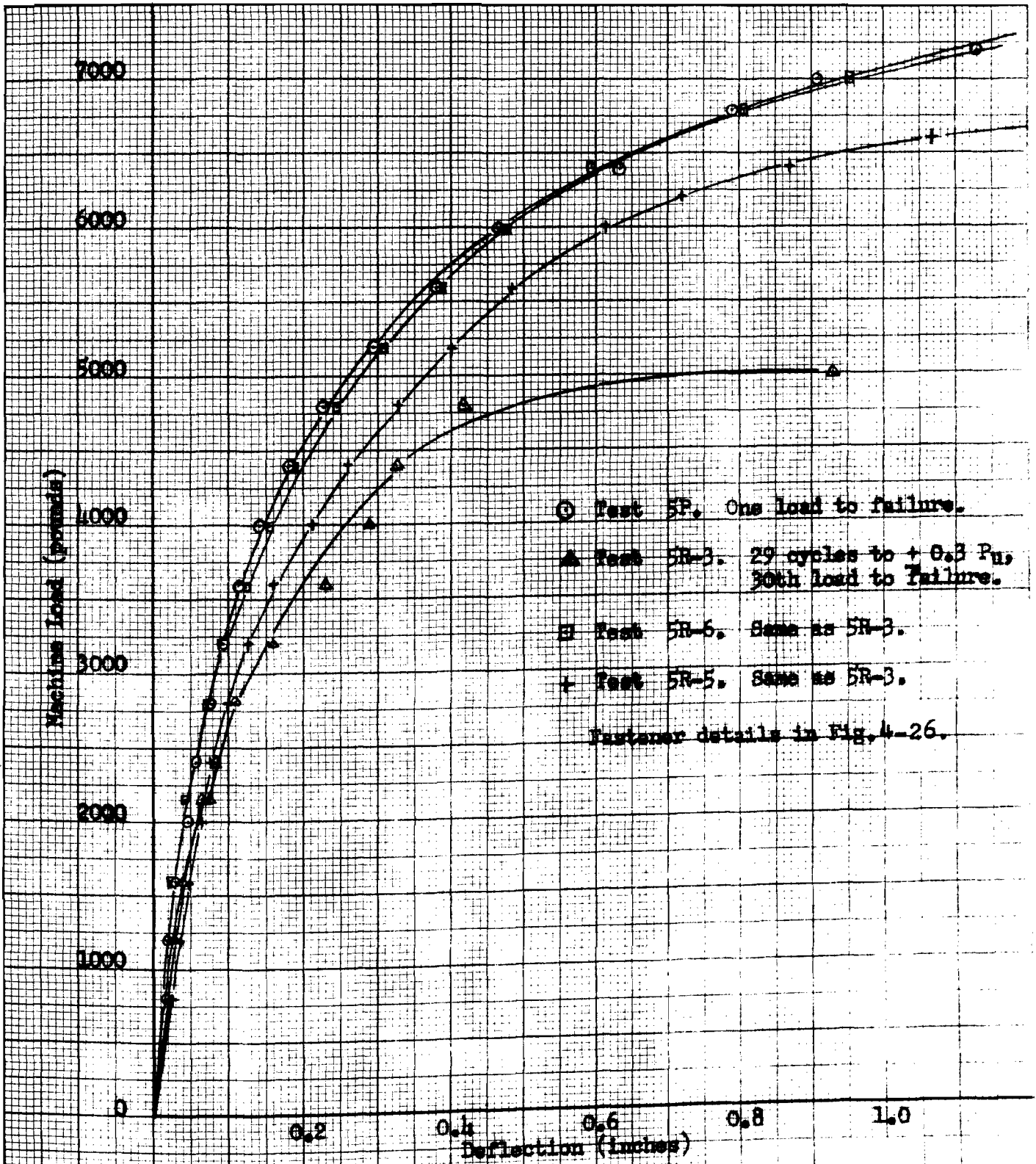


Fig. 4-7. Standard corrugated diaphragms with intermediate fasteners. Load reversal influences as compared to a statically loaded diaphragm. Intermediate sidelap fasteners are # 10 S.M.S.

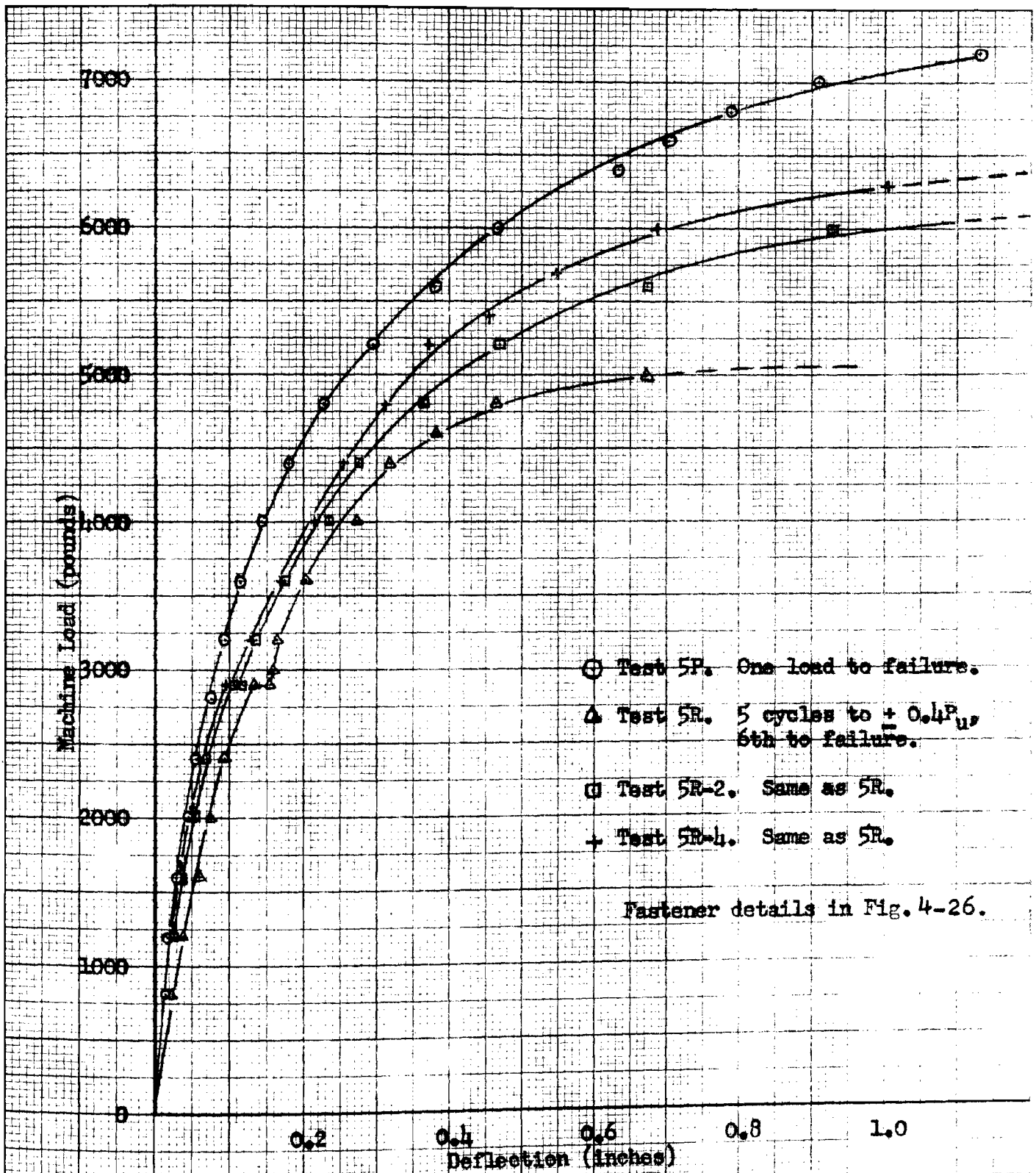


Fig. 4-8. Standard corrugated diaphragms with intermediate fasteners. Load reversal influences as compared to a statically loaded diaphragm. Intermediate sidelap fasteners are # 10 S.M.S.

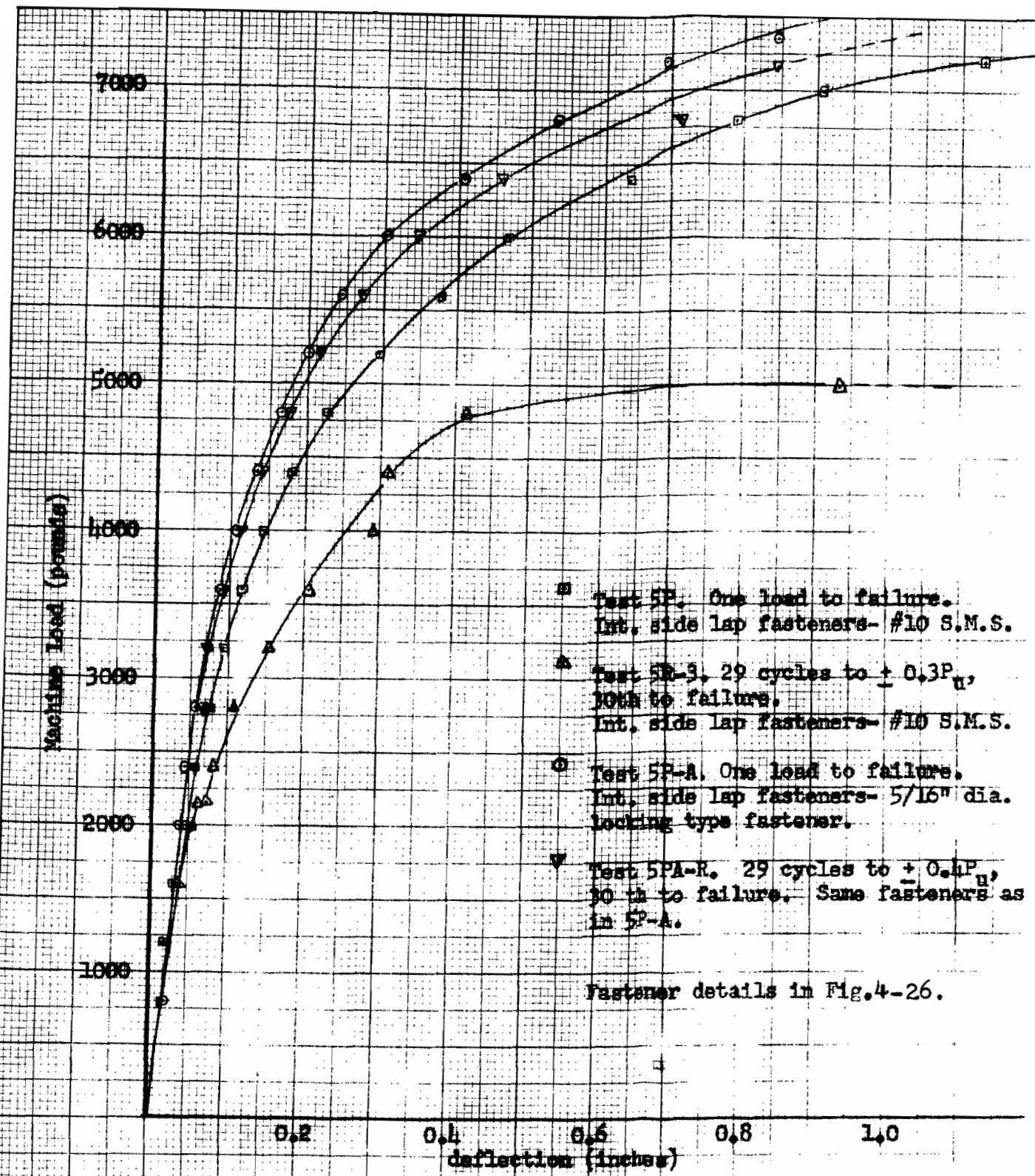
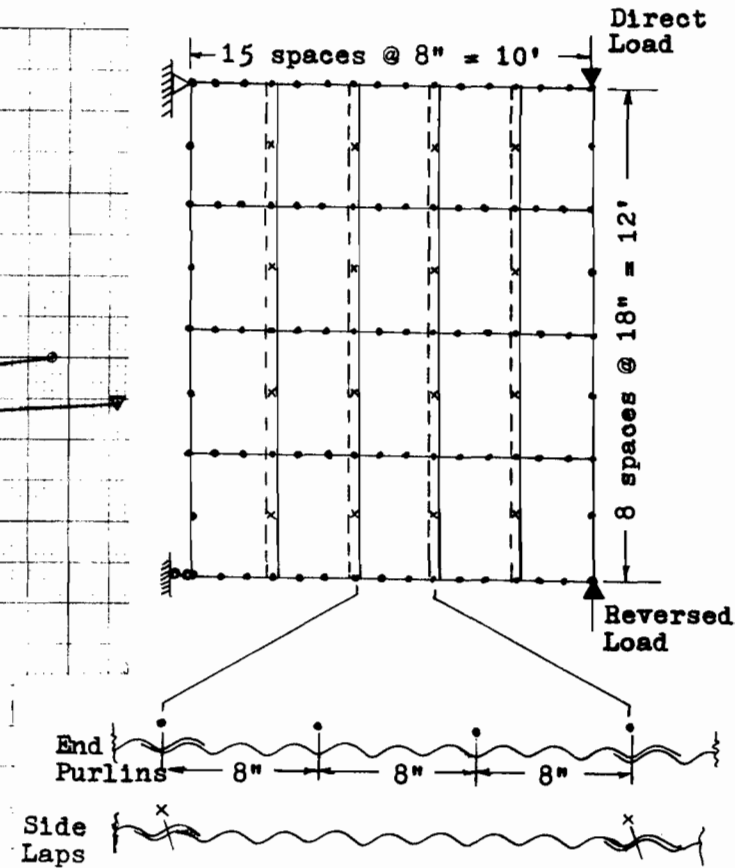
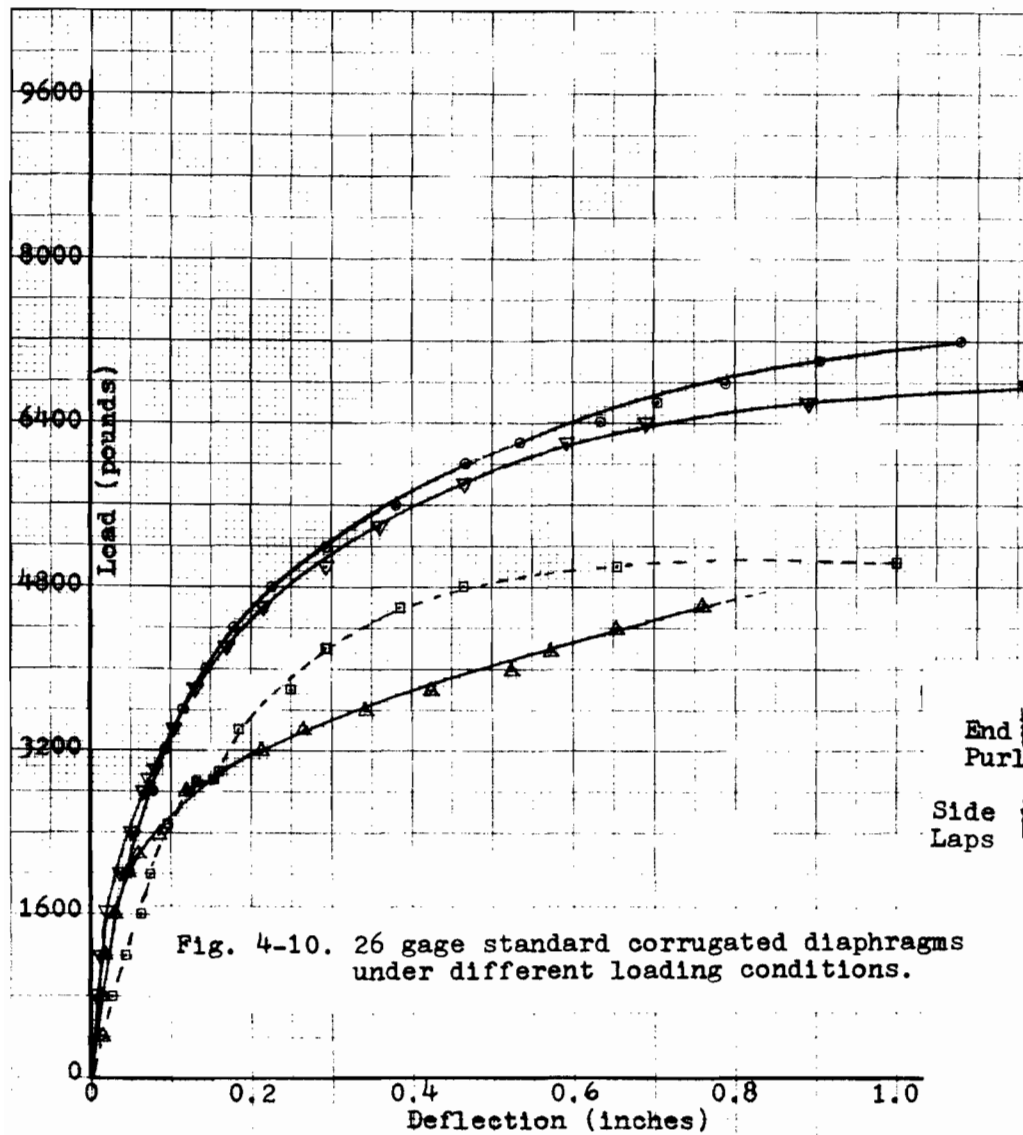
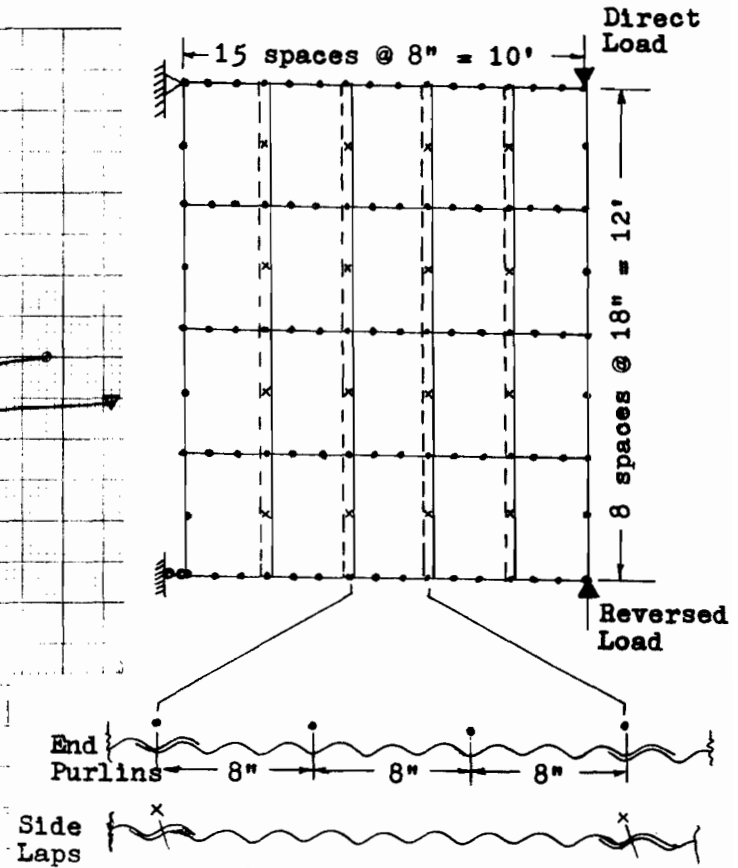
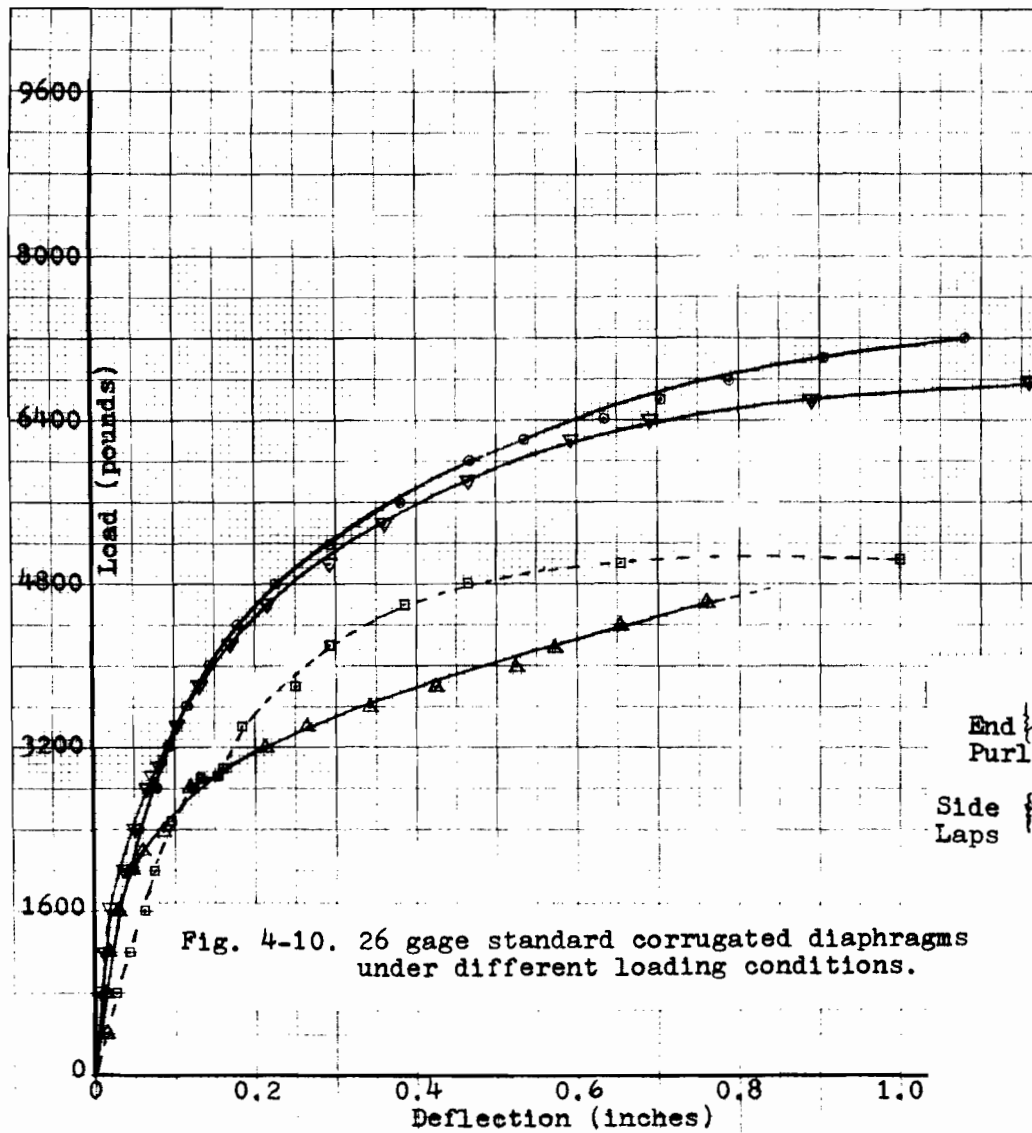


Fig.4-9. A comparison of 26 gage standard corrugated diaphragms under two conditions of load and with two different types of intermediate side lap fasteners.



- - # 14 Screws. Panel-to-frame.
  - x - # 10 Screws. Panel-to-panel.
  - - Test 5P. Connection details above.
  - - Test 5R. Same.
  - ▽ - Test 5Z. Same connections.
  - △ - Test 4P. Same as 5P except no intermediate fasteners.
- All tests with 4 prefixes did not have intermediate fasteners.



- - # 14 Screws. Panel-to-frame.
  - × - # 10 Screws. Panel-to-panel.
  - - Test 5P. Connection details above.
  - - Test 5R. Same.
  - ▽ - Test 5Z. Same connections.
  - △ - Test 4P. Same as 5P except no intermediate fasteners.
- All tests with 4 prefixes did not have intermediate fasteners.

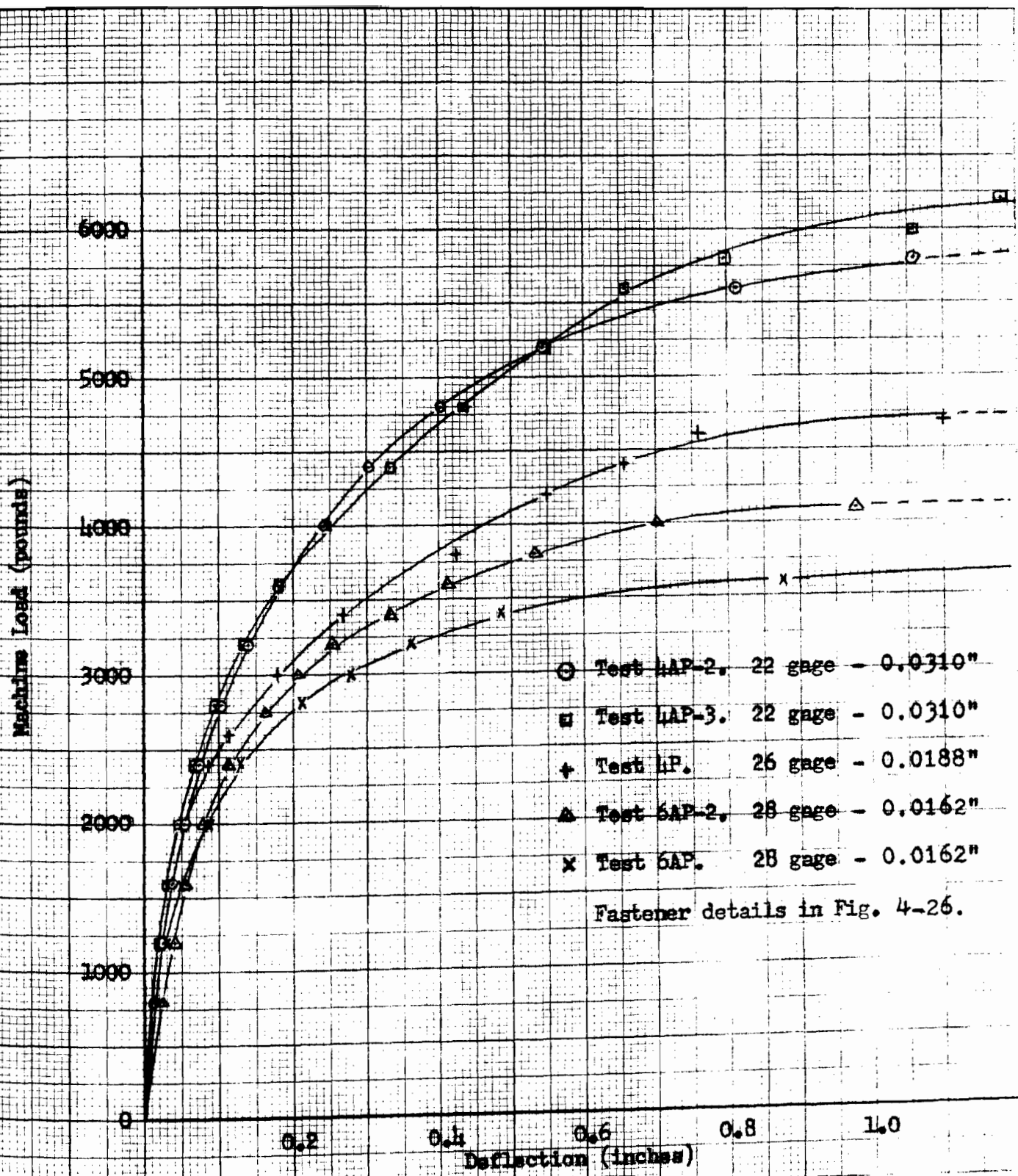


Fig. 4-11. Standard corrugated diaphragms of various thicknesses with no intermediate fasteners.

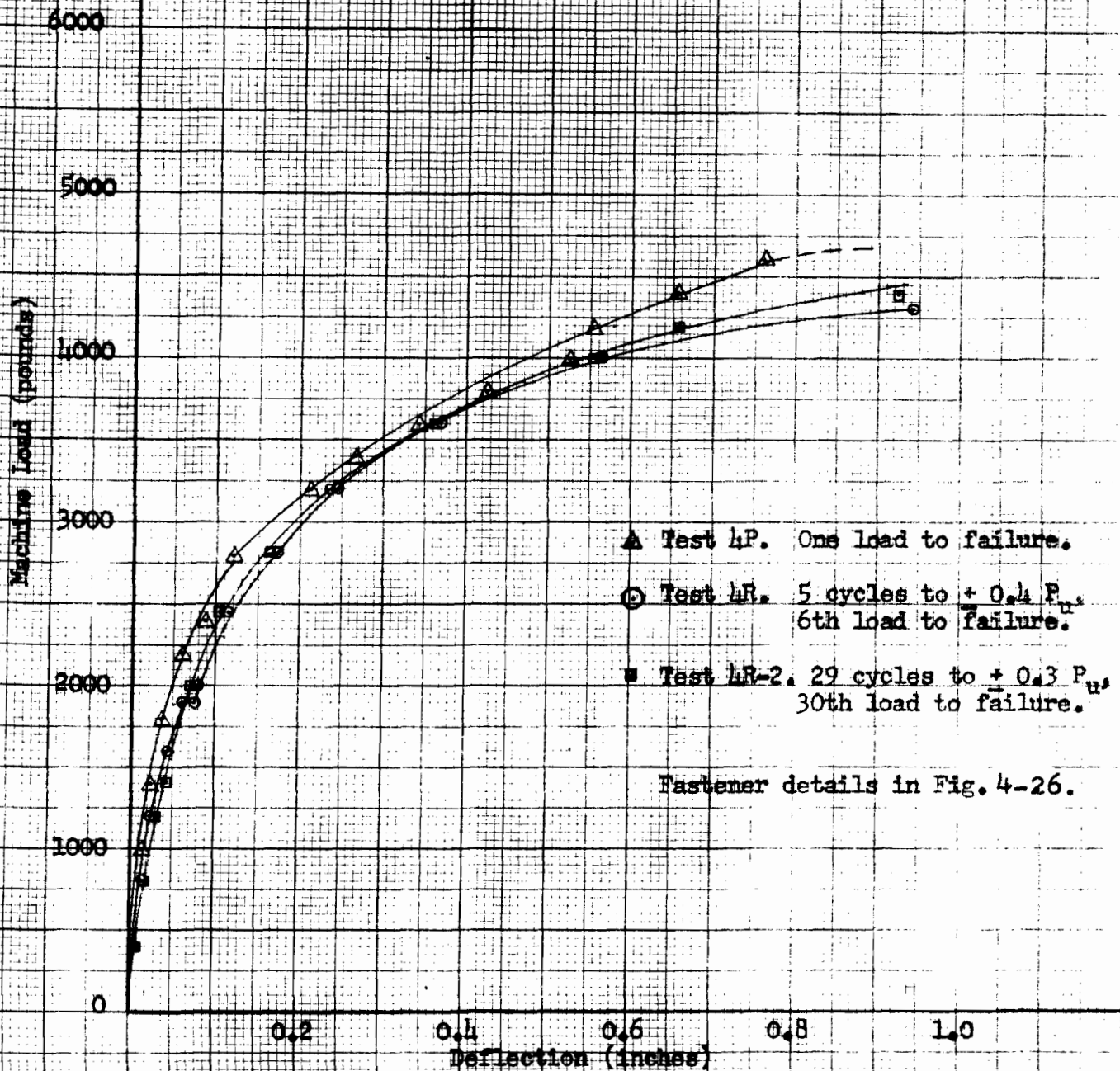


Fig. 4-12. Standard corrugated diaphragms without intermediate fasteners. Load reversal influences as compared to a statically loaded diaphragm.

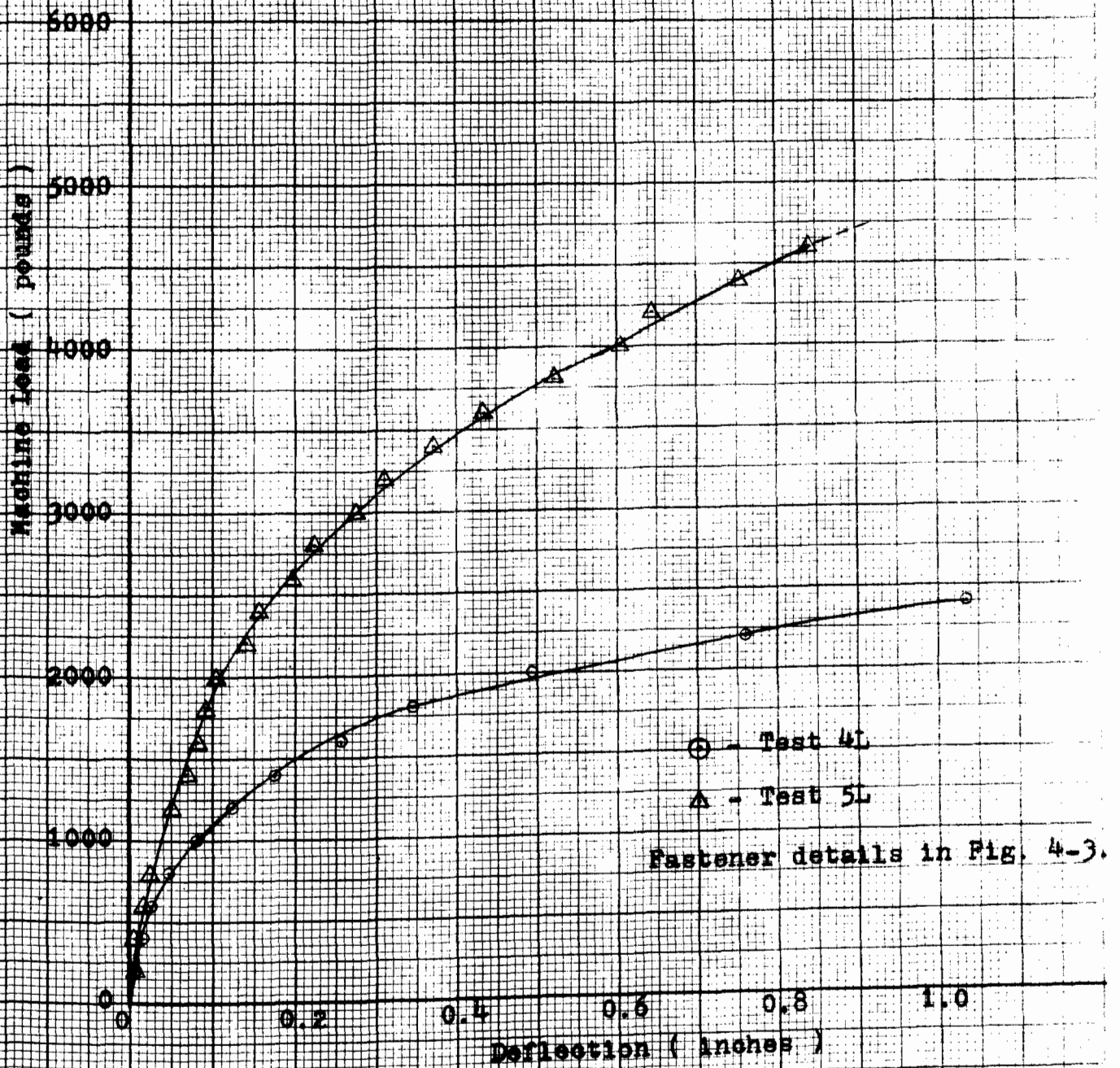


Fig. 4-1). Static load tests on 26 gage standard corrugated diaphragms having special perlin connections.

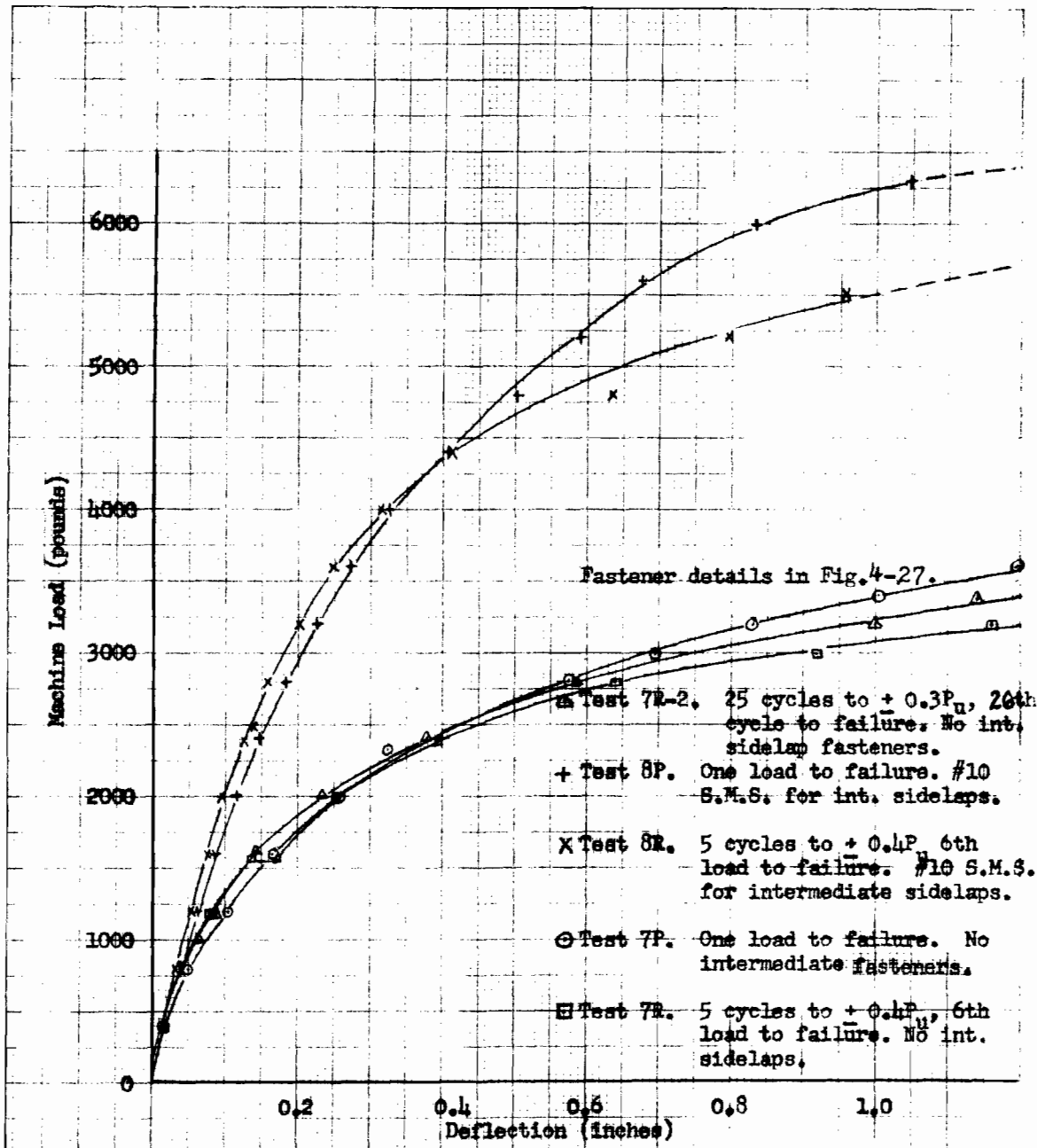


Fig. 4-14. 26 gage deep corrugated high strength diaphragms under different loading conditions and with two different fastener arrangements. Tests with a 7 prefix had no intermediate fasteners.

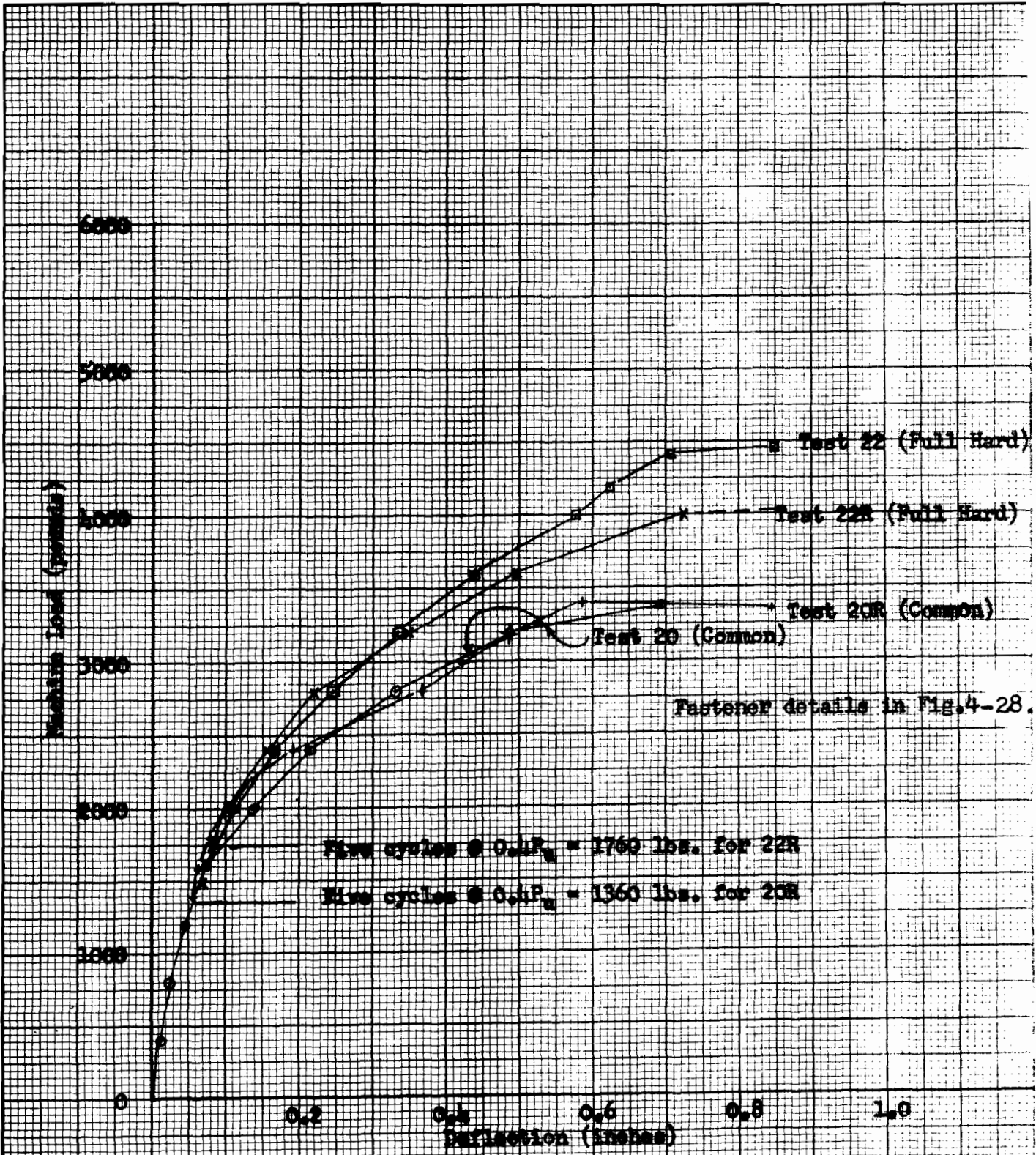
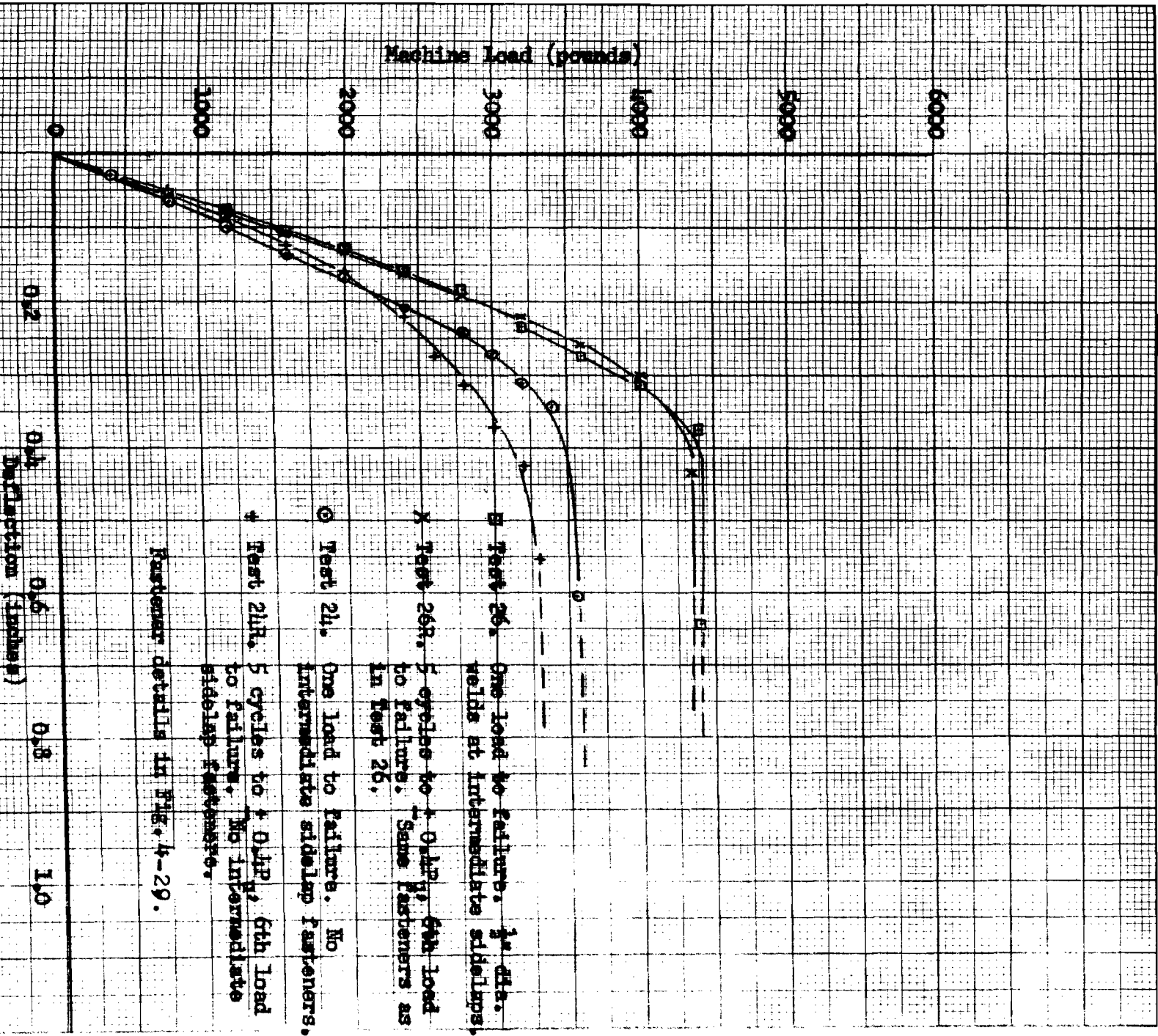


Fig. 4-15. Tests on diaphragms using both common and full hard material. 36" ribbed panels with no intermediate fasteners.



- A Test 26. One load to failure. 1/2 dia. welds at intermediate sidelaps.
  - B Test 26R. 5 cycles to 0.4HP, 6th load to failure. Some fasteners as in Test 26.
  - C Test 24. One load to failure. No intermediate sidelap fasteners.
  - D Test 24R. 5 cycles to 0.4HP, 6th load to failure. No intermediate sidelap fasteners.
- Fastener details in FIG. 4-29.

Fig. 4-16.32 gage welded ribs rib roof decks with different loading conditions and different fastener arrangements. Tests 24 and 24R did not have intermediate fasteners.

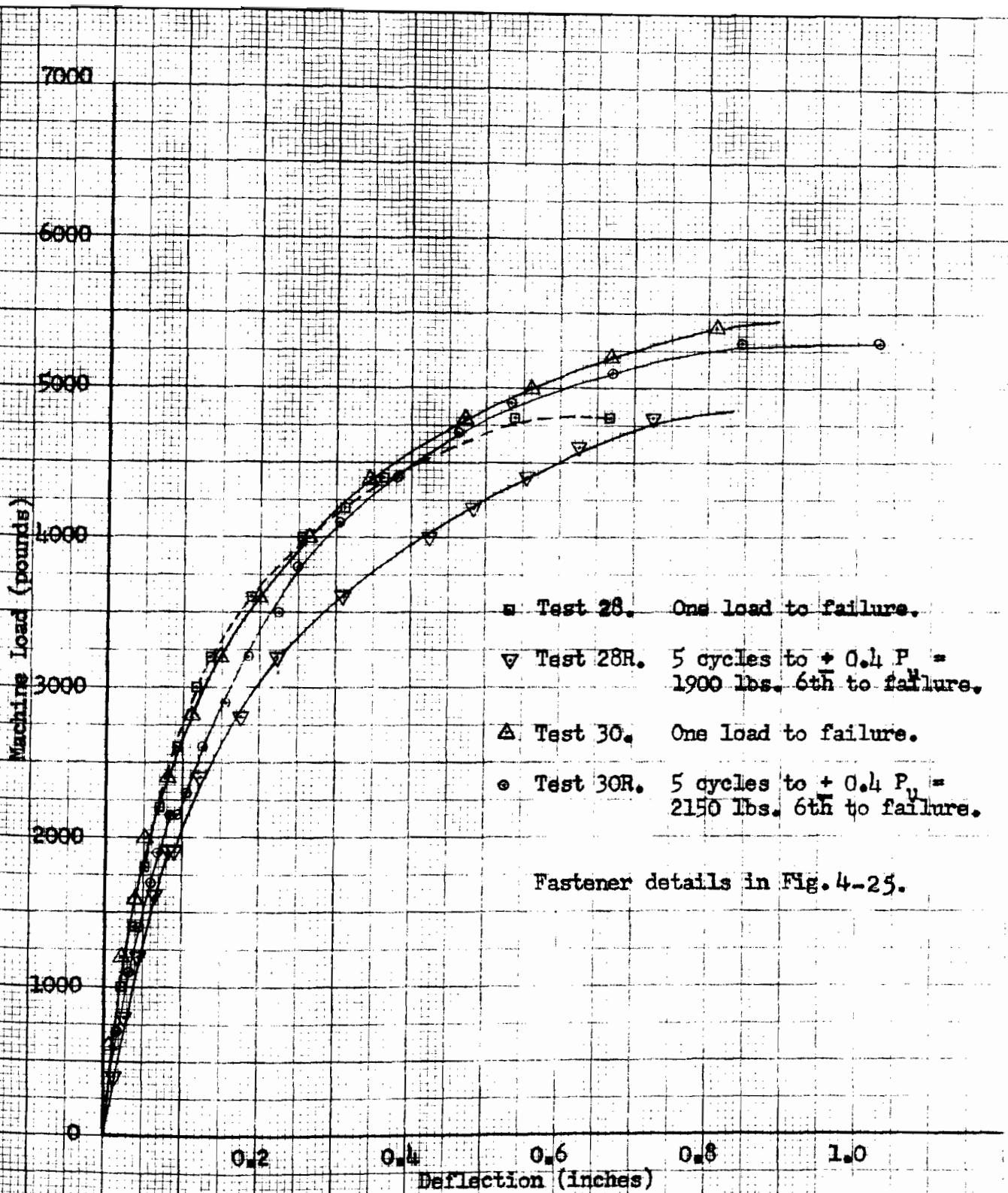


Fig. 4-17. Direct and reversed load tests on 26 gage standard corrugated diaphragms without intermediate edge fasteners but having intermediate sidelap fasteners at interior points.

Load P (pounds)

1400

1200

1000

800

600

400

200

0.1      0.2      0.3      0.4      0.5

Deflection  $\Delta$  (inches)

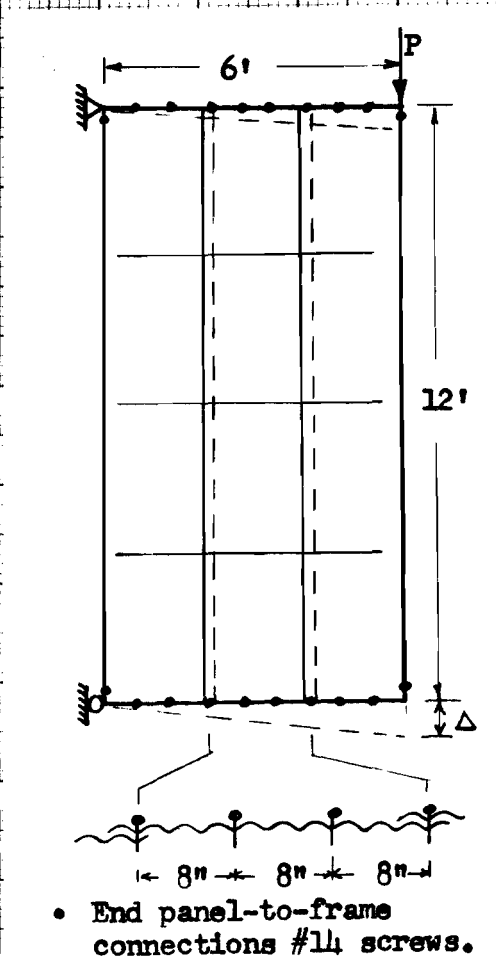
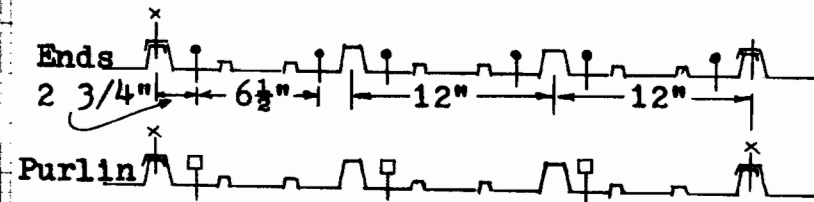
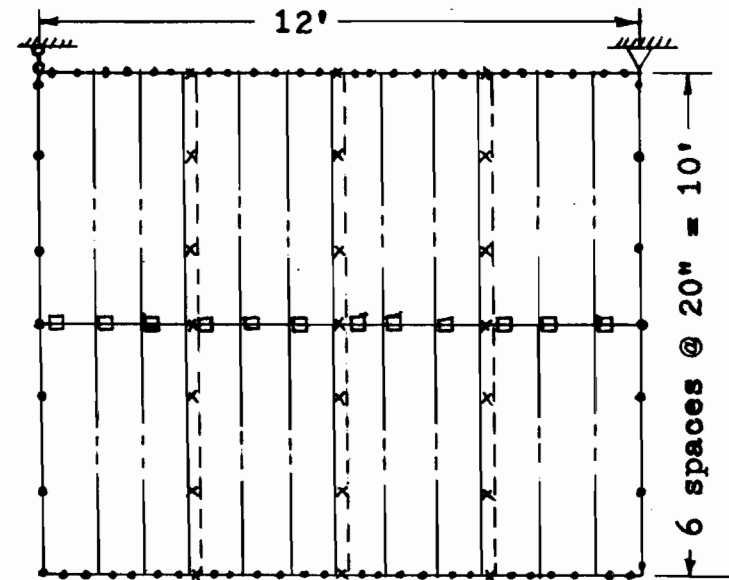
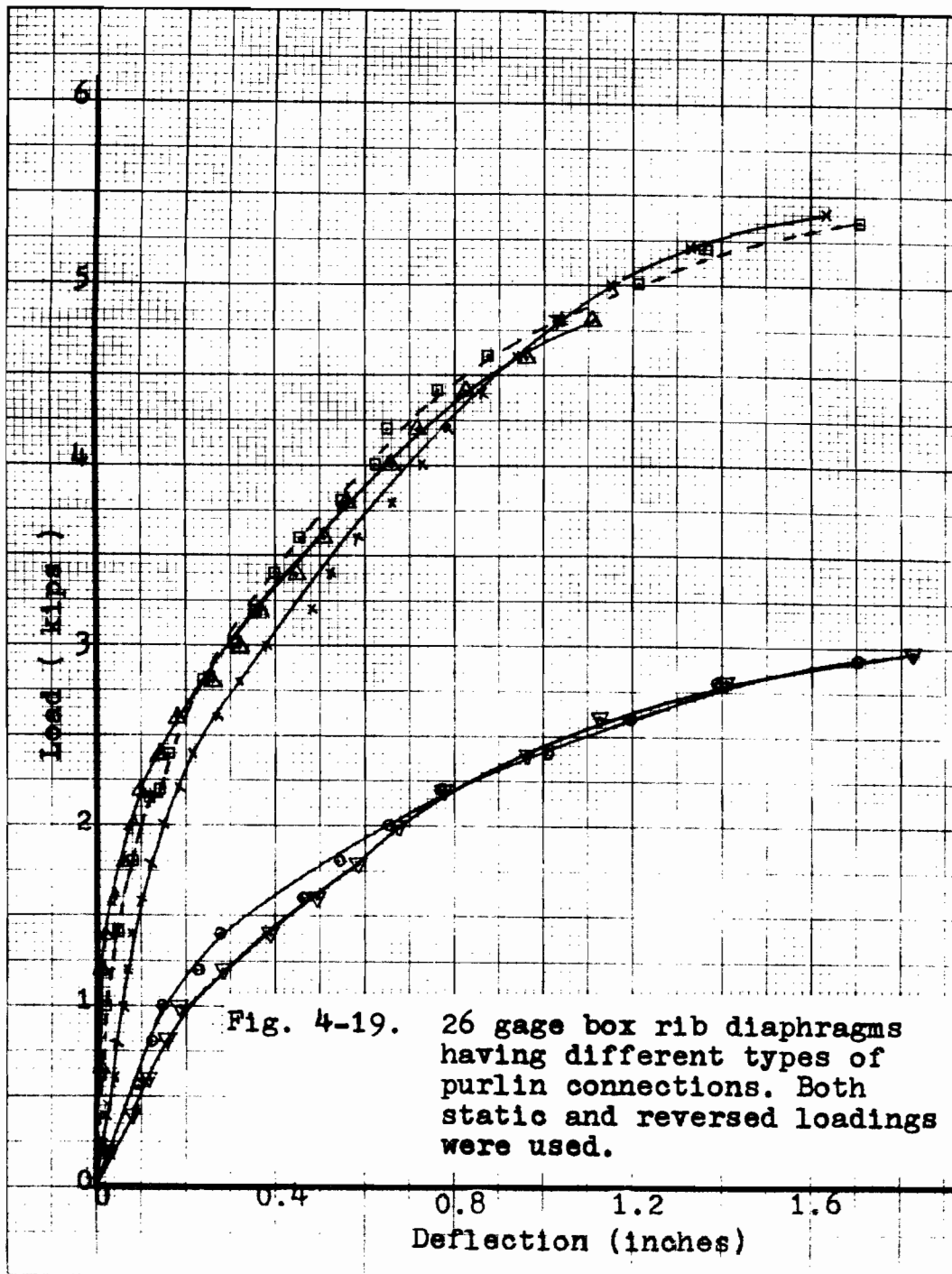


Fig. 4-18.. Load-deflection curve for a 26 gage standard corrugated diaphragm having connections at panel ends only.



- x - Panel-to-panel lock rivets.
- o - Panel-to-frame lock rivets.
- - Non load resisting connection.
- △ - Test 12L. Connection details above.
- - Test 11L. Same except no int. fasteners.
- × - Test 12P. Details above but replace non load resist. connections with # 14 screws.
- - Test 12R. Details same as 12P.
- ▽ - Test 11P. Same as 12P but no intermediate fasteners.

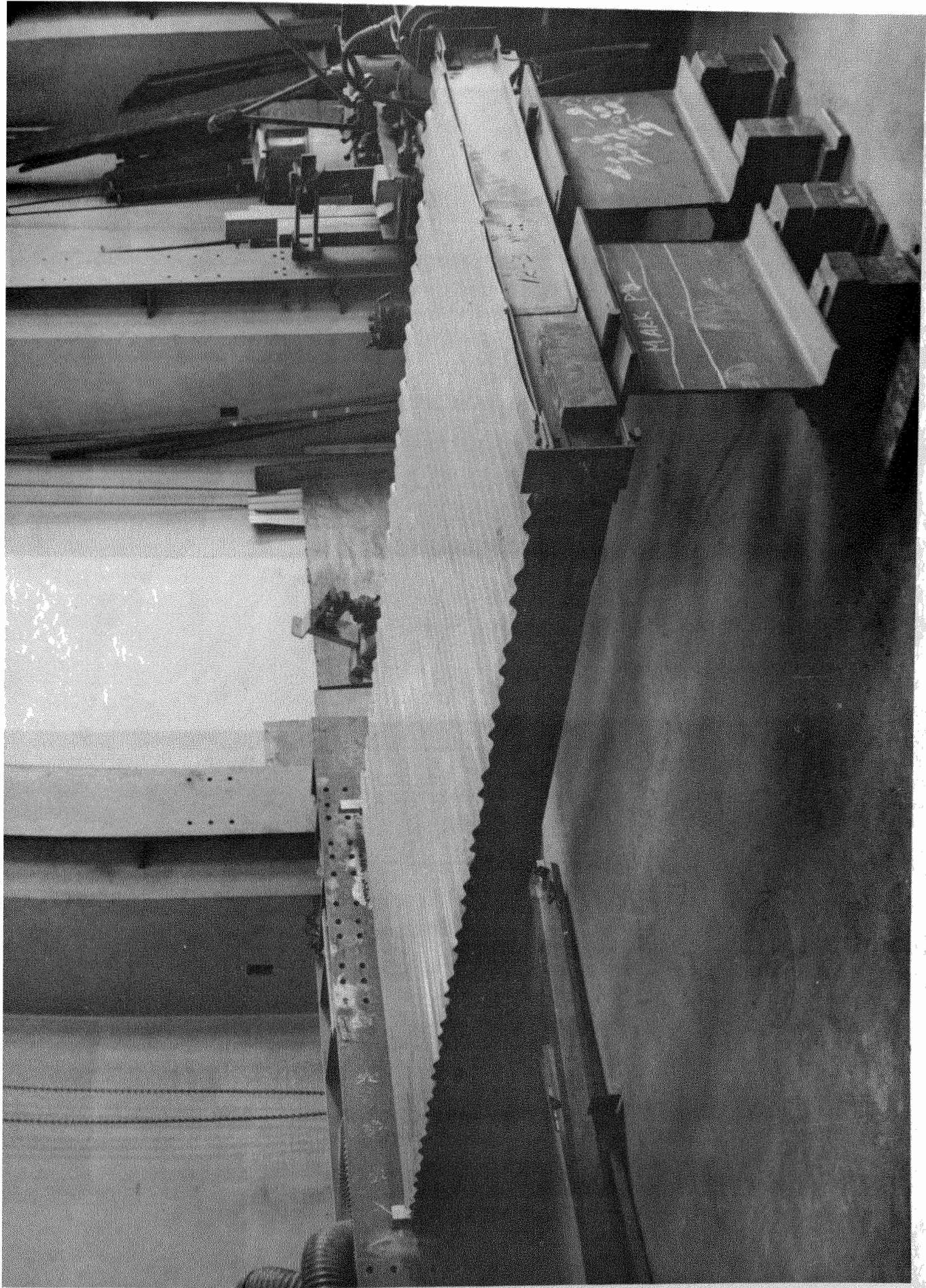


Fig. 4-20.

26 Gage Standard Corrugated Diaphragm ( 6' x 10' ).

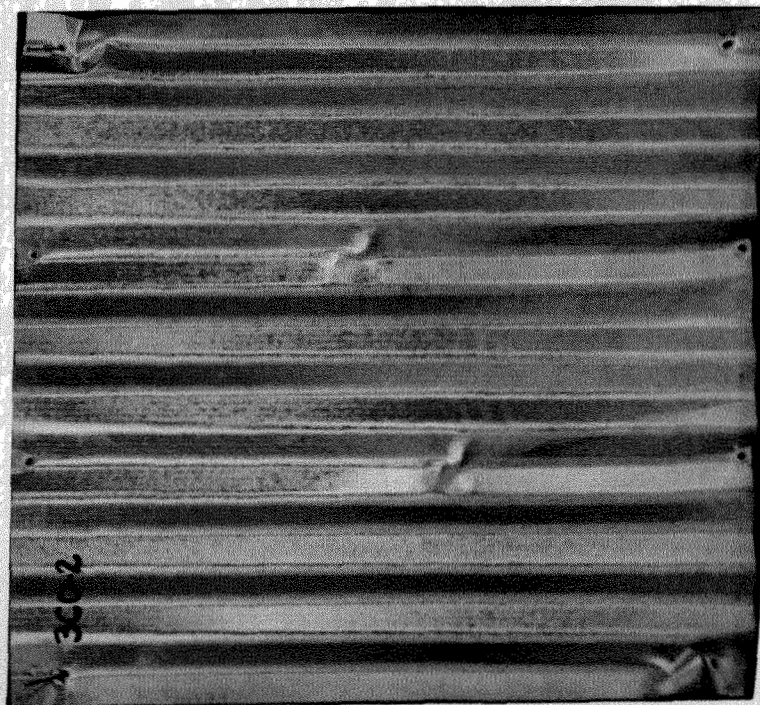
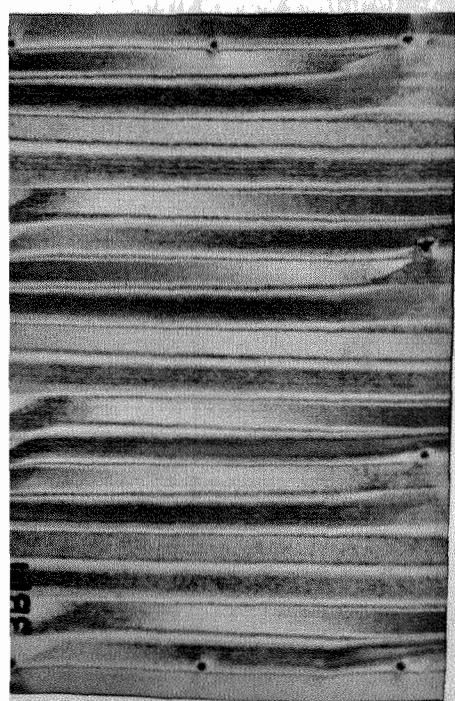
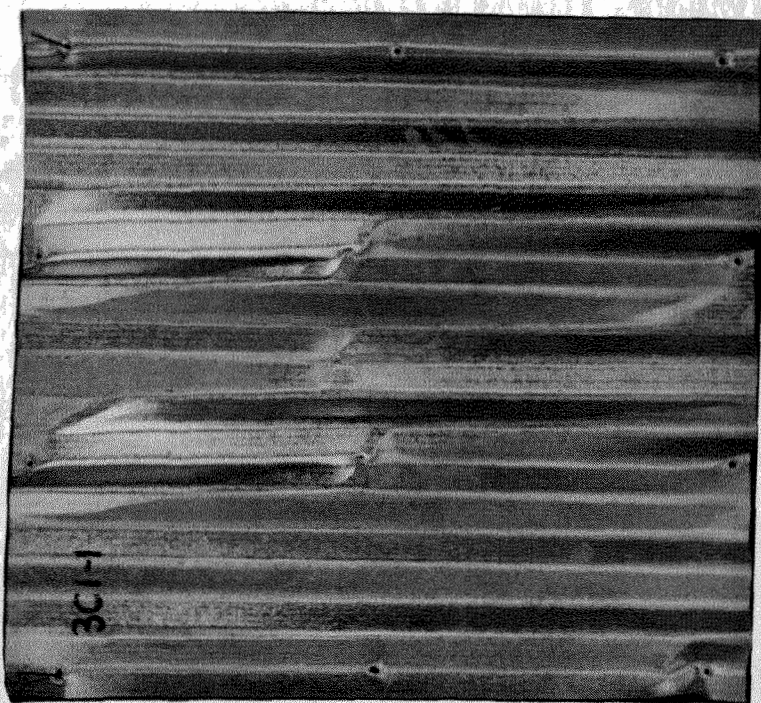
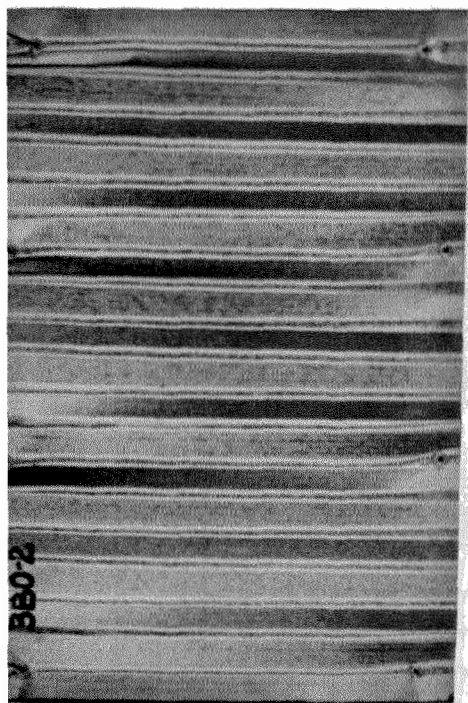


Fig. 4-21.

26 Gage Standard Corrugated Small Size Diaphragms.

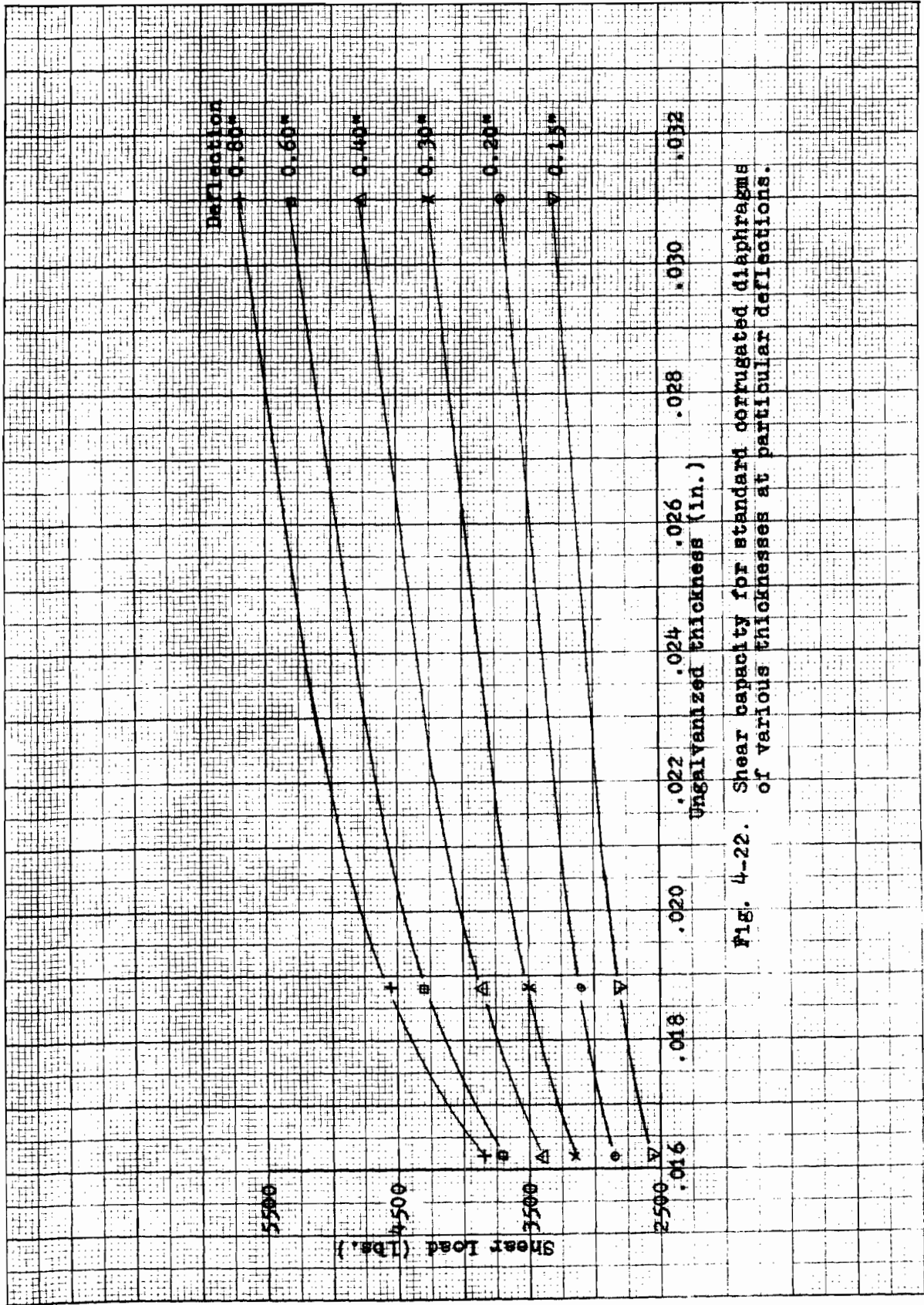


Fig. 4-22. Shear capacity for standard corrugated diaphragms of various thicknesses at particular deflections.

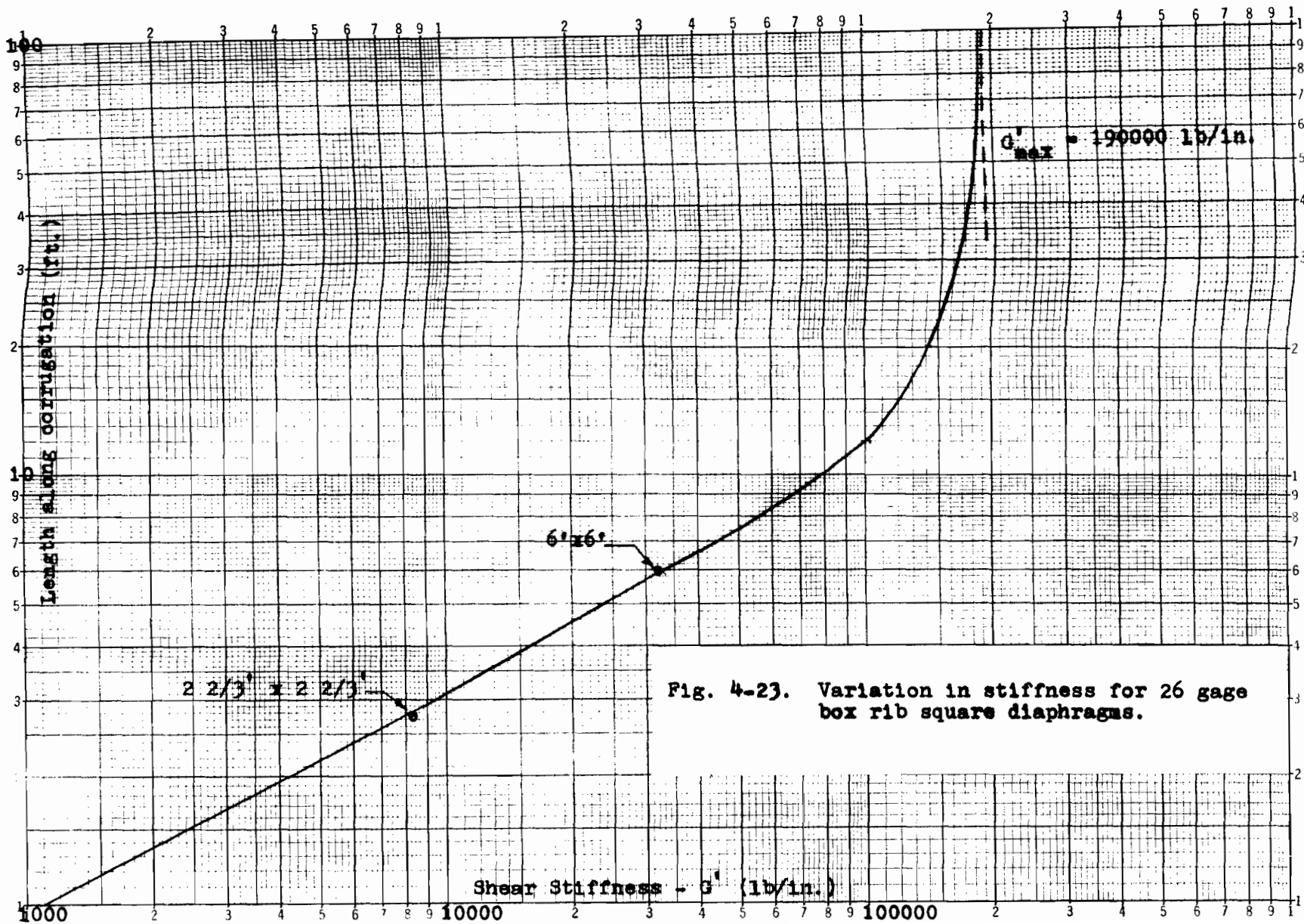


Fig. 4-23. Variation in stiffness for 26 gage box rib square diaphragms.

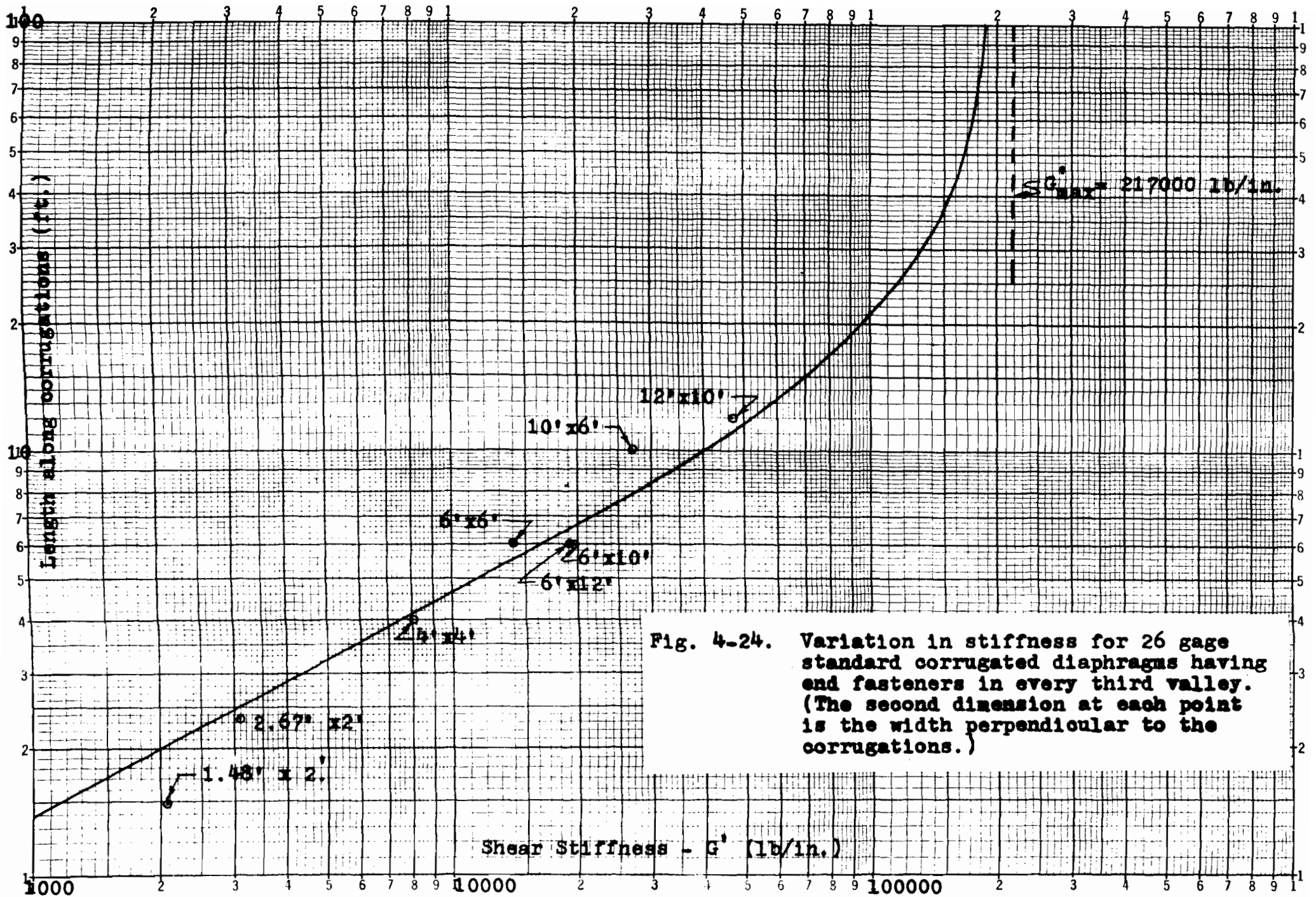


Fig. 4-24. Variation in stiffness for 26 gage standard corrugated diaphragms having end fasteners in every third valley. (The second dimension at each point is the width perpendicular to the corrugations.)

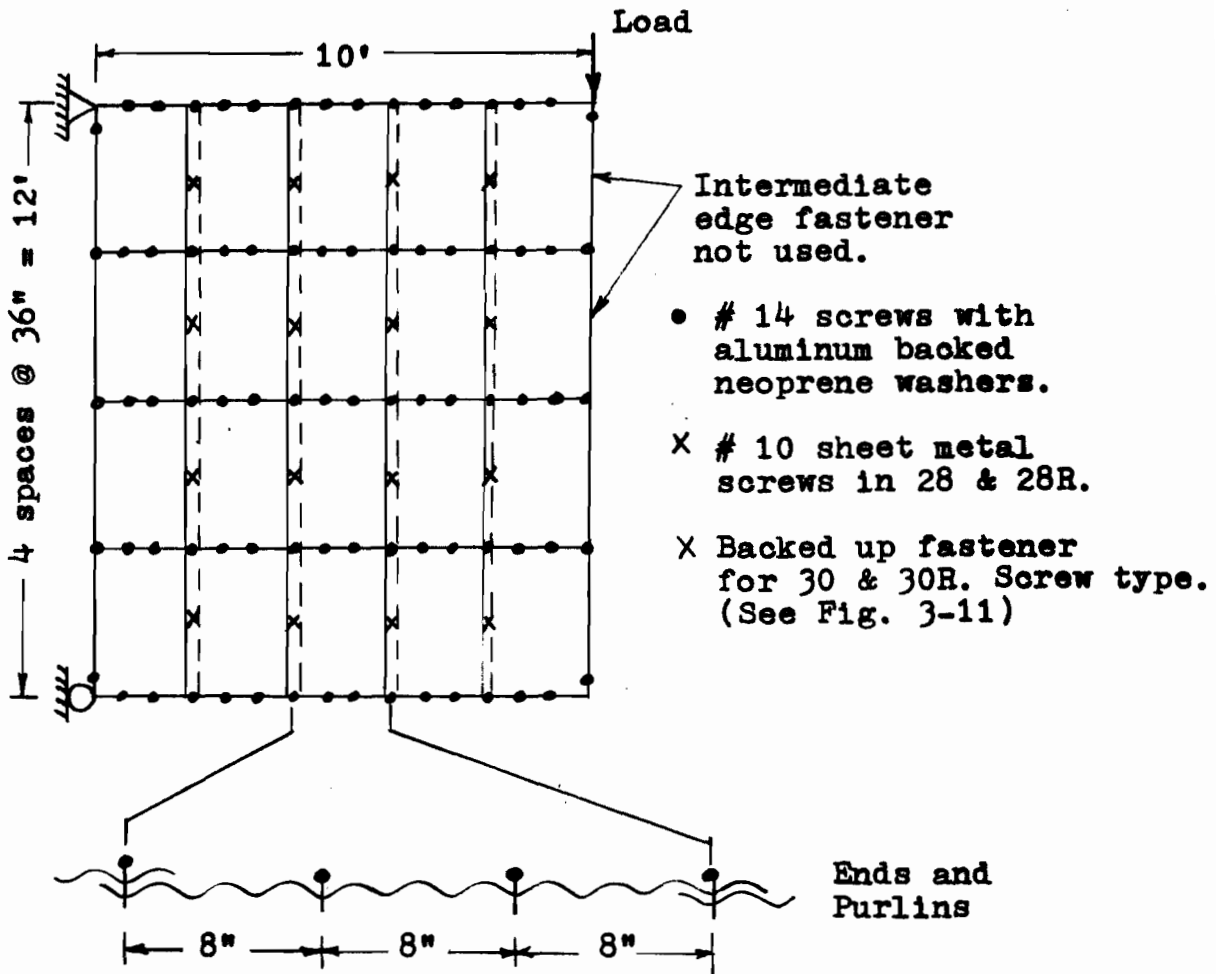


Fig. 4-25. Fastener arrangement for 26 gage standard corrugated tests 28, 28R, 30, and 30R.



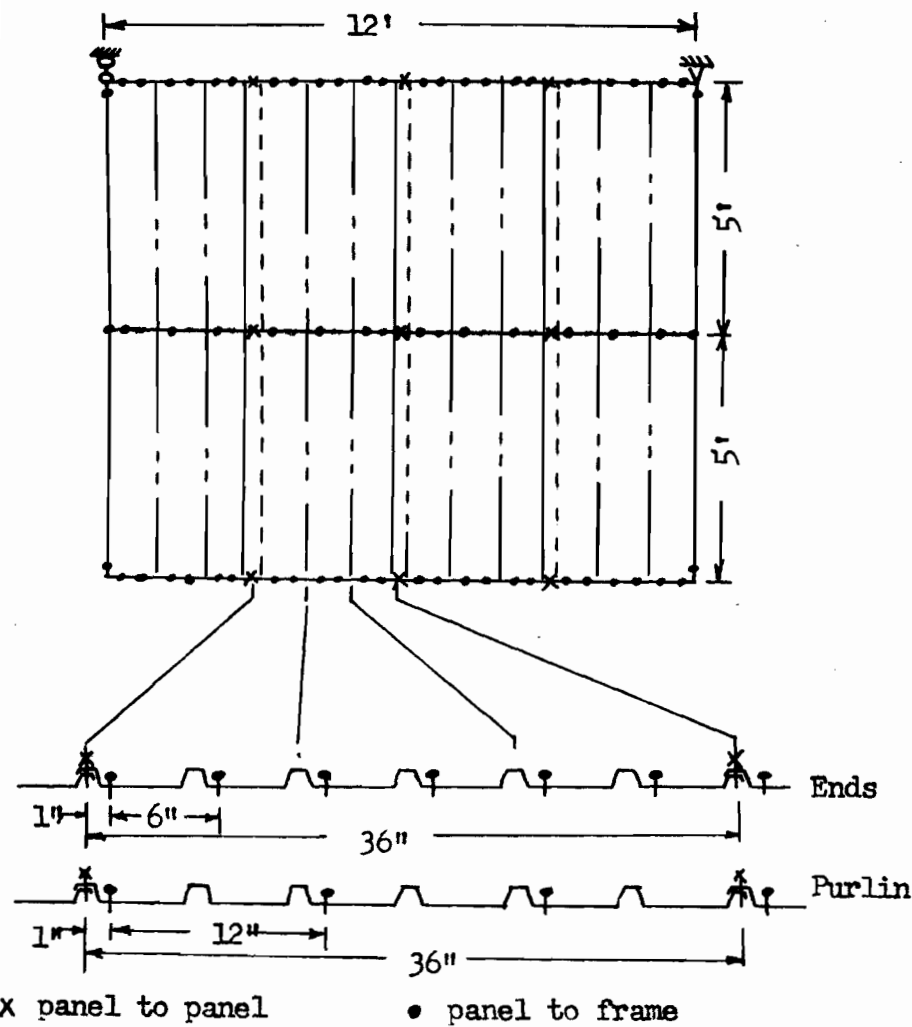
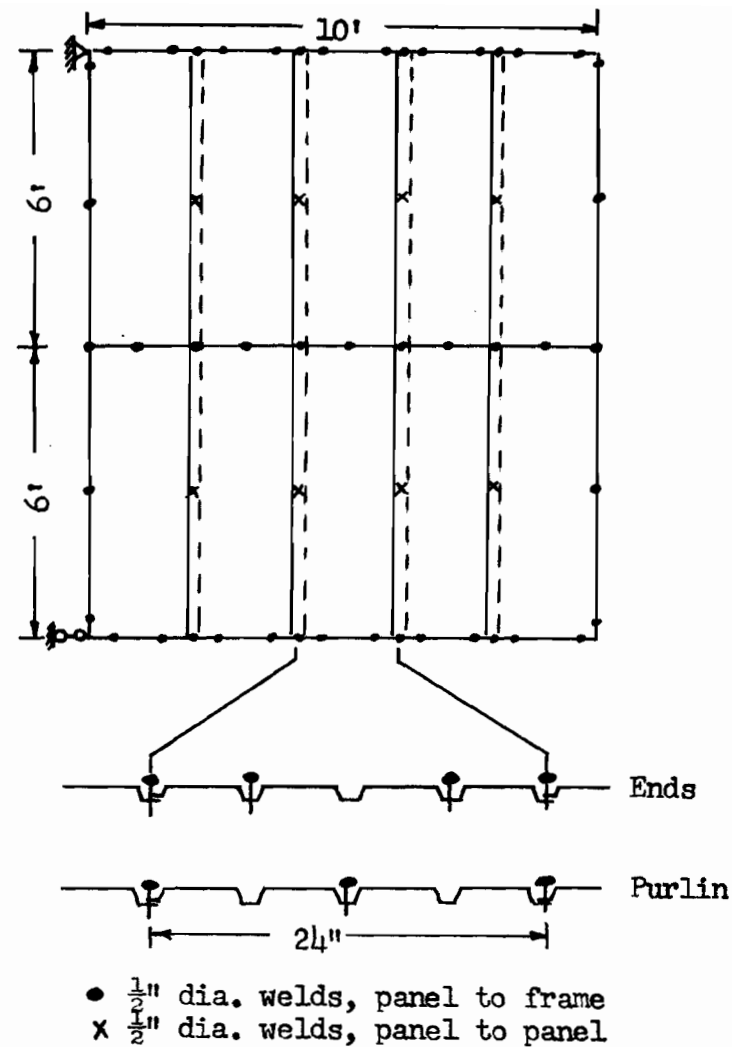


Fig. 4-28. Box rib tests 20, 20R, 22, and 22R. All connections were made with # 14 screws.



No intermediate fasteners in 24 or 24R.

Fig. 4-29. Fastener arrangements for Tests 24, 24R, 26, and 26R.

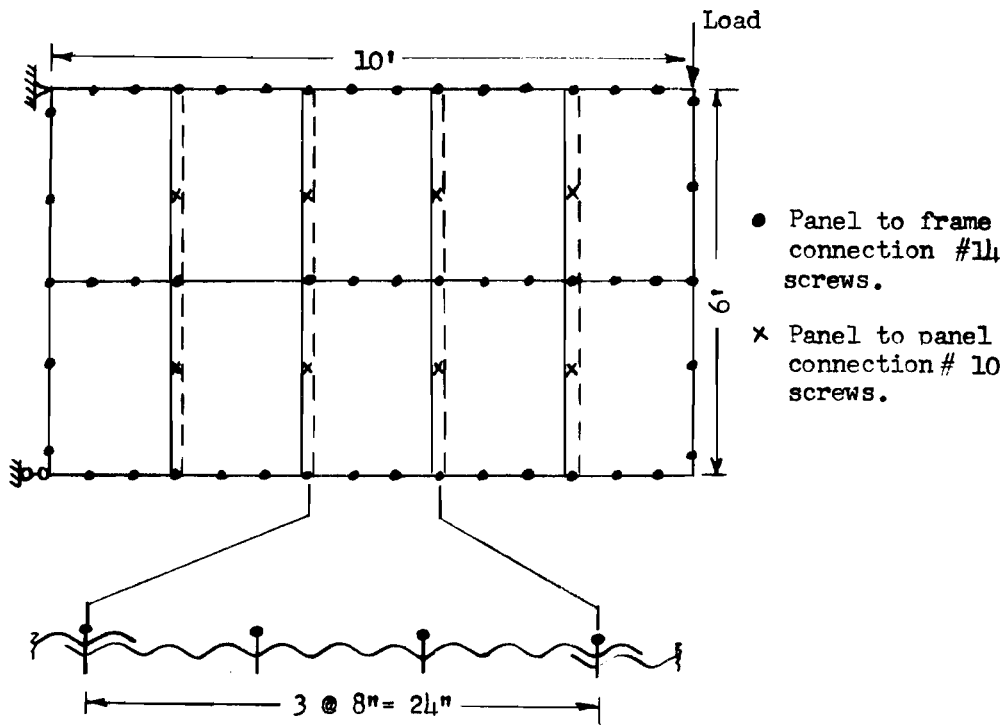


Fig. 4-30. 72" x 120" 26 gage standard corrugated tests. End fasteners in every third valley.

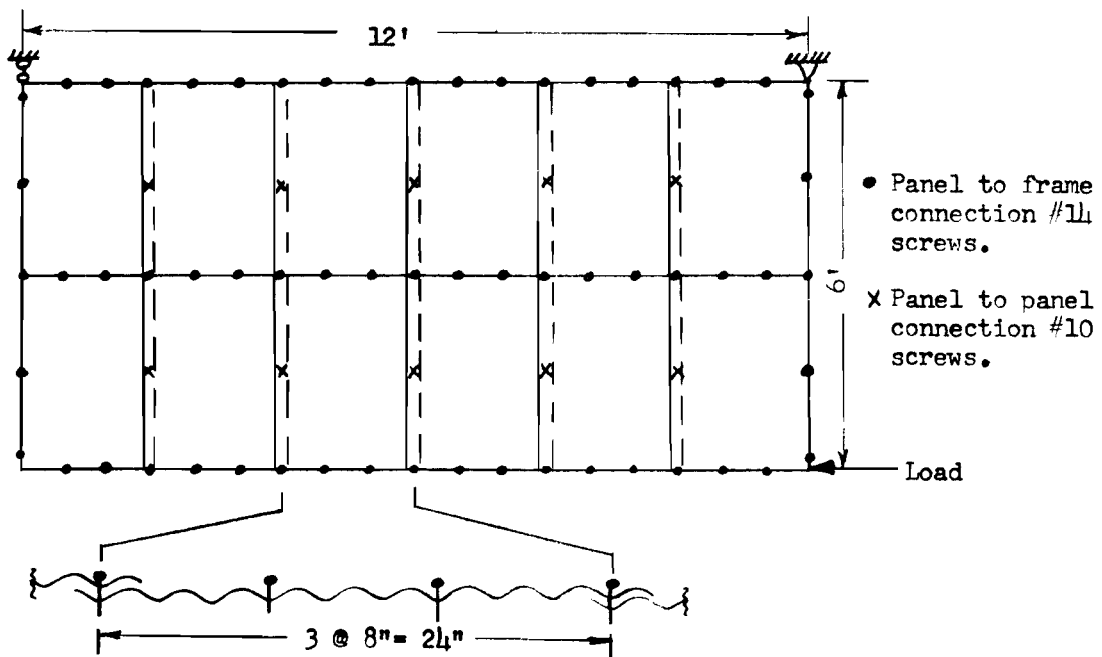


Fig. 4-31. 72" x 144" 26 gage standard corrugated tests. End fasteners in every third valley.

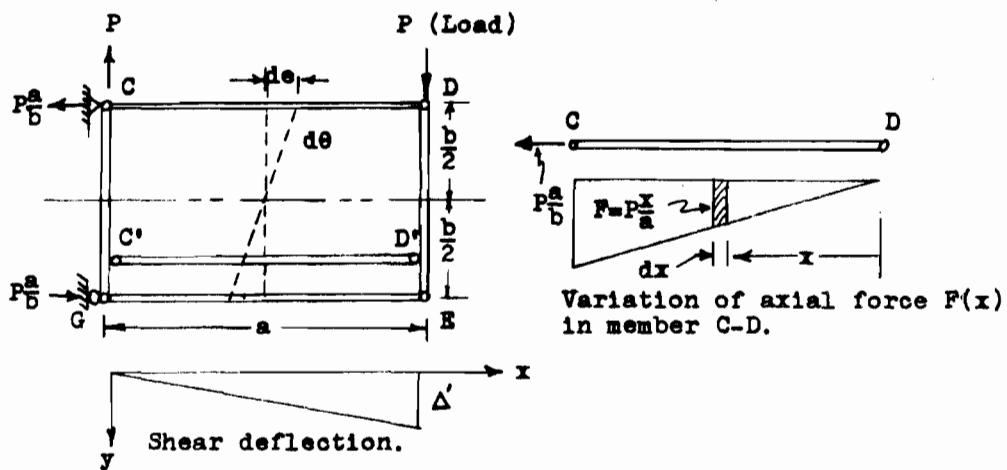


Fig. 5-1. Cantilever test frame showing differential elongations in the marginal members.

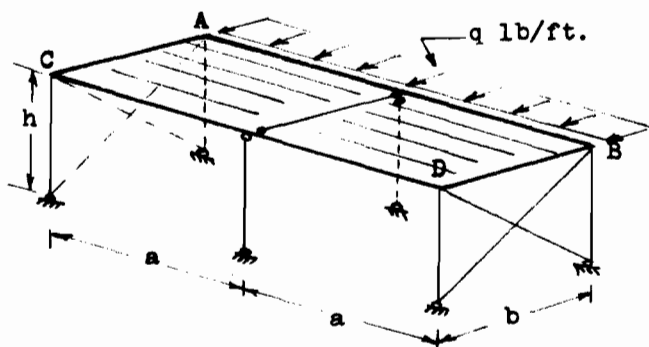


Fig. 5-2. Portal frame building with simple beam roof diaphragm.

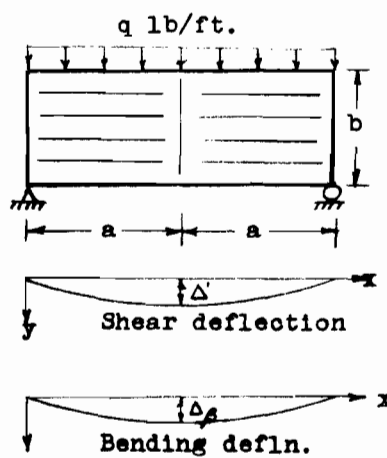


Fig. 5-3. Simple beam diaphragm.

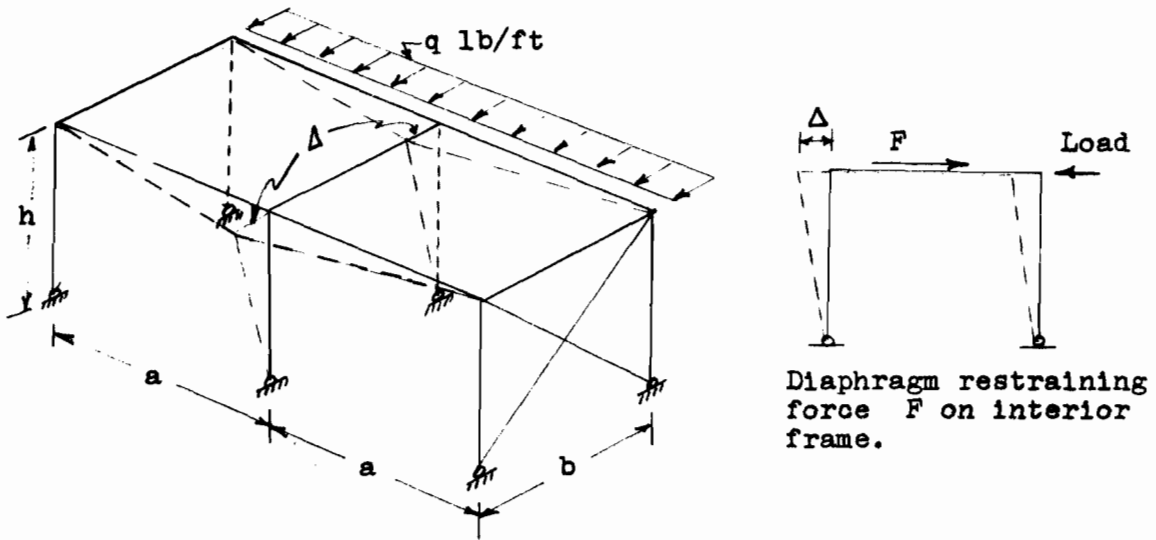


Fig. 5-4. Two bay portal frame building with rigid knee frames.

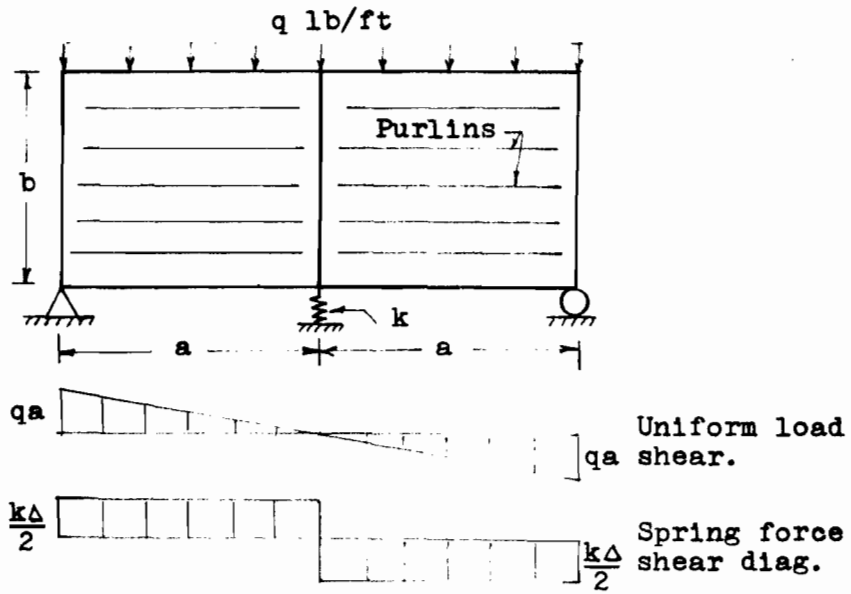


Fig. 5-5. Beam diaphragm with spring support.

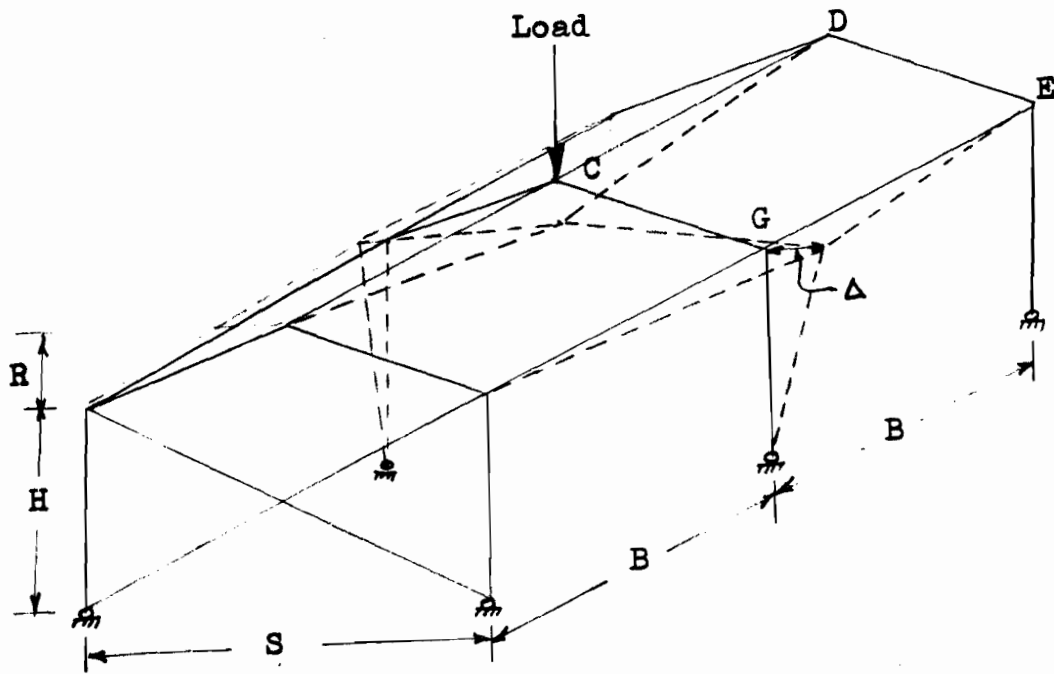


Fig. 6-1. Mill building showing spread of eaves.

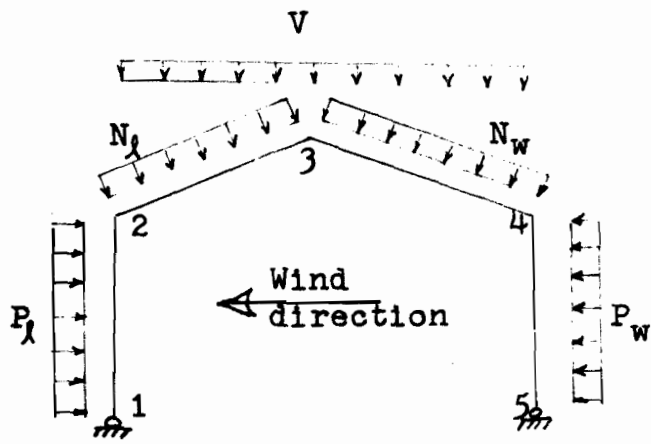


Fig. 6-2. Positive sign convention for loads.

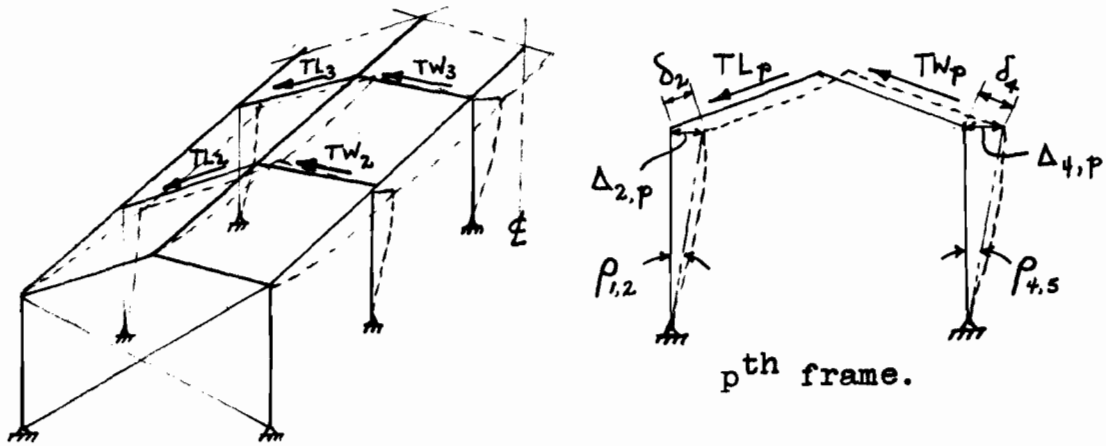


Fig. 6-3. Mill building showing the restraining forces due to diaphragm action.

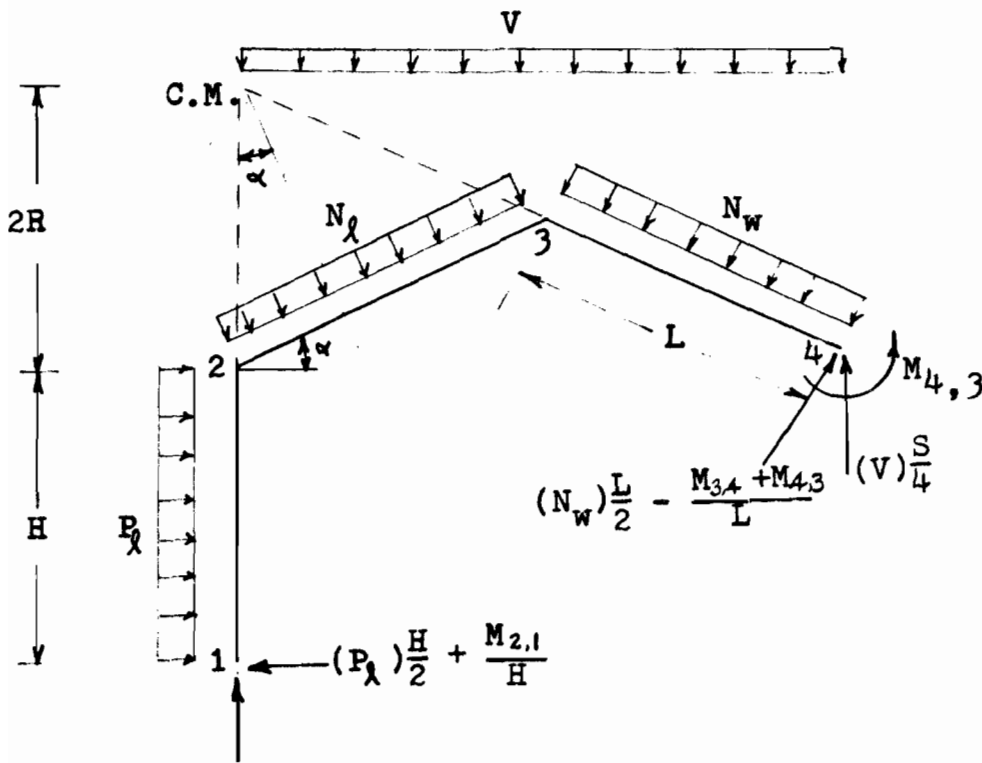


Fig. 6-4. Frame freebody.

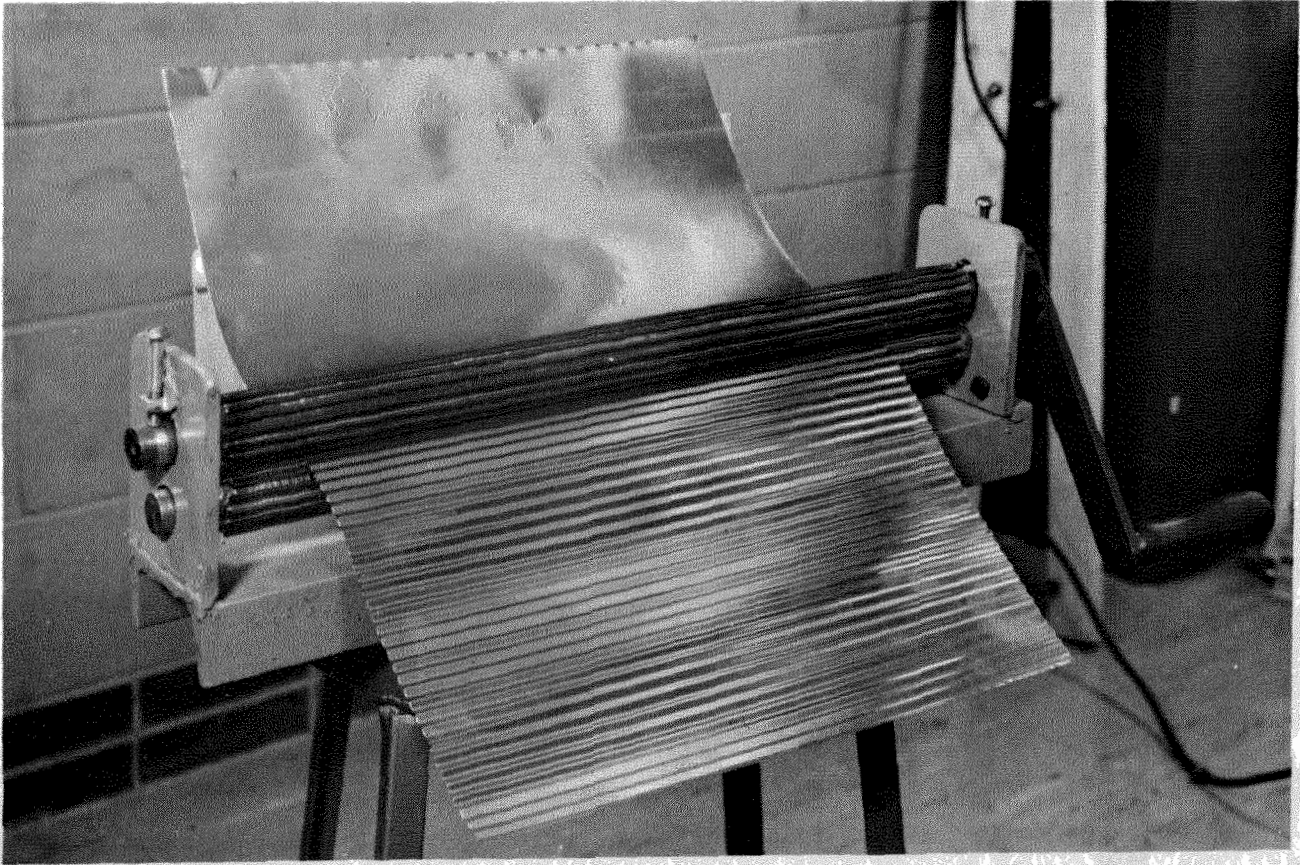


Fig. 6.5. Model corrugating machine.

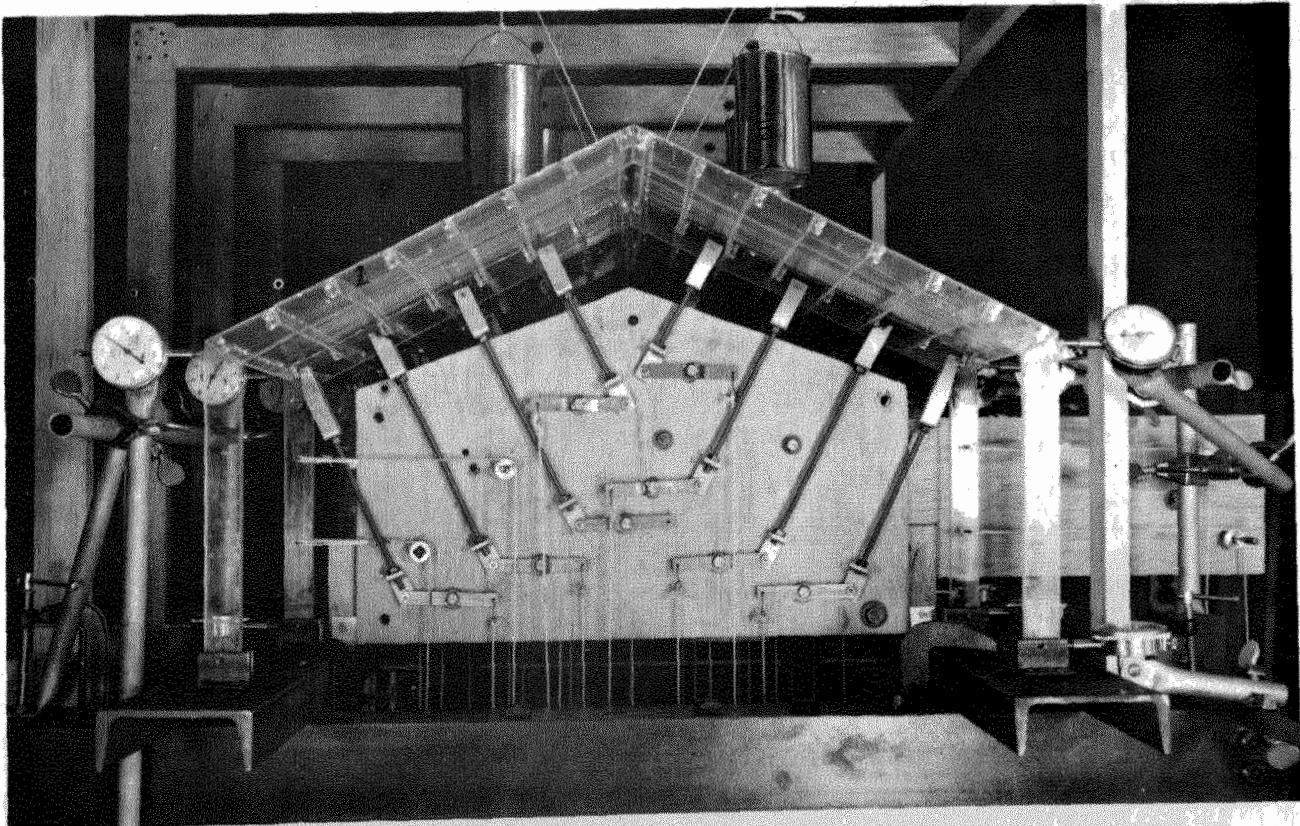


Fig. 6.6. Model building end view showing loading devices.

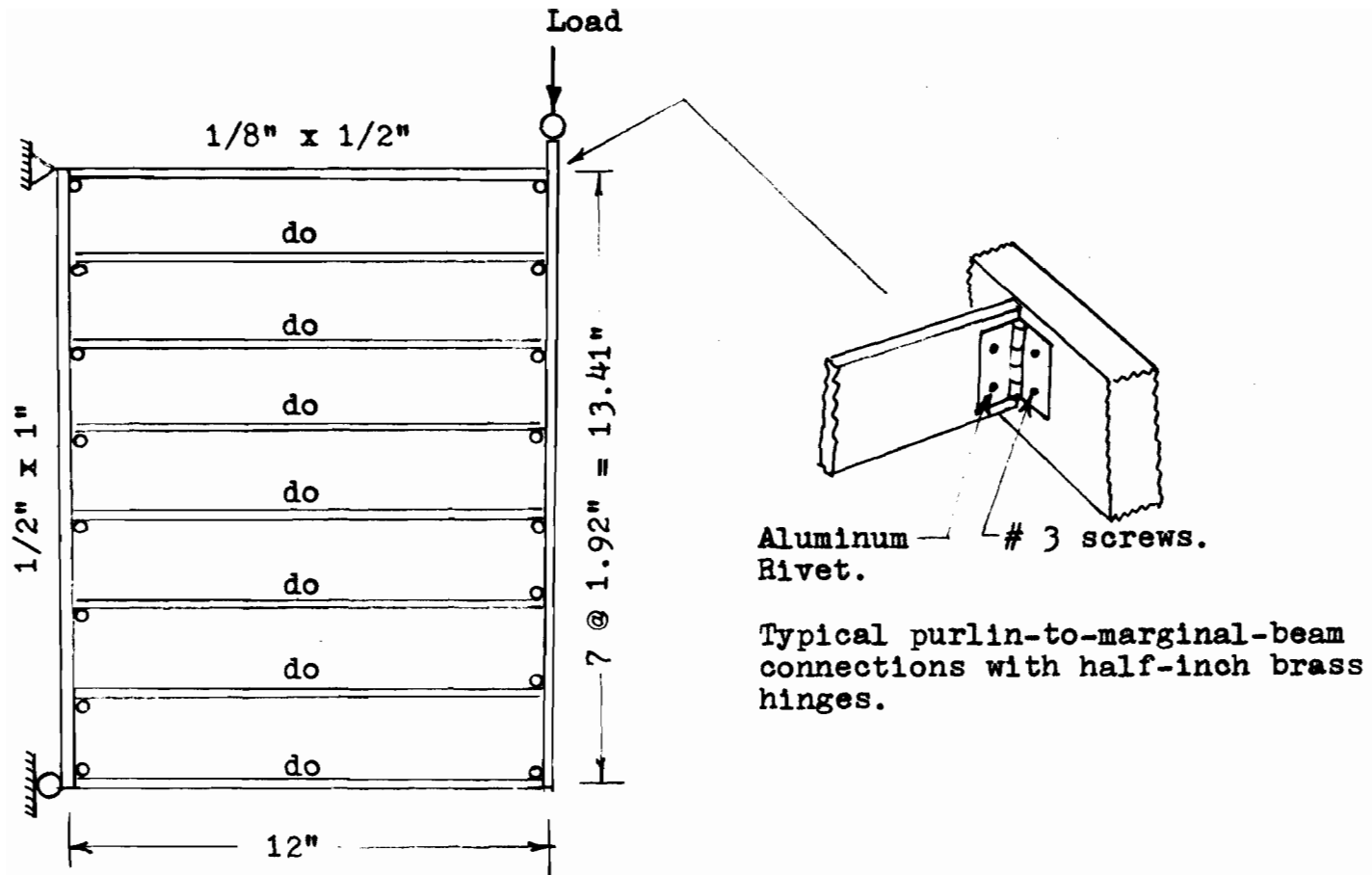


Fig. 6-7. Model diaphragm test frame showing pinned connections.

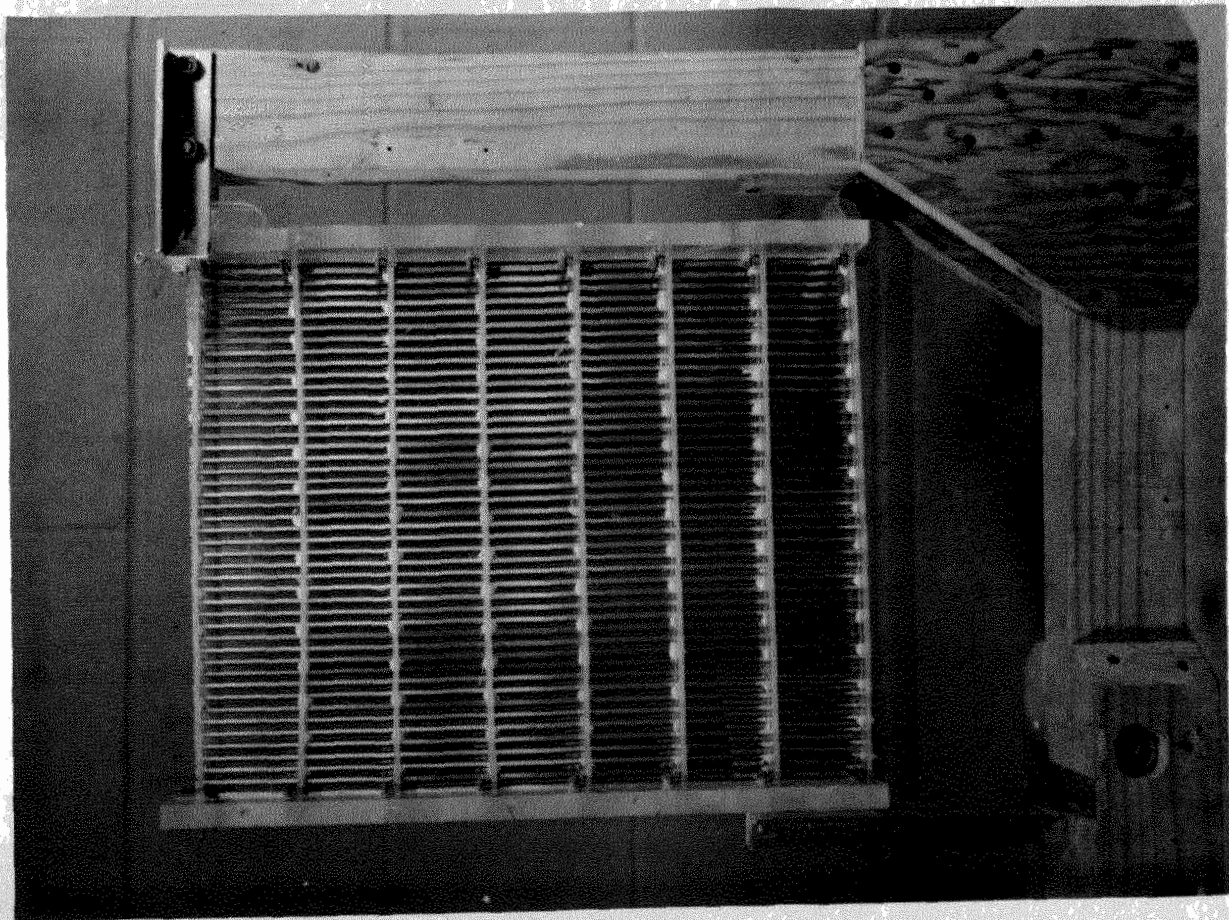


Fig. 6-8. Bottom view of model diaphragm.

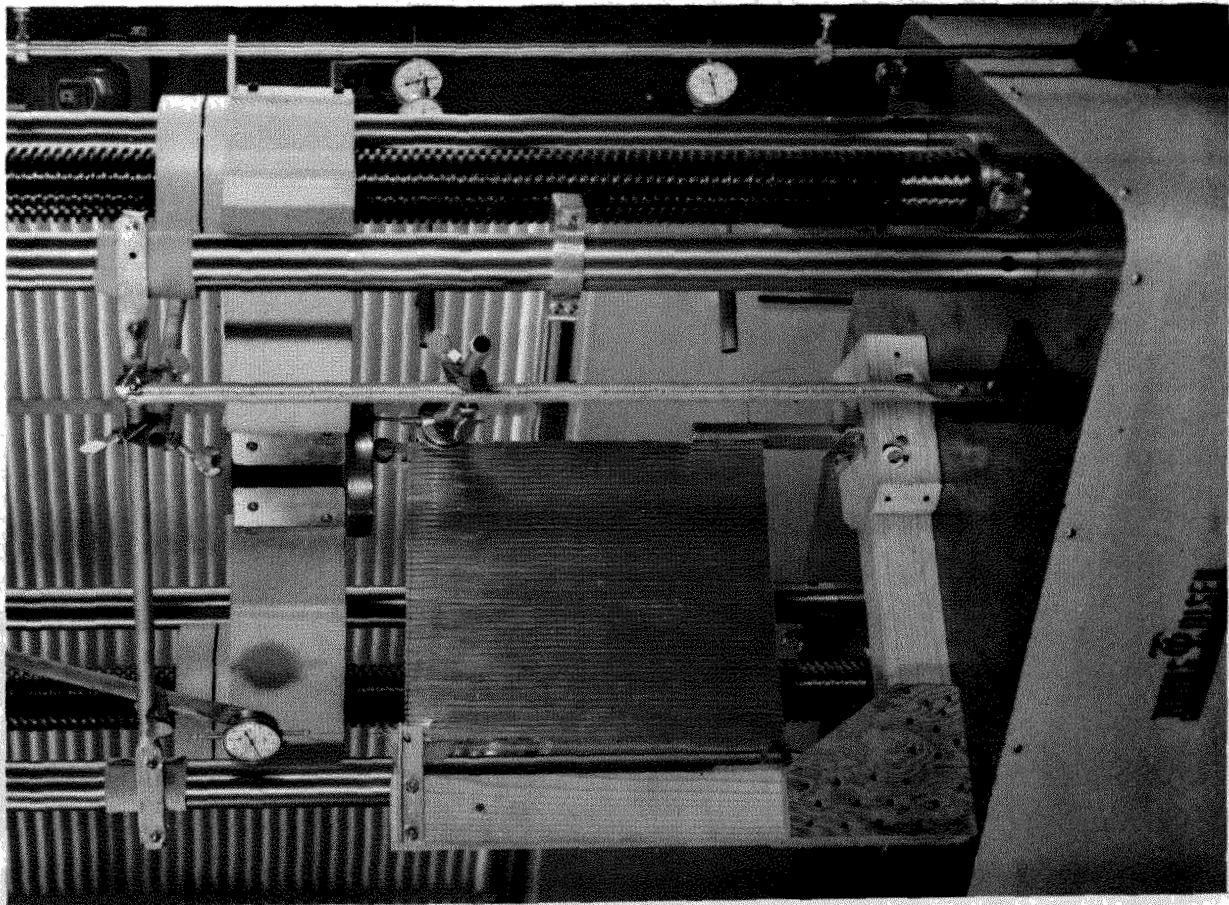
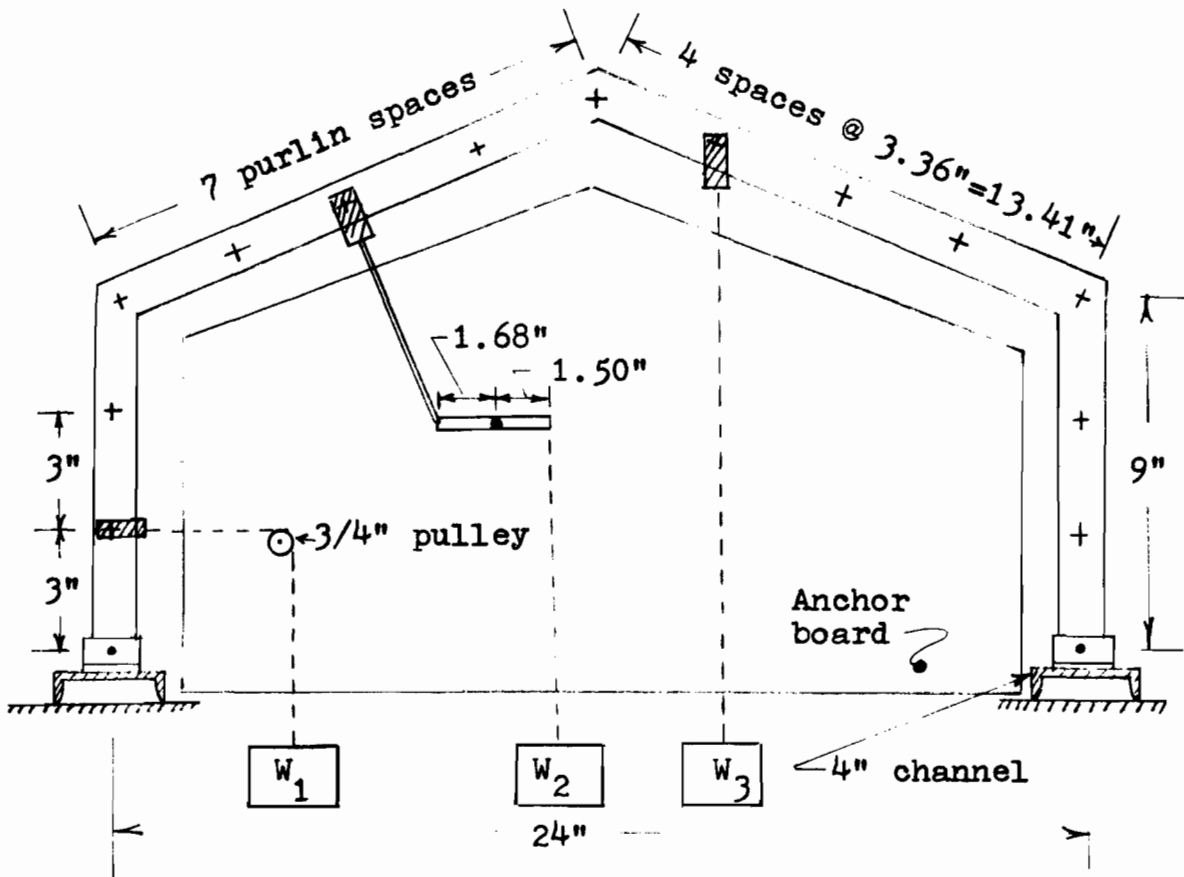


Fig. 6.9. Model diaphragm shear test.



$W_1$ : Lateral loads. Two per column.

$W_2$ : Normal outward loads.

$W_3$ : Vertical gravity loads.

Fig. 6-9a. Model building frame showing one of each load type.

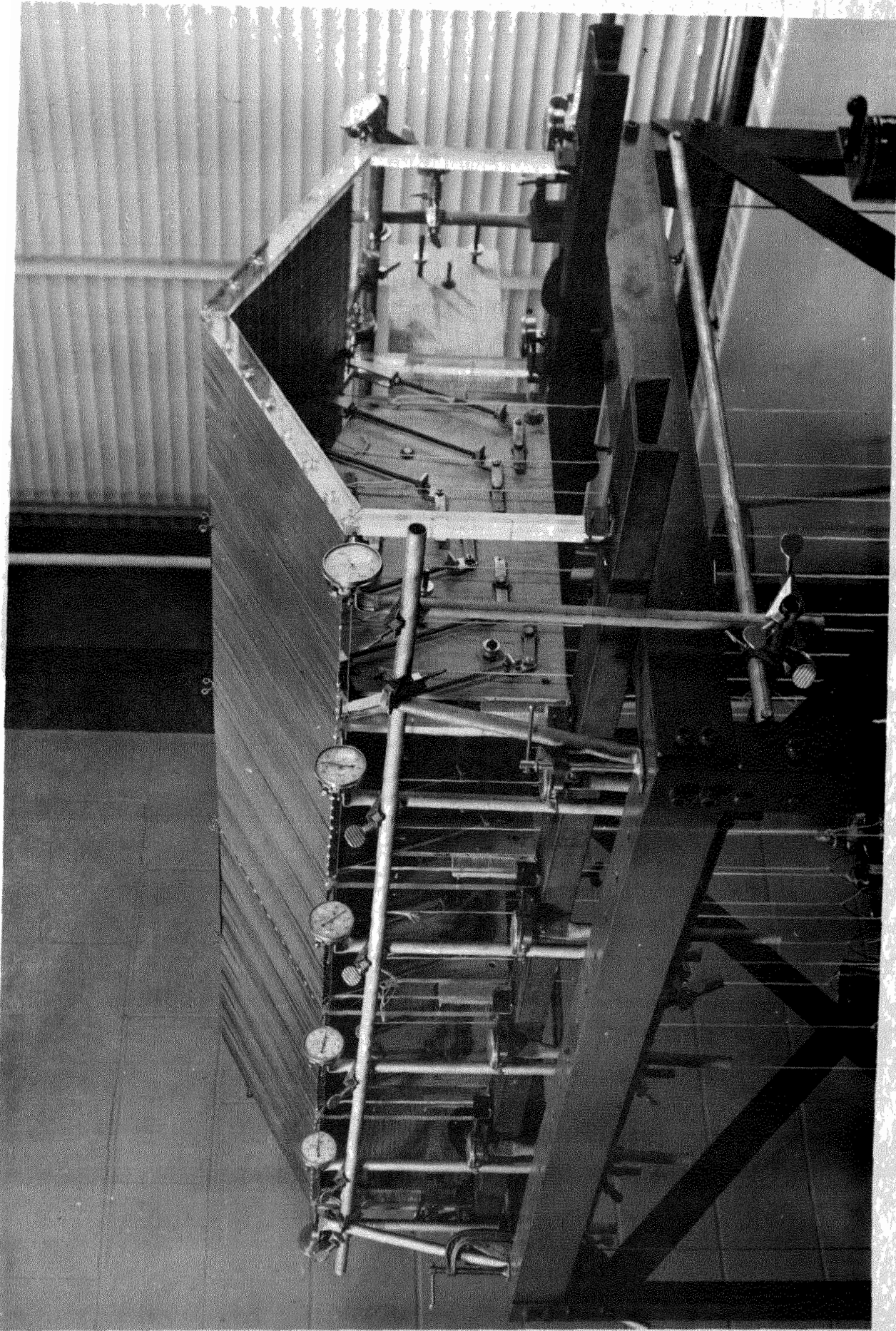


Fig.6.10 General view of model building with end wall removed.

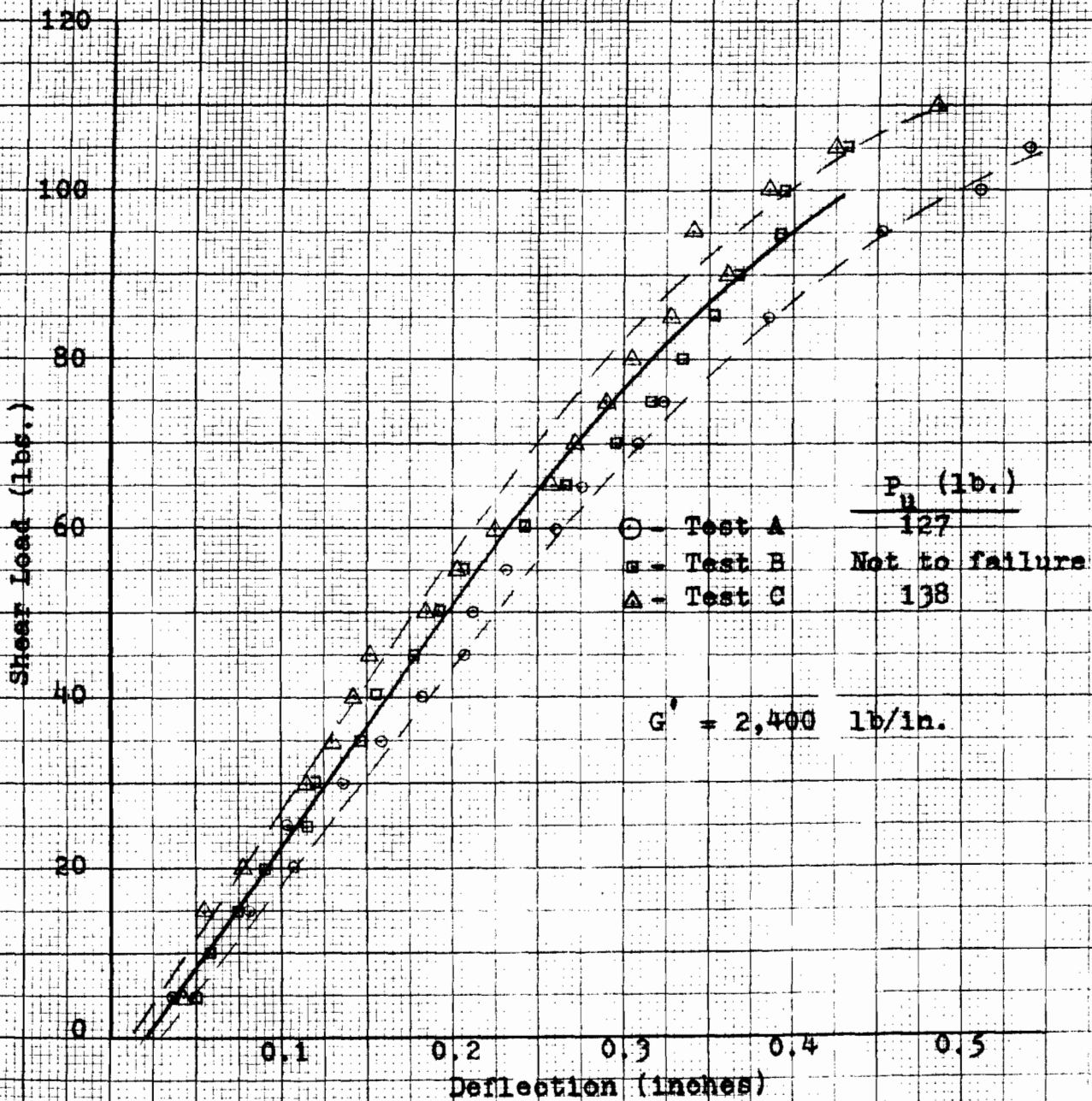


Fig. 6-11. Model diaphragm test results.

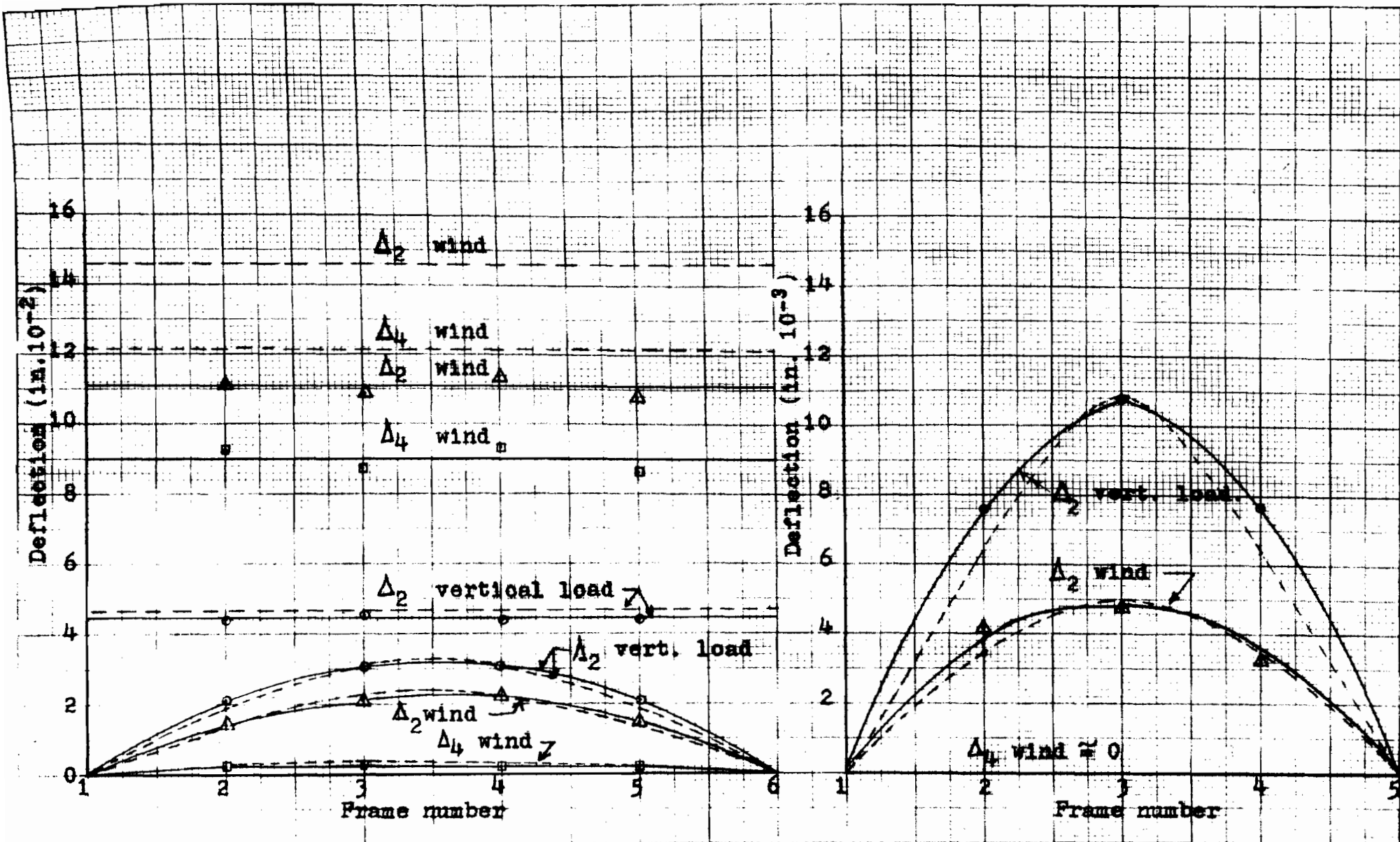
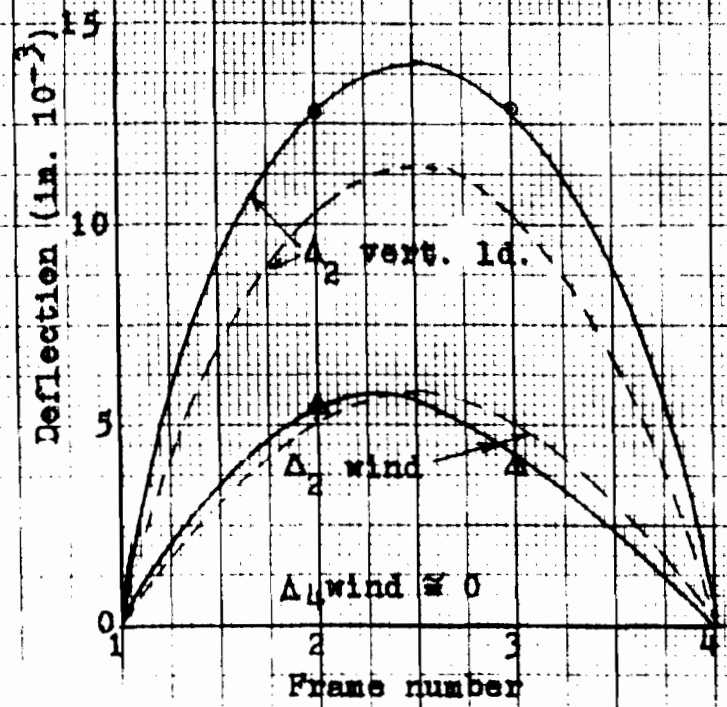
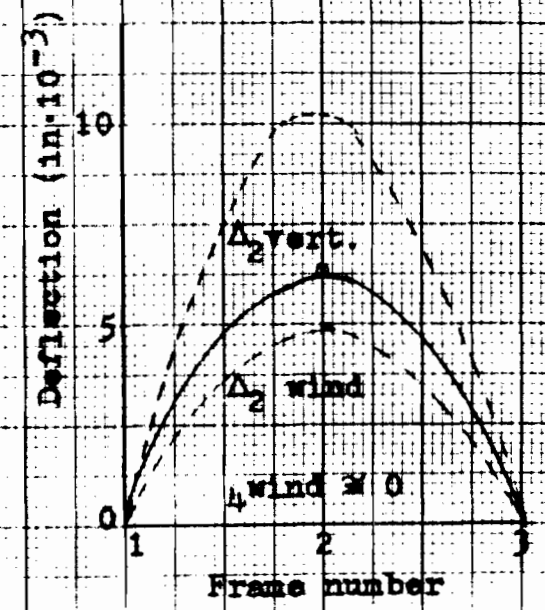


Fig. 6-12. Model mill building test results for buildings having indicated number of frames. Horizontal lines indicate values when diaphragms are not used. - - - Computer. \_\_\_\_\_ Measured.



a. Three bay building.



b. Two bay building.

Fig. 6-13. Model mill buildings. Horizontal lines give values when diaphragms are not used. For comparisons, see Fig. 6-12.

----- Computer  
 \_\_\_\_\_ Measured

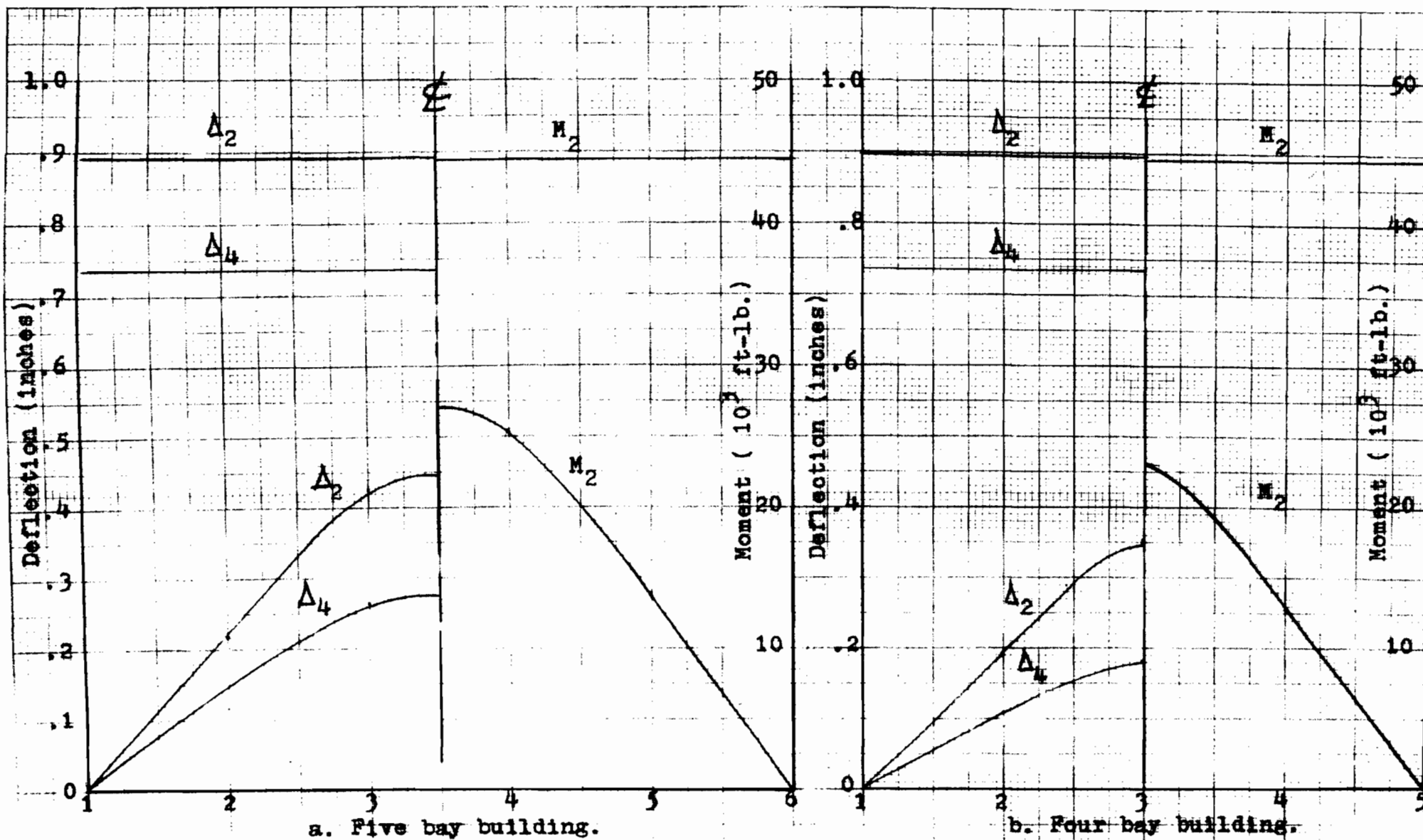
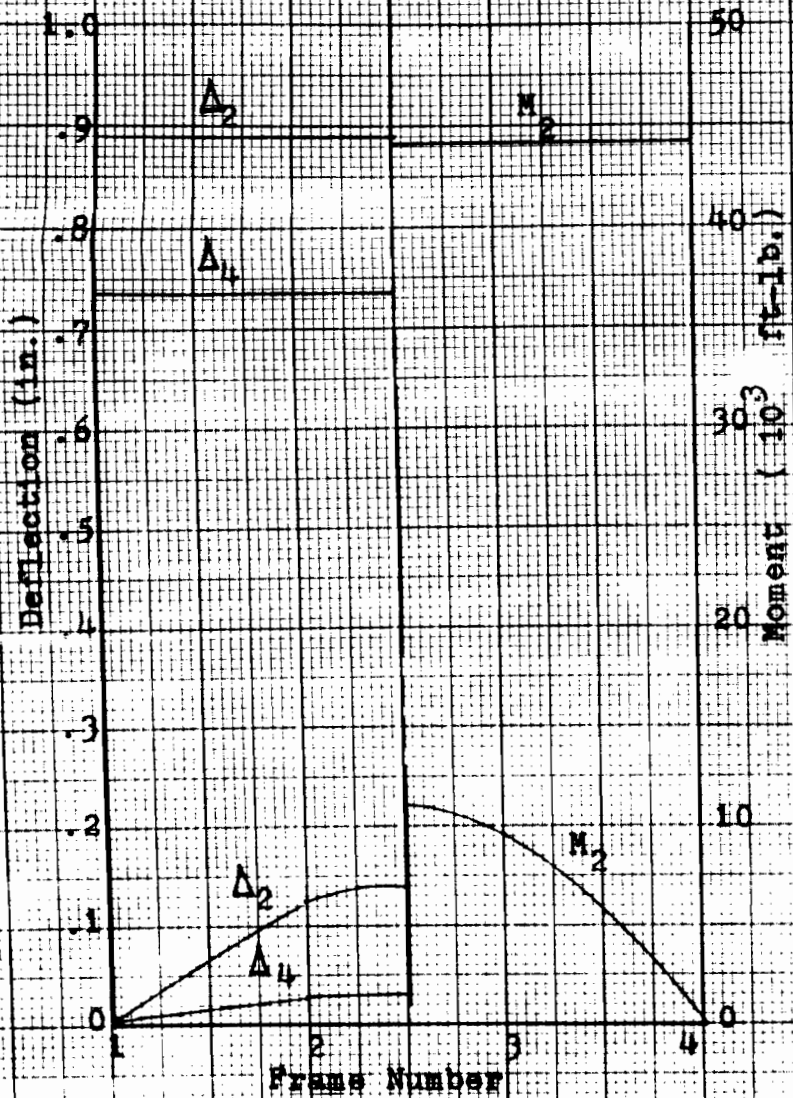
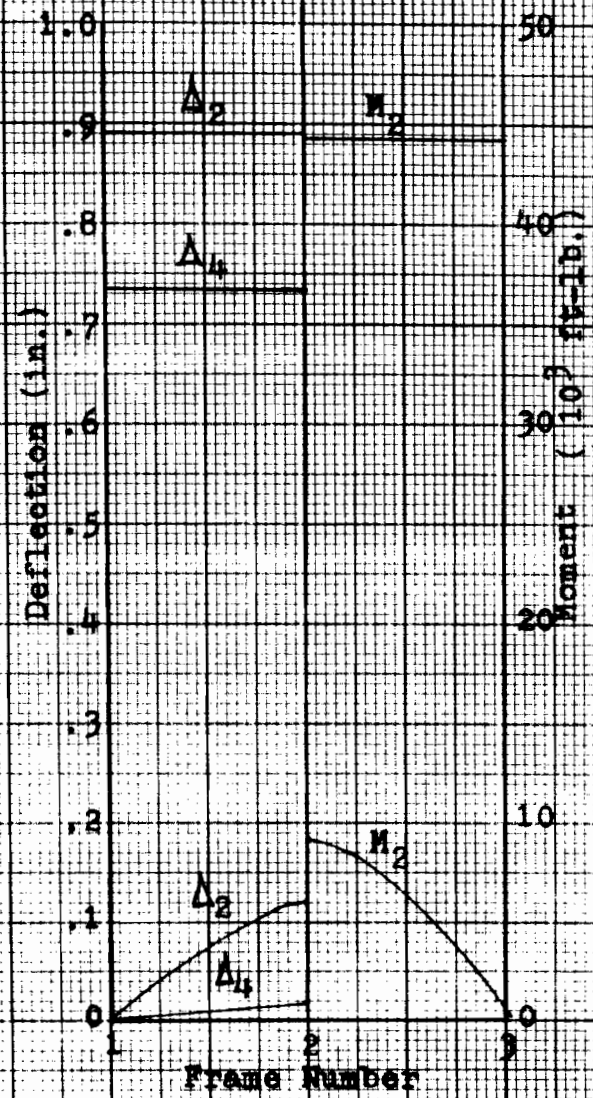


Fig. 6-14. Typical mill building eave moments and deflections from wind loads. Values are symmetrical about the building centerline. Horizontal lines are from solution which discounts diaphragm action.



a. Three bay building.



b. Two bay building.

Fig. 6-15. Typical mill building eave moments and deflections from wind loads. Values are symmetrical about the building centerline. Horizontal lines are from solution which discounts diaphragm action.